

De promotie zal plaats vinden in het Groot-Auditorium  
der Rijksuniversiteit, Rapenburg 73,  
en is voor iedereen toegankelijk.

Receptie na de promotie in het Academiegebouw.

Met tijdrovende parkeermoeilijkheden bij het  
Academiegebouw moet rekening worden gehouden.

## STELLINGEN

### I

Onderzoek aan het viscomagnetische effect in nematische vloeibare kristallen biedt de mogelijkheid de coëfficiënt te meten die het effect bepaalt dat reciprook is aan het effect van stromings-dubbele-breking.

P.G. de Gennes, *The Physics of Liquid Crystals*, Clarendon Press, Oxford, 1974  
S. Hess, *Z. Naturforsch.* **30a** (1975) 1224

### II

De looptijdmethode wordt bij het onderzoek van de beweging van ionen in vloeibaar He II gewoonlijk toegepast met een wolframspunt als ionenbron. Met een hete wolframdraad als bron kan men ook zonder sterke elektrische velden bij de bron grote stroomsterkten verkrijgen.

J.D.P. van Dijk, G.M. Postma, J. Wiebes and H.C. Kramers, *Physica*, to be published  
H. Hori, O. Ichikawa and M. Wake, *J. Phys. Soc. Jap.* **35** (1973) 1184  
M. Date, H. Hori and O. Ichikawa, *J. Phys. Soc. Jap.* **35** (1973) 1190

### III

Om na te gaan of het toenemen van de viscositeit van ammoniak onder invloed van een magneetveld samenhangt met het elektrisch dipoolmoment, dient de stromings-dubbele-breking te worden onderzocht in ammoniak-edelgas mengsels.

### IV

Het gebruik van de aanduiding "collision induced" voor bijdragen tot de verstrooiings-intensiteit die het gevolg zijn van dubbelverstrooiing, is verwarrend en dient te worden vermeden.

W.M. Gelbart, *Adv. Chem. Phys.* **26** (1974) 1

### V

Het is wenselijk in een tabel die de waarden van de fundamentele constanten uit de natuurkunde bevat, ook de waarde van de universele gravitatieconstante op te nemen.

*J. Phys. Chem. Ref. Data* **2** (1973) 663  
Jaarboek van de Nederlandse Natuurkundige Vereniging 1974-1975

## VI

In meeratomige gassen is de produktie van een impulsmomentpolarisatie van de vorm  $\langle J \rangle$  door een visceuze stroming, op grond van symmetrie-overwegingen, slechts mogelijk in aanwezigheid van een magnetveld.

## VII

Bij de analyse van de experimentele gegevens over het kritisch gedrag van thermodynamische grootheden in de buurt van een magnetische fase-overgang is kennis van de magnetostrictieve distorsies, die bij het overgangspunt optreden, van groot belang.

M.E. Fisher, Rev. Mod. Phys. **46** (1974) 597

## VIII

Het verdient aanbeveling resultaten van metingen van totale botsingsdoorsneden, verkregen onder verschillende experimentele omstandigheden, te presenteren in de vorm  $Q_{\text{exp}}(g/v)$ , waarin  $v$  de primaire bundelsnelheid is en  $g$  de relatieve snelheid van de botsingspartners.

K. Berkling, R. Helbing, K. Kramer, H. Pauly, Ch. Schlier and P. Toschek,  
Z. Phys. **166** (1962) 406

## IX

Het is wenselijk om bij de realisering van het beleidsvoornemen van de minister met betrekking tot het systeem van meervoudige bevoegdheden bij de nieuwe lerarenopleidingen voor de natuurwetenschappen, uit te gaan van een systeem waarbij het hoofdvak wordt gevormd door één van de afzonderlijke natuurwetenschappen en het bijvak door het geïntegreerde vakgebied "natuuroriëntatie".

Brief van de minister van Onderwijs en Wetenschappen aan de voorzitter van de vaste commissie voor Onderwijs en Wetenschappen van de Tweede Kamer der Staten  
Generaal d.d. 11 juni 1974  
Verslag Responsconferenties deelraamplannen onderbouw Lager Beroepsonderwijs,  
voorjaar 1976

## X

Het is mogelijk een gepolariseerde bundel van lineaire moleculen te produceren door gebruik te maken van de "seeded beam" techniek.

P.G. van Ditzhuyzen

6 oktober 1976

**THE VISCOMAGNETIC EFFECT OF SOME  
LINEAR AND SYMMETRIC TOP MOLECULES**

**PROEFSCHRIFT**

**TER VERKRIJGING VAN DE GRAAD VAN DOCTOR  
IN DE WISKUNDE EN NATUURWETENSCHAPPEN  
AAN DE RIJKSUNIVERSITEIT TE LEIDEN, OP GEZAG  
VAN DE RECTOR MAGNIFICUS DR. D.J. KUENEN,  
HOGLERAAR IN DE FACULTEIT DER WISKUNDE EN  
NATUURWETENSCHAPPEN, VOLGENS BESLUIT VAN  
HET COLLEGE VAN DEKANEN TE VERDEDIGEN OP  
WOENSDAG 6 OKTOBER 1976 TE KLOKKE 14.15 UUR**

**DOOR**

**PAUL GUSTAAF VAN DITZHUYZEN**

**GEBOREN TE HILVERSUM IN 1942**

**1976**

**DRUKKERIJ J.H. PASMANS, 'S-GRAVENHAGE**

Promotor: Prof. Dr. H.F.P. KNAAP

Dit proefschrift is tot stand gekomen mede  
onder leiding van Dr. L.J.F. Hermans

Ter gedachtenis  
aan mijn vader

Het in dit proefschrift beschreven onderzoek werd uitgevoerd als onderdeel van het programma van de werkgemeenschap voor Molecuulfysica van de Stichting voor Fundamenteel Onderzoek der Materie (F.O.M.) met financiële steun van de Nederlandse Organisatie voor Zuiver Wetenschappelijk Onderzoek (Z.W.O.).

## CONTENTS

PREFACE		7
CHAPTER I	THE VISCOMAGNETIC EFFECT IN POLAR GASES	9
	1. Introduction	9
	2. Theory	10
	2.1 Linear molecules	11
	2.2 Symmetric top molecules	16
	3. Experimental method	23
	4. Corrections	25
	4.1 Presence of short sides	25
	4.2 Deviations from the ideal Poiseuille flow	25
	4.3 Stray fields	26
	5. Experimental results	26
	5.1 General	26
	5.2 $\text{NH}_3$ and $\text{ND}_3$	30
	5.3 The magnitude of the cross sections	39
	6. Discussion	40
	6.1 The precise form of the angular momentum dependent polarizations	40
	6.2 The importance of the various polarizations	42
CHAPTER II	THE TEMPERATURE DEPENDENCE OF THE VISCOMAGNETIC EFFECT IN THE HYDROGEN ISOTOPES	46
	1. Introduction	46
	2. Measuring procedure and calculation of the results	48
	3. Purity of the gases	50
	4. Experimental results	50
	4.1 General	50
	4.2 The position of the curve	56
	4.3 The magnitude of the viscosity change	57
	5. Discussion	59



6. The behavior of the cross sections	59
6.1 $H_2$ and $D_2$	62
6.1.1 $\mathcal{C}(0001)$ for $H_2$ and $D_2$	63
6.1.2 $\mathcal{C}_{20}^{(02)}$ for $H_2$ and $D_2$	65
6.1.3 $\mathcal{C}(02)$ for $H_2$ and $D_2$	67
6.2 HD	69
6.2.1 $\mathcal{C}(0001)$ for HD	69
6.2.2 $\mathcal{C}_{20}^{(02)}$ for HD	69
6.2.3 $\mathcal{C}(02)$ for HD	69
Appendix	69
SAMENVATTING	76
CURRICULUM VITAE	78

The chapters of this thesis will be published in *Physica*.

## PREFACE

The transport properties of a dilute polyatomic gas are influenced by a magnetic or an electric field. Studies of these Senfleben-Beenakker effects are of interest since they give information on the kinetic theory of polyatomic gases and on the various collision processes which can occur between molecules with internal angular momentum. In this thesis the influence of a magnetic field on the viscosity (the viscomagnetic effect) is investigated. This effect can be explained as follows: the presence of a velocity gradient gives rise to a velocity polarization and, through collisions, to an angular momentum dependent polarization (alignment of the molecules). Upon application of a magnetic field this polarization is partially destroyed. This decreases the velocity polarization thus changing the viscosity. The various polarizations appearing in the theoretical description of the viscomagnetic effect can be even or odd powers in the angular momentum  $J$  giving rise to a decrease or an increase of the viscosity, respectively. For linear molecules the viscomagnetic effect can be well described by one single polarization which is even in the angular momentum. In the case of symmetric top molecules, however, it was found that in measurements on the influence of an electric field on the thermal conductivity, also odd-in- $J$  polarizations play a role. The presence of such polarizations has theoretical interest since in this case the collision operator is not self-adjoint, which indicates in classical terms that not every collision has its inverse. For a detailed investigation of those polarizations and the precise reason for their occurrence a systematic research program was set up. In contrast to experiments in electric fields, measurements in magnetic fields yield more possibilities in studying the influence of the orientation of the field on the viscosity and thermal conductivity. This offers a relatively simple method of disentangling the contributions from the various polarizations. The thermal conductivity measurements in a magnetic field are still in progress and will be described in the thesis of B.J. Thijsse. The measurements for the viscomagnetic effect on a number of polar molecules with various structures are presented in chapter I of this thesis. Two different viscosity changes have been measured for the linear molecules  $\text{CO}_2$ ,  $\text{OCS}$ ,  $\text{N}_2\text{O}$ ,  $\text{HCl}$ ,  $\text{DCl}$  and the symmetric top molecules  $\text{CH}_3\text{F}$ ,  $\text{CHF}_3$ ,  $\text{PF}_3$ ,  $\text{NF}_3$ ,  $\text{PH}_3$ ,  $\text{AsH}_3$ ,  $\text{NH}_3$ ,  $\text{ND}_3$  and  $\text{SF}_6$ . It was found that, with the exception of  $\text{NH}_3$  and  $\text{ND}_3$ , the effects of all gases, independent of the molecular structures, can be well described by one single polarization of type  $\overline{J\overline{J}}$ . The experimental results are compared with theory. Effective cross sections are obtained and are compared with results from the visco-electric effect.

In chapter II the viscomagnetic effect of  $\text{H}_2$  and  $\text{D}_2$  has been studied. Being in low rotational states due to their small moments of inertia, these homonuclear hydrogen isotopes offer the unique possibility of studying the various collisional processes in

different rotational quantum states. This can be achieved both by studying the temperature dependence of the effect as well as performing experiments on the ortho- and para-modifications of  $H_2$  and  $D_2$ . However, very high sensitivity is required in such experiments, the relative viscosity change being about a factor of 100 smaller than the effects measured to date. Experiments were performed on these gases in the temperature range from 140 K to room temperature. The results are compared with data for HD as obtained earlier by Burgmar *et al.* The data are combined with literature data on the volume viscosity and are expressed in terms of effective cross sections for several elastic and inelastic collision processes.

## CHAPTER I

## THE VISCOMAGNETIC EFFECT IN POLAR GASES

1. *Introduction.* It has been shown both experimentally and theoretically, that the transport properties of polyatomic gases can be influenced by an external field<sup>1,2,3,4,5,6</sup>). In this paper experiments on the influence of a magnetic field on the shear viscosity are presented. This phenomenon, called the viscomagnetic effect, can be described as follows: a velocity gradient in a gas of polyatomic molecules produces not only a non-isotropic distribution in velocity space but also, through collisions, a polarization of the molecular angular momenta. In this process the angle dependent part of the molecular interaction potential plays a crucial role. The polarization in the angular momenta can be partially destroyed by the action of a magnetic field (through the Larmor precession). Through collisions, in turn, the polarization in velocities decreases thus changing the viscosity. Therefore, the viscomagnetic effect gives information about collision processes in which the molecular angular momenta are involved, *i.e.*, about energetically inelastic as well as reorientation processes.

Earlier experiments on this viscomagnetic effect for diatomic molecules and spherical top molecules<sup>7,8</sup>) have shown that the change in viscosity can be well described on the basis of one particular type of angular momentum polarization. This polarization is of the form  $\overline{J_i J_j} R(J^2)$  where the symbol  $\overline{\quad}$  indicates the symmetric traceless part of a tensor *e.g.*,  $\overline{J_i J_j} = \frac{1}{2} J_i J_j + \frac{1}{2} J_j J_i - \frac{1}{3} \delta_{ij} J^2$ . The polynomial  $R(J^2)$  is a function of the scalar quantity  $J^2$ . Physically  $\langle \overline{J_i J_j} R(J^2) \rangle \neq 0$  implies an alignment of the rotational axes of the molecules. However, there are experimental indications that for molecules of more complicated structure, *e.g.*, symmetric top molecules, other angular momentum polarizations also play a role. Of special interest are odd-in- $J$  polarizations because of the information they give about the collision dynamics. The presence of such terms indicates that not each collision has its inverse, or, quantummechanically, that the collision operator is not self-adjoint. In the field effects, such terms give rise to an increase of the transport properties upon application of the field, as opposed to the even-in- $J$  polarizations which produce a decrease (see fig. 1). Indications for such odd-in- $J$  terms were found a) in measurements of the electric field effect on the thermal conductivity for molecules with large electric dipole moments<sup>9</sup>) and b) in measurements of the electric and magnetic field effects on the viscosity of  $\text{NH}_3$  and  $\text{ND}_3$ <sup>10,11</sup>). It is, however, from these experiments not clear whether the presence of these odd-in- $J$  polarizations are essentially due to the electric dipole moment or to the more complicated structure of the molecules, and whether it was limited in the case of the viscosity to the ammonia molecules. In order

to settle this question a research program was initiated to investigate the field effects on viscosity and thermal conductivity of such molecules. A disentanglement of contributions arising from different types of polarization can reliably be performed only if more than one element of the viscosity or thermal conductivity tensor is determined. This requires experiments in external fields which can be oriented in different directions with respect to the apparatus. Such a procedure is difficult in practice when using electric fields but is rather simple when using magnetic fields. The magnetic field effect on thermal conductivity is investigated by Thijsse<sup>12</sup>). Results for the field effect on viscosity are presented in this chapter for a) simple (linear) molecules with an electric dipole moment (OCS, N<sub>2</sub>O, HCl and DCl), b) symmetric top molecules, with an electric dipole moment (CH<sub>3</sub>F, CHF<sub>3</sub>, PF<sub>3</sub>, NF<sub>3</sub>, NH<sub>3</sub>, ND<sub>3</sub>, PH<sub>3</sub> and AsH<sub>3</sub>) and c) molecules without electric dipole moment (SF<sub>6</sub> and CO<sub>2</sub>). Since the theoretical description of the magnetic field effects of molecules with a more complicated structure is slightly different from that of linear molecules, first a short outline of the theory of the viscomagnetic effect on both types of molecules is given in the next section.

2. *Theory.* The shear viscosity of a polyatomic gas in a magnetic field can be described by five independent coefficients<sup>4</sup>): three even-in-field coefficients  $\eta_0^+$ ,  $\eta_1^+$  and  $\eta_2^+$  and two odd-in-field coefficients  $\eta_1^-$  and  $\eta_2^-$ . The relation between this notation and the one of De Groot and Mazur<sup>13,14</sup>) is:  $\eta_0^+ = \eta_1$ ,  $\eta_1^+ = \eta_3$ ,  $\eta_2^+ = 2\eta_2 - \eta_1$ ,  $\eta_1^- = \eta_5$  and  $\eta_2^- = -\eta_4$ . In this thesis results for  $\eta_0^+$  and  $\eta_2^+$  are given.

A velocity gradient in a gas causes a deviation of the distribution function  $f$  from the equilibrium value  $f^{(0)}$ . For small deviations this is expressed by

$$f = f^{(0)} \left( 1 - \underline{\underline{B}} : \overline{\underline{v}v_0} \right) \quad (1)$$

where for polyatomic molecules

$$f^{(0)} = \left( \frac{m}{2\pi kT} \right)^{\frac{3}{2}} \frac{n}{Q} \exp \left\{ -W^2 - \frac{\mathcal{H}_{\text{rot}}}{kT} \right\} \quad (2)$$

with  $m$  the molecular mass,  $n$  the number density,  $Q$  the internal state partition function,  $\mathcal{H}_{\text{rot}}$  the rotational Hamiltonian of the molecule and  $\underline{W} = (m/2kT)^{\frac{1}{2}} (\underline{v} - \underline{v}_0)$  the reduced peculiar velocity. The quantity  $\overline{\underline{v}v_0}$  is the symmetric traceless part of the stream velocity gradient tensor. In order to determine the field dependence of the shear viscosity the distribution function  $f$  and thus the tensor of second rank,  $\underline{\underline{B}}$ , has to be known. This tensor can be calculated from the linearized Waldmann-Snyder equation<sup>5,6</sup>)

$$2 \overline{\underline{W} \underline{W}} = \mathcal{R} \underline{\underline{B}} - \frac{i}{\hbar} [\underline{\mu} \cdot \underline{H}, \underline{\underline{B}}], \quad (3a)$$

where  $\mathcal{R}$  is the collision (super)operator,  $\underline{H}$  is the magnetic field strength,  $\underline{\mu}$  the molecular magnetic dipole moment and  $\underline{\underline{B}}$  is given by

$$\underline{\underline{B}} = \underline{\underline{B}}(\underline{H}; \underline{W}, \underline{J}, J_z). \quad (3b)$$

Here,  $\underline{J}$  is the angular momentum and  $J_z$  its component along the figure axis.  $\underline{\underline{B}}$  is then expanded in terms of tensors with even parity which can be constructed from  $\underline{W}$ ,  $\underline{J}$  and  $J_z$ . Note that  $J_z$  has odd parity. The polarizations in  $\underline{J}$ -space are produced from the velocity polarization through torques acting on the molecules during collisions (in which the nonspherical part of the interaction potential is essential). The angular momentum dependent polarizations of even parity, which can be influenced by magnetic fields, can be denoted as far as their tensorial structure is concerned by  $\underline{J}$ ,  $\underline{J}\underline{J}$ ,  $\overline{\underline{W} \underline{W}} \underline{J}$ ,  $\overline{\underline{W} \underline{W}} \underline{J}\underline{J}$ ,  $\overline{\underline{W} \underline{W}} \underline{J}\underline{J}\underline{J}$ ,  $\underline{W} \underline{J} J_z$ ,  $\underline{W} \underline{J}\underline{J} J_z$ , etc. The simple polarization of type  $\underline{J}$  will be disregarded since it contributes to the effect only in fourth order of the off-diagonal effective cross-sections. The Waldmann-Snyder equation (eq. 3a)) has been solved both for linear and for symmetric top molecules<sup>6,15</sup>. The contributions to the viscosity coefficients arising from the various types of polarizations are given for linear molecules in section 2.1 and for symmetric tops in section 2.2.

**2.1 Linear molecules.** The rotational Hamiltonian in eq. (2) for linear molecules can be written as

$$\mathcal{H}_{\text{rot}} = \frac{\hbar^2}{2I_1} \underline{J}^2 \quad (4)$$

where  $I_1$  is the moment of inertia about the rotational axis perpendicular to the internuclear axis. For diamagnetic molecules the magnetic dipole moment is related to the molecular angular momentum by

$$\underline{\mu} = \mu_N g_1 \underline{J} \quad (5)$$

where  $\mu_N$  is the nuclear magneton,  $g_1 \equiv g$  is the rotational g-factor perpendicular to the internuclear axis and  $\underline{J}$  the angular momentum in units  $\hbar$ . In the presence of a magnetic field, the magnetic moments and thus the angular momenta precess around the field direction, which gives rise to a partial destruction of the angular momentum dependent polarizations. This, in turn, changes the velocity polarization, thus changing the viscosity.

At this point it is convenient to introduce for the polarizations the general notation  $[W]^{(p)} [J]^{(q)}$  where the symbol  $[ ]^{(k)}$  indicates the totally symmetric traceless tensor of rank  $k$ ; thus  $[J]^{(2)} = \overline{JJ}$ . Using the results of Coope and Snider<sup>4</sup>) and Eggermont *et al.*<sup>16</sup>) one can derive a general expression for the viscosity coefficients

$$\frac{\eta_{\mu}}{\eta(0)} = \frac{\eta^{[0]}}{\eta(0)} + (-1)^q \frac{\mathfrak{S}^2(20)}{\mathfrak{S}(20) \mathfrak{S}(pq)} \Omega(2,p,q) \sum_{\alpha,\beta} \binom{2 \ p \ q}{-\mu \ \alpha \ \beta}^2 \frac{1}{1 + i\beta\omega\tau_{pq}} \quad (6)$$

where  $\eta^{[0]}$  is the value of the viscosity coefficient when  $J$  polarizations are ignored (see eq. (13)),  $\eta(0)$  is the field free viscosity coefficient and

$$\Omega(j_1, j_2, j_3) = \frac{(J+1)! (J-2j_1)! (J-2j_2)! (J-2j_3)!}{(2j_1)! (2j_2)! (2j_3)!} \frac{3 - (-1)^J}{2} \quad (7)$$

with  $J = j_1 + j_2 + j_3$ . In eq. (6), the quantities  $\binom{2 \ p \ q}{-\mu \ \alpha \ \beta}$  are the well known 3j-symbols (see *e.g.* ref. 17), while

$$\omega = \frac{g \mu_N H}{\hbar} \quad \text{and} \quad \tau_{pq} = \frac{1}{n \langle v \rangle_0 \mathfrak{S}(pq)} \quad (8)$$

are precession frequency and the decay time for the  $[W]^{(p)} [J]^{(q)}$  polarization, respectively. Here  $n$  is the number density,  $\langle v \rangle_0 = \left(\frac{8kT}{\pi\mu}\right)^{1/2}$  the mean relative velocity, with  $\mu$  the reduced mass,  $\mathfrak{S}(20)$  and  $\mathfrak{S}(pq)$  are effective cross sections for the production and decay of the  $[W]^{(p)} [J]^{(q)}$  polarization, respectively, as defined in refs. 6 and 18. Using

$$\eta_{\mu} = \eta_{\mu}^{+} + i\eta_{\mu}^{-}$$

one finds for the even-in-field coefficients

$$\frac{\eta_{\mu}^{+} - \eta(0)}{\eta(0)} = -(-1)^q \frac{\mathfrak{S}^2(20)}{\mathfrak{S}(20) \mathfrak{S}(pq)} \Omega(2, p, q) \sum_{\alpha,\beta} \binom{2 \ p \ q}{-\mu \ \alpha \ \beta}^2 \frac{\beta^2 \omega^2 \tau_{pq}^2}{1 + \beta^2 \omega^2 \tau_{pq}^2}$$

$$\text{with } \mu = 0, 1, 2 \quad (9a)$$

and for the odd-in-field coefficients

$$\frac{\eta_{\mu}^{-}}{\eta(0)} = -(-1)^q \frac{\mathfrak{S}^2(pq)^{20}}{\mathfrak{S}(20) \mathfrak{S}(pq)} \Omega(2,p,q) \sum_{\alpha, \beta} \binom{2p}{-\mu \quad \alpha \quad \beta}^2 \frac{\beta \omega \tau_{pq}}{1 + \beta^2 \omega^2 \tau_{pq}^2}$$

with  $\mu = 1, 2.$  (9b)

Using the above expressions, the contributions to the viscosity coefficients arising from the polarizations of tensorial type  $\overline{JJ}$ ,  $\overline{WW}J$ ,  $\overline{WW} \overline{JJ}$  and  $\overline{WW} \overline{JJJ}$  can be written as

$\overline{JJ}$	$\overline{WW}J$	$\overline{WW} \overline{JJ}$	$\overline{WW} \overline{JJJ}$	
$\frac{\eta_0^+ - \eta(0)}{\eta(0)} =$	$+\frac{6}{4} \Psi_{2,1} f(\xi_{2,1})$	$-\frac{1}{24} \Psi_{2,2} \{2f(\xi_{2,2}) + 8g(2\xi_{2,2})\}$	$+\frac{1}{10} \Psi_{2,3} \{4f(\xi_{2,3}) + 10g(2\xi_{2,3})\}$	
$\frac{\eta_1^+ - \eta(0)}{\eta(0)} = -\Psi_{0,2} f(\xi_{0,2})$	$+\frac{5}{4} \Psi_{2,1} f(\xi_{2,1})$	$-\frac{1}{24} \Psi_{2,2} \{7f(\xi_{2,2}) + 6g(2\xi_{2,2})\}$	$+\frac{1}{10} \Psi_{2,3} \{5f(\xi_{2,3}) + 5g(3\xi_{2,3})\}$	
$\frac{\eta_2^+ - \eta(0)}{\eta(0)} =$	$-\Psi_{0,2} f(2\xi_{0,2})$	$+\frac{2}{4} \Psi_{2,1} f(\xi_{2,1})$	$-\frac{1}{24} \Psi_{2,2} \{6f(\xi_{2,2}) + 4g(2\xi_{2,2})\}$	$+\frac{1}{10} \Psi_{2,3} \{3f(\xi_{2,3}) + 5f(2\xi_{2,3}) + 5g(3\xi_{2,3})\}$
$\frac{\eta_1^-}{\eta(0)} = -\Psi_{0,2} g(\xi_{0,2})$	$+\frac{1}{4} \Psi_{2,1} g(\xi_{2,1})$	$-\frac{1}{24} \Psi_{2,2} \{-5g(\xi_{2,2}) + 6g(2\xi_{2,2})\}$	$+\frac{1}{10} \Psi_{2,3} \{-g(\xi_{2,3}) + 5g(3\xi_{2,3})\}$	
$\frac{\eta_2^-}{\eta(0)} =$	$-\Psi_{0,2} g(2\xi_{0,2})$	$+\frac{2}{4} \Psi_{2,1} g(\xi_{2,1})$	$-\frac{1}{24} \Psi_{2,2} \{6g(\xi_{2,2}) + 4g(2\xi_{2,2})\}$	$+\frac{1}{10} \Psi_{2,3} \{3g(\xi_{2,3}) + 5g(2\xi_{2,3}) + 5g(3\xi_{2,3})\}$

(10)

where

$$f(m\xi) = \frac{(m\xi)^2}{1 + (m\xi)^2} \quad \text{and} \quad g(m\xi) = \frac{m\xi}{1 + (m\xi)^2} \quad (11)$$

with  $m = 0, 1, 2, 3$  and

$$\xi_{pq} = \omega \tau_{pq} = \frac{g_L \mu_N kT}{\hbar \langle v \rangle_0 \mathfrak{S}(pq)} \frac{H}{p} \quad (12)$$

with  $p$  the pressure. The field free viscosity coefficient,  $\eta(0)$ , is related to the cross section describing the decay of the velocity polarization,  $\mathfrak{S}(20)$ , by

$$\eta(0) \approx \eta[0] = \frac{kT}{\langle v \rangle_0 \mathfrak{S}(20)} \quad (13)$$



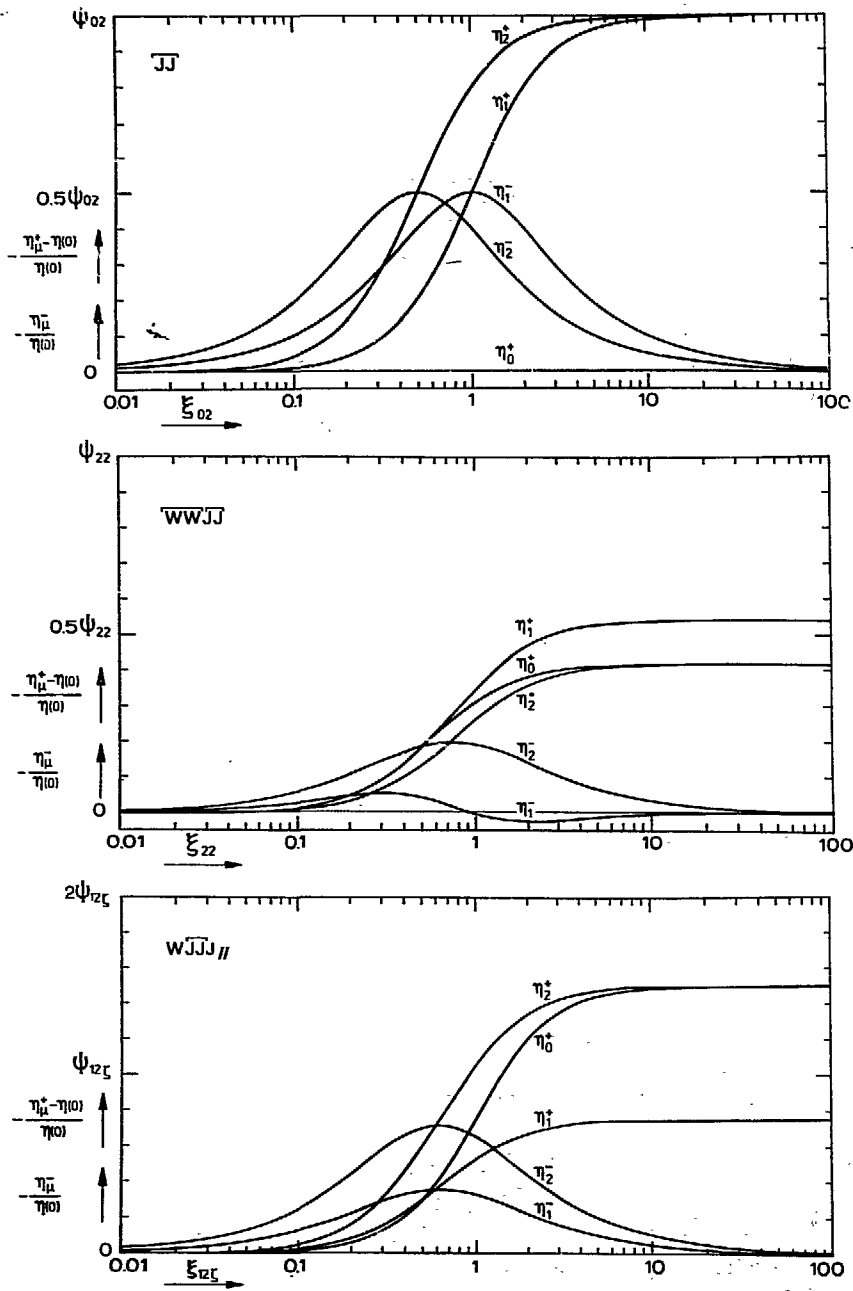


Fig. 1a The contributions of three even-in- $J$  polarizations to  $-\frac{\eta_{\mu}^{+} - \eta(0)}{\eta(0)}$  (for  $\mu = 0, 1, 2$ ) and  $-\frac{\eta_{\mu}^{-}}{\eta(0)}$  (for  $\mu = 1, 2$ ). The field parameter  $\xi_{pq} = \omega r_{pq}$  is proportional to  $H/p$  (see eq. (12)).

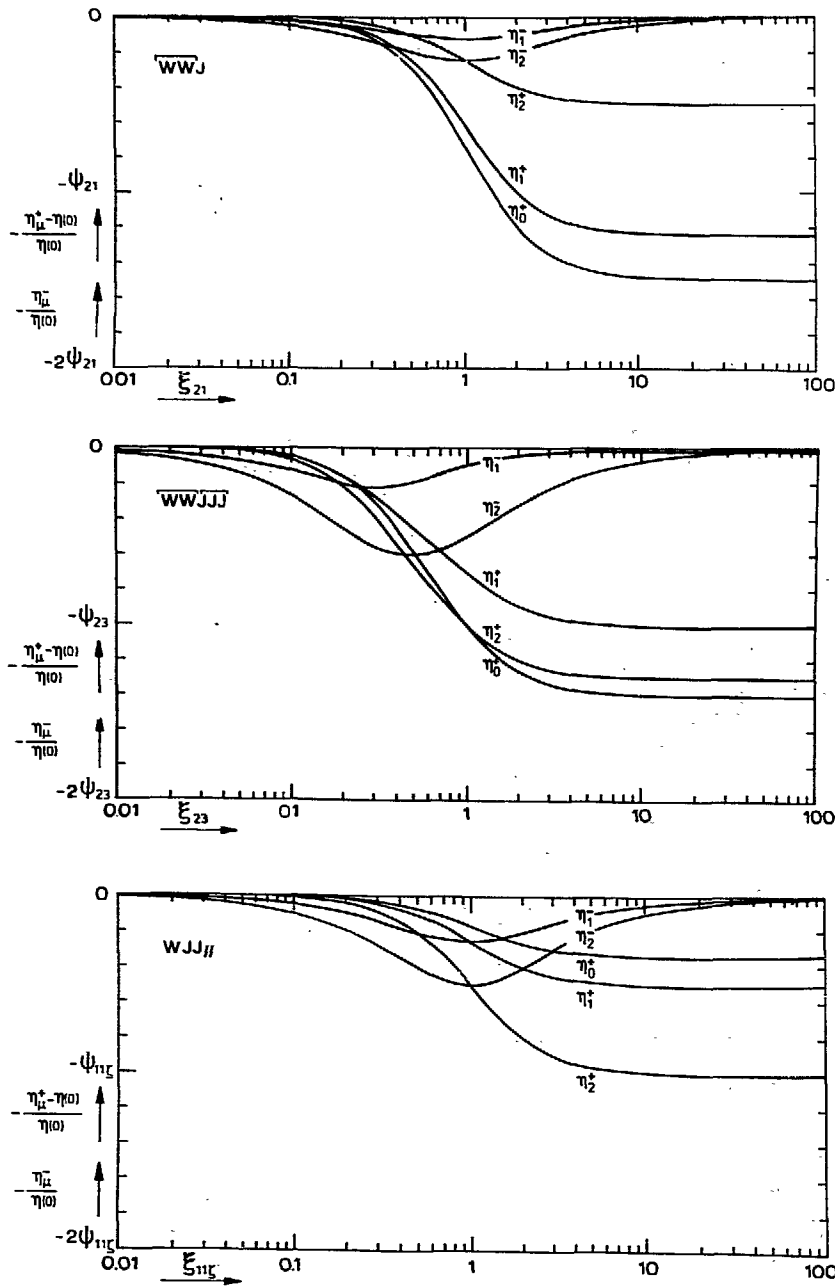


Fig. 1b The contributions of three odd-in- $J$  polarizations to  $-\frac{\eta_\mu^+ - \eta(0)}{\eta(0)}$  (for  $\mu = 0, 1, 2$ ) and  $-\frac{\eta_\mu^-}{\eta(0)}$  (for  $\mu = 1, 2$ ). The field parameter  $\xi_{pq} = \omega\tau_{pq}$  is proportional to  $H/p$  (see eq. (12)).

The positive quantities  $\Psi_{pq}$  in eqs. (10) determine the magnitude of the viscosity change arising from the various polarizations. They are given by

$$\Psi_{pq} = \frac{\mathfrak{S}_{(pq)}^{20}}{\mathfrak{S}(20) \cdot \mathfrak{S}(pq)} \quad (14)$$

In earlier experiments the quantities  $\Psi_{21}$ ,  $\Psi_{22}$  and  $\Psi_{23}$  were found to be very small for linear molecules such as  $N_2$ ,  $CO$ ,  $H_2$ ,  $HD$ ,  $D_2$  (see refs. 7, 8), the  $\overline{J\overline{J}}$ -polarization being far dominant in such molecules. In fig. 1 the relative viscosity changes corresponding to eqs. (10) are given as a function of the field parameter  $\xi_{pq} = \omega\tau_{pq}$ . It should still be noted that the field parameter  $\xi_{pq}$  is assumed to be independent of the quantum mechanical state of the molecules. For linear molecules, the precession frequency is indeed independent of the rotational state. The assumption that the decay of polarization can be described with one  $\tau_{pq}$  or one effective relaxation time is generally not quite true as was shown in experiments on Depolarized Rayleigh scattering<sup>19</sup>). In fact, the reorientation efficiency for angular momentum depends on the rotational state of the molecules. However, it was found that for heavier molecules, transfer of polarization between different rotational states limits the spread in time scales, and a description with one effective time scale is quite good. Consequently, for the linear molecules studied here, single parameter curves for each type of polarization as given by eqs. (10) can be expected.

**2.2 Symmetric top molecules.** For symmetric top molecules, the non-equilibrium distribution function also depends on the pseudo-scalar  $J_I$ , which has the same parity and time reversal properties as  $\underline{W}$  (see eq. (3)). The lowest order terms containing  $J_I$  are found to be  $\underline{W\overline{J}J_I}$  and  $\underline{W\overline{J\overline{J}}J_I^{20}}$ . It should be noted that the presence of  $J_I$  in the term  $\underline{W\overline{J}J_I}$  does not change its odd-in- $\underline{J}$  behaviour. The resulting scheme for the contributions from the various polarizations is given in Table I. The symbols used are defined in eqs. (11) through (14) while the quantities related to the two polarizations involving  $J_I$  are labeled with the extra index  $\zeta$ , e.g.,  $\mathfrak{S}(11\zeta)$  describes the decay of the  $\underline{W\overline{J}J_I}$  polarization, and  $\Psi_{11\zeta}$  describes the magnitude of the viscosity change from that polarization.

The expressions in table I are valid when the parameter  $\xi_{pq} = \omega\tau_{pq}$  is independent of the rotational (J, K)-state of the individual molecules. The spread in collision times  $\tau_{pq}$  will be neglected here. Assuming the same argument as given for linear molecules to be valid here, a state averaged cross section  $\mathfrak{S}(pq)$  is used. In section 6.1 we will come back to this point. However, the spread in precession frequencies  $\omega$  cannot be neglected for symmetric top molecules. This spread will now be discussed.

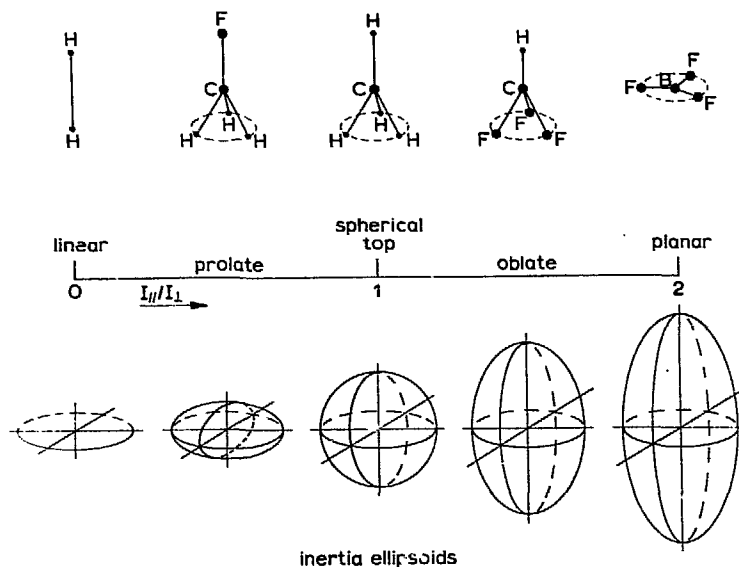


Fig. 2 The moments of inertia  $I_{\parallel}$  and  $I_{\perp}$  for various symmetric top molecules

The rotational Hamiltonian for symmetric top molecules can be written as

$$\mathcal{H}_{\text{rot}} = \frac{\hbar^2}{2I_{\perp}} J^2 + \frac{\hbar^2}{2I_{\parallel}} \left(1 - \frac{I_{\parallel}}{I_{\perp}}\right) J_z^2 \quad (15)$$

where  $I_{\perp}$  and  $I_{\parallel}$  are the moments of inertia perpendicular and parallel to the figure axis. The values of  $I_{\parallel}/I_{\perp}$  for various types of molecules are summarized schematically in fig. 2. For a symmetric top molecule the directions of the magnetic moment and the angular momentum generally do not coincide (fig. 3), the rotational  $g$ -value being anisotropic:

$$\underline{\mu} = \mu_N \underline{g} \cdot \underline{J} \quad (16)$$

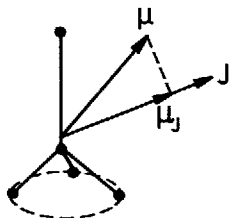


Fig. 3 The magnetic moment  $\underline{\mu}$  and its component along the direction of the angular momentum  $\underline{J}$  for a symmetric top molecule.

Table I. The contributions to the viscosity coefficients from various polarizations

$\overline{II}$	$\overline{WW} I$	$\overline{WW} \overline{II}$	$\overline{WW} \overline{III}$	$\overline{W} I J_r$	$\overline{W} \overline{II} J_r$	
$\frac{\eta_0^+ - \eta(0)}{\eta(0)} =$	$+\frac{6}{4}\Psi_{21}f(\xi_{21})$	$-\frac{1}{24}\Psi_{22}\{2f(\xi_{22}) + 8f(2\xi_{22})\}$	$+\frac{1}{10}\Psi_{23}\{4f(\xi_{23}) + 10f(2\xi_{23})\}$	$+\frac{2}{6}\Psi_{11}f(\xi_{11})$	$-\frac{1}{4}\Psi_{12}f(6f(\xi_{12}))$	
$\frac{\eta_1^+ - \eta(0)}{\eta(0)} = -\Psi_{02}f(\xi_{02})$	$+\frac{5}{4}\Psi_{21}f(\xi_{21})$	$-\frac{1}{24}\Psi_{22}\{7f(\xi_{22}) + 6f(2\xi_{22})\}$	$+\frac{1}{10}\Psi_{23}\{5f(\xi_{23}) + 5f(3\xi_{23})\}$	$+\frac{3}{6}\Psi_{11}f(\xi_{11})$	$-\frac{1}{4}\Psi_{12}\{f(\xi_{12}) + 2f(2\xi_{12})\}$	
$\frac{\eta_2^+ - \eta(0)}{\eta(0)} =$	$-\Psi_{02}f(2\xi_{02})$	$+\frac{2}{4}\Psi_{21}f(\xi_{21})$	$-\frac{1}{24}\Psi_{22}\{6f(\xi_{22}) + 4f(2\xi_{22})\}$	$+\frac{1}{10}\Psi_{23}\{3f(\xi_{23}) + 5f(2\xi_{23}) + 5f(3\xi_{23})\}$	$+\frac{6}{6}\Psi_{11}f(\xi_{11})$	$-\frac{1}{4}\Psi_{12}\{2f(\xi_{12}) + 4f(2\xi_{12})\}$
$\frac{\eta_1^-}{\eta(0)} = -\Psi_{02}g(\xi_{02})$	$+\frac{1}{4}\Psi_{21}g(\xi_{21})$	$-\frac{1}{24}\Psi_{22}\{-5g(\xi_{22}) + 6g(2\xi_{22})\}$	$+\frac{1}{10}\Psi_{23}\{-g(\xi_{23}) + 5g(3\xi_{23})\}$	$+\frac{3}{6}\Psi_{11}g(\xi_{11})$	$-\frac{1}{4}\Psi_{12}\{g(\xi_{12}) + 2g(2\xi_{12})\}$	
$\frac{\eta_2^-}{\eta(0)} =$	$-\Psi_{02}g(2\xi_{02})$	$+\frac{2}{4}\Psi_{21}g(\xi_{21})$	$-\frac{1}{24}\Psi_{22}\{6g(\xi_{22}) + 4g(2\xi_{22})\}$	$+\frac{1}{10}\Psi_{23}\{3g(\xi_{23}) + 5g(2\xi_{23}) + 5g(3\xi_{23})\}$	$+\frac{6}{6}\Psi_{11}g(\xi_{11})$	$-\frac{1}{4}\Psi_{12}\{2g(\xi_{12}) + 4g(2\xi_{12})\}$

Table II. Moments of inertia and rotational g-factors parallel and perpendicular to the figure axis

	$\frac{I^2}{2I_1k}$	$g = g_1$		$\frac{I^2}{2I_1k}$	$\frac{I_2}{I_1}$	$g_1$	$g_2$	$\frac{g_2 - g_1}{g_1}$	$\langle g \rangle_0$
	(K)			(K)					
CO <sub>2</sub>	0.56	-0.0551 <sup>23)</sup>	CH <sub>2</sub> F	1.2	0.166 <sup>29)</sup>	-0.062	+0.265 <sup>36)</sup>	-5.27	[-0.017]
OCS	0.29	-0.0287 <sup>24)</sup>	CHF <sub>3</sub>	0.50	1.83 <sup>30)</sup>	-0.0359	(-0.031) <sup>37)</sup>	-0.14	-0.034
N <sub>2</sub> O	0.60	-0.0761 <sup>25)</sup>	PF <sub>3</sub>	0.38	1.61 <sup>31)</sup>	-0.0659	-0.081 <sup>38)</sup>	+0.24	-0.072
HCl	15.0	+0.4594 <sup>26)</sup>	NF <sub>3</sub>	0.51	1.83 <sup>32)</sup>	-0.060	(-0.081 <sup>38)</sup>	+0.36	-0.069
DCl	7.8	—	PH <sub>3</sub> <sup>*</sup>	6.4	1.13 <sup>33)</sup>	-0.033	+0.017 <sup>39)</sup>	-1.52	[-0.017]
SF <sub>6</sub>	0.13	—	AsH <sub>3</sub>	5.4	1.00 <sup>34)</sup>	—	—	—	—
CH <sub>4</sub>	—	+0.3133 <sup>27)</sup>	NH <sub>3</sub>	14.3	1.57 <sup>35)</sup>	+0.563	+0.500 <sup>40)</sup>	-0.11	+0.538
CF <sub>4</sub>	—	-0.031 <sup>28)</sup>	ND <sub>3</sub>	7.4	1.63 <sup>35)</sup>	—	(+0.25)	—	—

Numbers between parentheses ( ) are estimated values.

\*One should note that the signs of  $g_1$  and  $g_2$  are not quite certain as is pointed out in ref. 39.

The second rank tensor  $\underline{g}$  can be written as

$$\underline{g} = g_l \underline{U} + (g_l - g_l) \underline{u} \underline{u} \quad (17)$$

where  $\underline{U}$  is the unit second rank tensor and  $\underline{u}$  is a unit vector along the figure axis. The subscripts refer to directions with respect to the figure axis. For the precession of the molecule around an external field direction only the magnetic moment  $\underline{\mu}_J$  along the direction of  $\underline{J}$  is of importance:

$$\underline{\mu}_J = \mu_N g \underline{J} \quad (18)$$

where

$$g = g_l \left[ 1 + \frac{g_l - g_l}{g_l} \frac{K^2}{J(J+1)} \right] \quad (19)$$

In the notation used here,  $\underline{J}$  and  $J_l$  represent operators, while  $J$  and  $K$  represent the corresponding quantum numbers. It follows from eq. (19) that for a symmetric top molecule the precession frequency of the molecular angular momentum around the field direction depends on its rotational ( $J, K$ )-state. The field dependence of the viscosity can now be described by a weighted sum of contributions of molecules with different precession frequencies<sup>6,15,21</sup>. If we only retain the polarizations that make important contributions to the viscomagnetic effect of the molecules under consideration, the expressions for the even-in-field coefficients are given by

$$\frac{\eta_0^+ - \eta(0)}{\eta(0)} = -\frac{6}{4} \Psi_{21} \langle f(\xi_{21}) \rangle_{av} \quad (20a)$$

$$\frac{\eta_1^+ - \eta(0)}{\eta(0)} = +\Psi_{02} \langle f(\xi_{02}) \rangle_{av} - \frac{5}{4} \Psi_{21} \langle f(\xi_{21}) \rangle_{av} \quad (20b)$$

$$\frac{\eta_2^+ - \eta(0)}{\eta(0)} = +\Psi_{02} \langle f(2\xi_{02}) \rangle_{av} - \frac{2}{4} \Psi_{21} \langle f(\xi_{21}) \rangle_{av} \quad (20c)$$

where

$$\xi_{pq} = \frac{g_l \mu_N kT}{\hbar \langle v \rangle_0 \mathcal{G}(pq)} \frac{H}{p} \left( 1 + \frac{g_l - g_l}{g_l} \frac{K^2}{J(J+1)} \right) \quad (21)$$

and the symbol  $\langle f(\xi_{pq}) \rangle_{av}$  represents an average of the field functions over the different  $J$  and  $K$  values (cf. eqs. (22) and (24)). Note that the averaged field functions  $\langle f(m \xi_{pq}) \rangle_{av}$  depend not only on  $g_{\parallel}$  and  $g_{\perp}$  but, through the averaging also on  $I_{\parallel}$  and  $I_{\perp}$ . When  $\xi_{pq}$  does not depend on  $K$  and  $J$  eqs. (20) reduce to the corresponding parts of eqs. (10). This is the case a) if only the value  $K=0$  is allowed (linear molecules) and b) if  $g_{\parallel} = g_{\perp}$  (e.g.,  $SF_6$ ). The actual form of the averaged field functions  $\langle f(m \xi_{pq}) \rangle_{av}$  depends on the precise form (normalization) of the angular momentum dependent part of the polarizations.

Theoretically, there has been a discussion over the last few years as to the precise form of the polarizations, especially on the polynomial  $R(J^2)$  of polarization  $\overline{J \cdot J} R(J^2)$ . We will treat here two possible choices:

- a) Starting from considerations involving the intermolecular potential one is tempted to try an analysis on the basis of the angular momentum in terms of its direction only, *i.e.*, essentially  $\underline{J}/|\underline{J}|$ . In this case, one has for the angular momentum tensor- and vector-polarizations

$$\frac{\overline{J \cdot J}}{(\overline{J \cdot J} : \overline{J \cdot J})^{1/2}} \quad \text{and} \quad \frac{\underline{J}}{(J^2)^{1/2}},$$

respectively. The average of the field functions takes the form

$$\langle f(m \xi_{pq}) \rangle_{av} = \left\langle \frac{(m \xi_{pq})^2}{1 + (m \xi_{pq})^2} \right\rangle_0 \quad (22)$$

with the equilibrium average  $\langle \rangle_0$  given by

$$\langle A(K, J) \rangle_0 = \frac{\sum_{J=0}^{\infty} \sum_{K=-J}^{+J} A(K, J) (2J+1) \exp \left[ -\frac{\hbar^2}{2I_{\parallel} kT} \{J(J+1) + (\frac{I_{\perp}}{I_{\parallel}} - 1) K^2\} \right]}{\sum_{J=0}^{\infty} \sum_{K=-J}^{+J} (2J+1) \exp \left[ -\frac{\hbar^2}{2I_{\parallel} kT} \{J(J+1) + (\frac{I_{\perp}}{I_{\parallel}} - 1) K^2\} \right]} \quad (23)$$

- b) When a Chapman-Enskog procedure is followed, where  $\underline{J}$  is treated analogous to  $\underline{W}$ , magnitude as well as direction have to be considered. In this case the theoretical expression for the average of the field functions is given by<sup>22</sup>,

$$\langle f(m \xi_{pq}) \rangle_{av} = \frac{1}{\langle [\underline{J}]^{(q)} \circ^q [\underline{J}]^{(q)} \rangle_0} \langle [\underline{J}]^{(q)} \circ^q [\underline{J}]^{(q)} \frac{(m \xi_{pq})^2}{1 + (m \xi_{pq})^2} \rangle_0, \quad (24)$$

where  $\circ^q$  indicates a  $q$ -fold contraction.

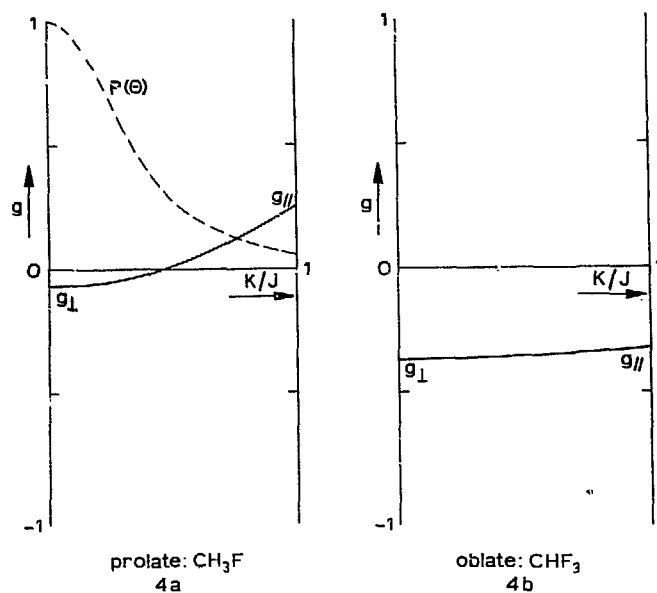


Fig. 4 The rotational  $g$ -factor as a function of  $K/J = \cos \theta$  (classical limit).  
 a. the prolate symmetric top molecule  $\text{CH}_3\text{F}$ .  
 b. the oblate symmetric top molecule  $\text{CHF}_3$ .  
 The dotted line in fig. 4a represents the probability distribution  $P(\theta)$  (see eq. (26)).

We will now assess the spread in field functions resulting from the averaging over different  $(J, K)$ -states. First, the dependence of  $g$  on  $J$  and  $K$  is of importance. In fig. 4 the value of  $g$  is given in the classical limit as a function of  $K/J$  for two typical cases. For the oblate symmetric tops  $\text{CHF}_3$  or  $\text{NH}_3$ , one has typically (see table II) that  $g_{\parallel}$  and  $g_{\perp}$  have the same sign and roughly the same magnitude. For these molecules  $|\frac{g_{\parallel} - g_{\perp}}{g_{\perp}}| \ll 1$  so that the spread in  $g$ -values is rather small as illustrated in fig. 4b. For the prolate symmetric top  $\text{CH}_3\text{F}$ , on the other hand,  $g_{\parallel}$  and  $g_{\perp}$  have opposite signs while  $|g_{\parallel}| > |g_{\perp}|$ . As illustrated in fig. 4a this gives a large variation of  $g$ -values, some molecules having  $g$ -values close to zero and thus requiring extremely large fields to precess sufficiently fast. However, even in this case no large spread of field functions should be expected since for strongly prolate molecules only the lowest  $K$ -values are appreciably populated. In the classical limit this can be easily illustrated. Replacing the sums in eq. (22) by integrations one has



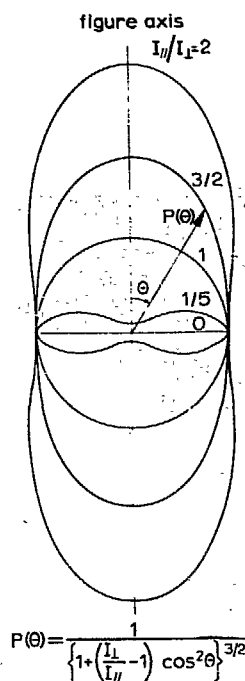


Fig. 5 The probability distribution for the orientation of the angular momentum  $\underline{I}$  with respect to the figure axis for various values of  $I_{//}/I_T$  in a polar diagram. For clearness of representation the curves have been scaled to the same value at  $\theta = \pi/2$ .

$$\frac{1}{Q} \int_{-1}^{+1} \int_0^{\infty} \exp \left[ -\frac{\hbar^2}{2I_T kT} \left\{ 1 + \left( \frac{I_{//}}{I_T} - 1 \right) \cos^2 \theta \right\} J^2 \right] \frac{\{m \xi_{pq}(\cos \theta)\}^2}{1 + \{m \xi_{pq}(\cos \theta)\}^2} J^2 dJ d\left(\frac{K}{J}\right) =$$

$$2 \sqrt{\frac{I_T}{I_T}} \int_{-1}^{+1} P(\theta) \frac{\{m \xi_{pq}(\cos \theta)\}^2}{1 + \{m \xi_{pq}(\cos \theta)\}^2} d(\cos \theta) \quad (25)$$

with

$$P(\theta) = \frac{1}{\left\{ 1 + \left( \frac{I_{//}}{I_T} - 1 \right) \cos^2 \theta \right\}^{3/2}} \quad (26)$$

where  $\cos \theta = K/J$  and  $\xi_{pq}$  depends on  $\cos \theta$  only (see eq. (21)). In fig. 5 the weight factor  $P(\theta)$  is plotted. The same procedure applied to the average of eq. (24) yields a weight factor similar to eq. (26), only with  $3/2$  replaced by  $3/2 + q$ . In this case even more weight is given to the low  $K/J = \cos \theta$  values. One should realize that these

expressions with  $P(\theta)$  serve only as an illustration of the effect of the different weightings. For some of the molecules considered here the number of K-states involved is not high enough to replace the summation over the quantum states by an integral.

In conclusion one can say that in most cases investigated, no appreciable broadening of the experimental curves should be expected. This simplifies the analysis for most of the symmetric top molecules under investigation, because the field function averages of eqs. (22) or (24) can be approximated by

$$\langle f(\eta, \xi_{pq}) \rangle_{av} \approx f(\eta, \langle \xi_{pq} \rangle_0). \quad (27)$$

The result is that a simple behaviour of the form of eqs. (10) can be expected with the field parameter  $\xi_{pq}$  replaced by an average value  $\langle \xi_{pq} \rangle_0$ . A clear exception is  $\text{PH}_3$  which can be expected to show a large broadening, since it is nearly a spherical top while its values for  $g_l$  and  $g_s$  have opposite signs. Unfortunately, the viscomagnetic effect for this gas was found to be too small to be investigated.

**3. Experimental method.** Since the molecules of interest here, such as the symmetric top molecules, tend to have very small magnetic moments (or rotational g-factors), very high magnetic fields are necessary in order to achieve molecular precession frequencies high enough so as to compete with the collision frequency. In the experiments a superconducting magnet was employed, giving fields up to 75 kOe in a 10 cm room temperature bore (homogeneity 99%). The fact that the axial field is fixed in the vertical direction, puts some limitations on the design of the experimental set up if one wishes to determine more than one element of the viscosity tensor. In the present apparatus, two even-in-field coefficients,  $\eta_0^+$  and  $\eta_2^+$ , can be determined by using four identical capillaries with rectangular cross section (thickness  $t = 0.1$  cm, width  $w = 1$  cm, length  $l = 7$  cm), arranged in a Wheatstone bridge circuit as shown in fig. 6. The arrangement is such that either the lower pair of capillaries  $c_1$  and  $c_4$  are in the field center (position I of the apparatus) or the top pair of capillaries  $c_2$  and  $c_3$  (position II of the apparatus). The orientation of the capillaries is indicated in fig. 7. According to ref. 41 the field-induced unbalance of the bridge is now related to changes in the viscosity by

$$2 \frac{\delta p}{\Delta p} = - \frac{\eta_2^+ - \eta(0)}{\eta(0)} \quad (\text{position I}) \quad (28a)$$

and

$$2 \frac{\delta p}{\Delta p} = - \frac{\frac{1}{4}\eta_2^+ + \frac{3}{4}\eta_0^+ - \eta(0)}{\eta(0)} \quad (\text{position II}) \quad (28b)$$

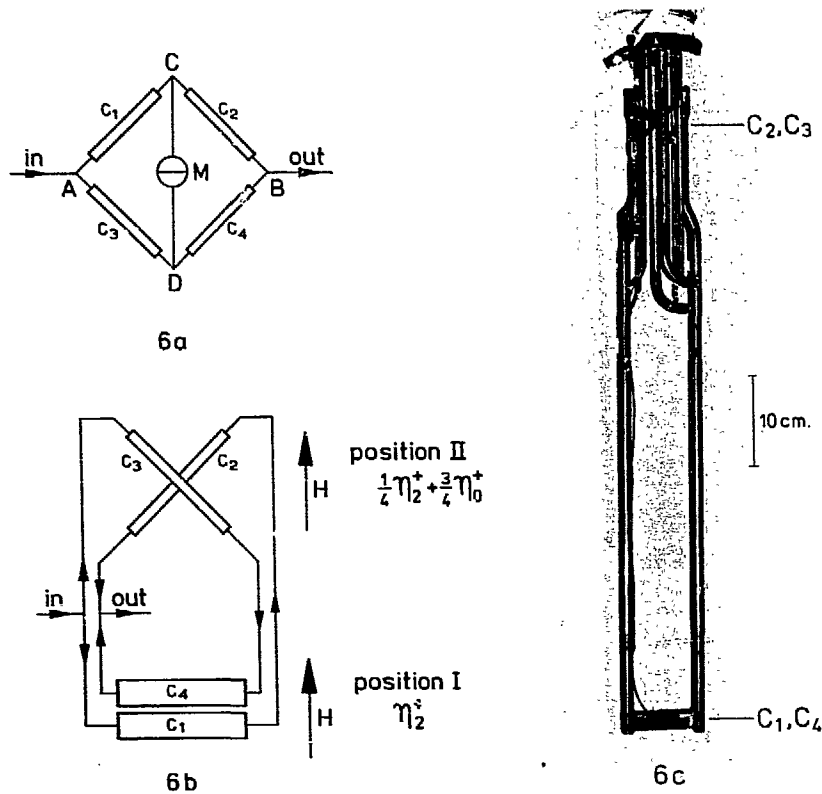


Fig. 6 a. Schematic diagram of the Wheatstone bridge.  
 b. The arrangement of the capillaries in the apparatus.  
 c. Photograph of the apparatus with vacuum jacket removed.

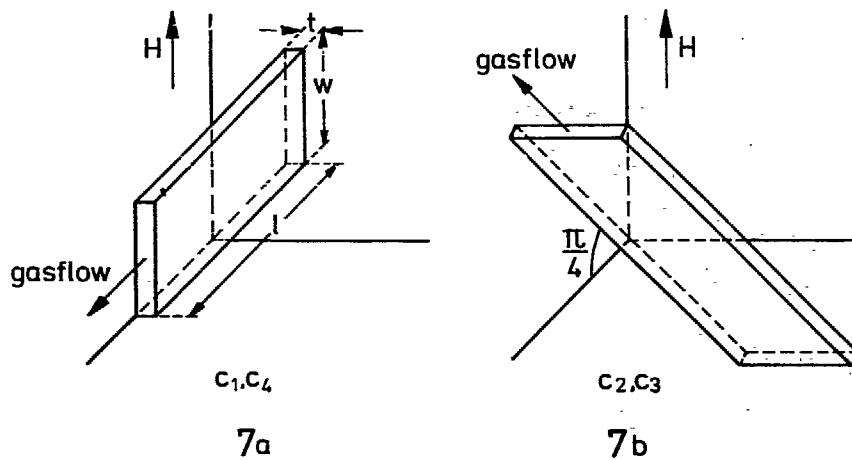


Fig. 7 The orientation of the capillaries with respect to the magnetic field;  
 a. capillaries  $c_1$  and  $c_4$  (cf. arrangement II in scheme II of ref. 41).  
 b. capillaries  $c_2$  and  $c_3$  (cf. arrangement I in scheme II of ref. 41).

where  $\delta p$  is the pressure difference between points C and D of the bridge (see fig. 6a),  $\Delta p$  is the pressure difference between the entrance and the exit of the bridge. The unbalance of the bridge,  $\delta p$ , is detected by a high-sensitivity differential manometer M (sensitivity of  $10^{-5}$  torr). From the experimental results in the positions I and II it is possible to determine  $\eta_2^+$  and  $\eta_0^+$  separately; this last viscosity coefficient is of special interest because a polarization of type  $\overline{[I]}$  does for tensorial reasons not contribute to  $\eta_0^+$  (see eq. (10)) while it is usually the dominant contribution to  $\eta_1^+$  and  $\eta_2^+$ .

In order to test the apparatus, experiments on HD and He have been performed. The results for HD were found to agree within the experimental error with those of Hulsman *et al.*<sup>7)</sup> As should be expected, for He no effect could be detected.

4. Corrections. 4.1 Presence of short sides. In the foregoing section eqs. (28a) and (28b) have been based on the assumption that the capillaries consist of two infinitely wide parallel plates placed at a small distance. Between such plates a second derivative of the flow velocity exists; however, since in the experimental set up the plates have a finite width, also a Poiseuille profile is build up between the short sides giving rise to a – be it small – second derivative of the flow velocity. This causes a correction on eqs. (28a) and (28b); following Hulsman *et al.*<sup>7)</sup> one finds for our set up

$$2 \frac{\delta p}{\Delta p} f = - \frac{\eta_2^+ - \eta(0)}{\eta(0)} (1 - \epsilon) - \frac{\eta_1^+ - \eta(0)}{\eta(0)} \epsilon \quad \text{in position I} \quad (29a)$$

and

$$2 \frac{\delta p}{\Delta p} f = - \frac{1/4 \eta_2^+ + 3/4 \eta_0^+ - \eta(0)}{\eta(0)} (1 - \epsilon) - \frac{1/2 \eta_1^+ + 1/2 \eta_2^+ - \eta(0)}{\eta(0)} \epsilon \quad \text{in position II,} \quad (29b)$$

where  $\epsilon = 1/2 \times 0.630 \frac{t}{w}$ . With  $t/w = 0.1$  in the apparatus we have  $\epsilon = 0.0315$ . The quantity  $f$  is a correction factor which is discussed in the next section.

4.2 Deviations from the ideal Poiseuille flow. The correction factor  $f$  appearing in eqs. (29a) and (29b) takes into account the deviations from the ideal Poiseuille flow and the Knudsen effect on the viscosity changes. Following refs. 7 and 8 it is given by

$$f = \left[ \frac{2(p_C + K_\alpha)}{(p_A + K_\alpha) + (p_B + K_\alpha)} \right] \left[ 1 + \frac{1}{20} (m + 1/2 \ln \frac{p_A}{p_B}) \frac{1}{\ell} \text{Re} \right] \left[ 1 + \frac{K_\beta}{p} \right] \quad (30)$$

The indices A, B and C indicate different points of the bridge (see fig. 6). The numbers  $K_\alpha$  and  $K_\beta$  describe Knudsen corrections and are discussed below. The quantity  $m$  depends on the shape of the entrance of the capillary and is assumed to be 0.75 in accordance to ref. 7,  $l$  is the length of the capillary and  $Re$  is Reynolds number equal to  $2G/w\eta(0)$ , where  $G$  is the mass flow per unit time through the bridge. The first factor in eq. (30), taking into account the expansion of the gas, is always between 1 and 1.03. The second factor arises from pressure losses caused by the acceleration of the gas at both the entrance of the capillary and in the capillary itself and is extensively discussed in refs. 7 and 8. This factor is always between 1 and 1.01.

The third factor,  $[1 + K_\beta/p]$ , is the Knudsen correction on the magnitude of the effect ( $p$  is the mean pressure in the bridge); this factor was usually between 1 and 1.3 and did not exceed 1.6 at the lowest pressures. Also on the position of the effect a Knudsen correction was applied in the familiar way<sup>7,8</sup>) using a reduction factor  $(1 + K_\gamma/p)^{-1}$ . This factor was not smaller than 0.85. The quantities  $K_\beta$  and  $K_\gamma$  (see table III) are determined experimentally in the usual way by plotting the uncorrected experimental data versus  $1/p$  and extrapolating to  $1/p=0$ . Following Hulsman *et al.*<sup>7</sup>) Knudsen numbers  $n_\beta$  and  $n_\gamma$  are introduced defined by  $K_{\beta,\gamma} = n_{\beta,\gamma} p\xi/t$  where the quantity  $\xi$  is a mean free path defined by  $\xi = \frac{4}{5} \frac{\eta}{p} \sqrt{\frac{8kT}{\pi m}}$ , where  $m$  is the molecular mass. This definition is in agreement with the definition used in refs. 7 and 8. Similarly the Knudsen correction on the field free flow,  $K_\alpha$ , can be written as  $K_\alpha = n_\alpha p\xi/t$ . For all gases it is found that  $n_\alpha = 6$  in accordance with ref. 7. The values for  $n_\beta$  and  $n_\gamma$  found for the various gases are presented in table III. Within the experimental accuracy these values are independent of the type of field effect (positions I and II) and in agreement with those obtained in refs. 7 and 8.

**4.3 Stray fields.** Since the top and bottom capillaries are 60 cm apart (see fig. 6c) the field strength at the out-of-field capillaries was found to be only 1% of the field at the in-field capillaries. The correction for this stray field effect depends on the  $H/p$ -region studied, being 1.5% at most. Also a correction for the influence of the magnetic field on the flow resistance in the gas leads is applied. This correction is small (less than 3%) since the leads are rather wide (1 cm diameter).

**5. Experimental results. 5.1 General.** Experiments were performed at 293 K on the linear molecules  $CO_2$ ,  $OCS$ ,  $N_2O$ ,  $HCl$ ,  $DCl$ , on the symmetric top molecules  $CH_3F$ ,  $CHF_3$ ,  $PF_3$ ,  $NF_3$ ,  $NH_3$ ,  $ND_3$ ,  $PH_3$ ,  $AsH_3$  and on the regular octahedral molecule  $SF_6$ . These gases have been obtained commercially and their purities are given in table IV. No detectable effects were observed for  $HCl$  and  $DCl$  in the  $H/p$  range up to about 65 kOe/torr, sufficient to be near saturation. This puts an upper limit of approximately  $2 \times 10^{-5}$  to the relative viscosity change for these gases. For  $AsH_3$  no

Table III. Knudsen correction parameters

	$K_\beta$ (torr)	$K_\gamma$ (torr)	$n_\beta$	$n_\gamma$		$K_\beta$ (torr)	$K_\gamma$ (torr)	$n_\beta$	$n_\gamma$
CO <sub>2</sub>	0.39	0.08	13	3	CHF <sub>3</sub>	0.33	0.08	12	3
OCS	0.31	0.06	11	2	PF <sub>3</sub>	0.18	0.06	7	2
N <sub>2</sub> O	0.32	0.11	10	3	NF <sub>3</sub>	0.32	0.02	9	1
SF <sub>6</sub>	0.44	0.06	13	2	NH <sub>3</sub>	0.20	0.08	8	2
CH <sub>3</sub> F	0.22	0.09	10	4	ND <sub>3</sub>	0.36	0.10	9	2

Table IV. Purity of the gases

CO <sub>2</sub>	99.9%	CHF <sub>3</sub>	98.0% (1% air, 1% C <sub>k</sub> H <sub>l</sub> F <sub>m</sub> )
OCS	97.5% (1.4% CO <sub>2</sub> , 0.6% N <sub>2</sub> )	PF <sub>3</sub>	99.8%
N <sub>2</sub> O	98.0%	NF <sub>3</sub>	97.0%
HCl	99.0%	NH <sub>3</sub>	99.9%
DCl	99.0% (isotopic)	ND <sub>3</sub>	98.0% (isotopic)
SF <sub>6</sub>	99.8%	PH <sub>3</sub>	99.5%
CH <sub>3</sub> F	99.0%	AsH <sub>3</sub>	99.5%

effect was observed up to about 110 kOe/torr, while  $\text{PH}_3$  showed a very slight decrease of its viscosity (less than  $5 \times 10^{-5}$ ) at 100 kOe/torr.

For the calculation of the results in terms of viscosity coefficients from eq. (29), a successive approximation method can be used. A preliminary value of  $\{\eta_2^+ - \eta(0)\}/\eta(0)$  is obtained from eq. (29a) by neglecting the second term,  $\epsilon$  being 0.93. From this approximate value,  $\{\eta_1^+ - \eta(0)\}/\eta(0)$  is calculated on the basis of the (dominant)  $\overline{\text{J}}\overline{\text{J}}$ -type of polarization only, to give an improved value for  $\{\eta_2^+ - \eta(0)\}/\eta(0)$ . A similar procedure was used to determine  $\{\frac{1}{2}\eta_2^+ + \frac{3}{2}\eta_0^+ - \eta(0)\}/\eta(0)$ . That the correction term with  $\epsilon$  may be calculated on the basis of  $\overline{\text{J}}\overline{\text{J}}$ -type of polarization, will be justified below where it is established that such a polarization gives a good description for the experimental viscosity results. This is not true for  $\text{NH}_3$  and  $\text{ND}_3$  which will be treated separately in section 5.2.

We will now try to fit the experimental results on the basis of a  $\overline{\text{J}}\overline{\text{J}}$ -type of polarization only. Since the  $\overline{\text{J}}\overline{\text{J}}$ -polarization gives no field effect for  $\eta_0^+$  the theoretical curve for both sets of measured coefficients are determined by  $\eta_2^+$  only. The different formulae for  $\eta_2^+$  are (cf. eqs. (20), (22) and (24)):

$$\frac{\eta_2^+ - \eta(0)}{\eta(0)} = \Psi_{02} \left\langle \frac{4\xi_{02}^2}{1 + 4\xi_{02}^2} \right\rangle_0, \quad (31a)$$

$$\frac{\eta_2^+ - \eta(0)}{\eta(0)} = \Psi_{02} \frac{1}{\langle \overline{\text{J}}\overline{\text{J}} : \overline{\text{J}}\overline{\text{J}} \rangle_0} \langle \overline{\text{J}}\overline{\text{J}} : \overline{\text{J}}\overline{\text{J}} \frac{4\xi_{02}^2}{1 + 4\xi_{02}^2} \rangle_0 \quad (31b)$$

and the approximate formula

$$\frac{\eta_2^+ - \eta(0)}{\eta(0)} = \Psi_{02} \frac{4\langle \xi_{02} \rangle_0^2}{1 + 4\langle \xi_{02} \rangle_0^2}. \quad (31c)$$

The expression for  $\eta_0^+$  corresponding to eqs. (31a, b and c) reads

$$\frac{\eta_0^+ - \eta(0)}{\eta(0)} = 0. \quad (32)$$

Of the three curves corresponding to eqs. (31a, b and c) shape and position were found to be essentially indistinguishable as a function of  $H/p$  for all gases except for the prolate symmetric top,  $\text{CH}_3\text{F}$ , where the spread of  $g$ -values causes some broadening of the curve. This (small) broadening has been discussed in section 6.1.

The theoretical curves for the  $\overline{\text{J}}\overline{\text{J}}$ -polarization are now fitted to the two sets of measured points simultaneously. As seen in figs. 8 through 15, the fit is perfect within experimental error for  $\text{N}_2\text{O}$ ,  $\text{SF}_6$ ,  $\text{PF}_3$  and  $\text{NF}_3$ . The fit is somewhat less per-

fect for  $\text{CO}_2$ ,  $\text{OCS}$  and  $\text{CHF}_3$ . This suggests a small contribution from  $\eta_0^+$  which has to be attributed to the presence of a polarization of type  $\overline{\text{W}}\overline{\text{W}}\overline{\text{J}}\overline{\text{J}}$  or  $\overline{\text{W}}\overline{\text{J}}\overline{\text{J}}\overline{\text{J}}$  (see table I), although in the case of  $\text{OCS}$  and  $\text{CHF}_3$  the presence of impurities might also play a role in these deviations. For  $\text{CH}_3\text{F}$  a good fit is achieved when using either of the averaged theoretical curves given by eqs. (31a) and (31b), as seen in fig. 15. However, the curve corresponding to eq. (31c) describes the results somewhat less satisfactorily.

Now that the  $\overline{\text{J}}\overline{\text{J}}$ -polarization has been shown to give by far the dominant contribution to the field effects of these gases, their magnitude  $\Psi_{02}$  and the value  $(H/p)_{1/2}$  for which both curves reach half their saturation value are determined (see table V). It is found that two groups of values for  $\Psi_{02}$  can be distinguished: a)  $\Psi_{02}$  between  $2 \times 10^{-3}$  and  $4 \times 10^{-3}$ , and b)  $\Psi_{02} \leq 1 \times 10^{-3}$ . In this latter group we find molecules for which the rotational level splitting is large due to the presence of hydrogen atom(s):  $\text{HCl}$ ,  $\text{DCl}$ ,  $\text{CH}_4$ ,  $\text{CH}_3\text{F}$ ,  $\text{PH}_3$ ,  $\text{AsH}_3$ . Also  $\text{I}_2$  and  $\text{D}_2$  fit into this category (see chapter II).

The results for  $\Psi_{02}$  and  $(H/p)_{1/2}$  are now used to determine values for the cross sections  $\mathcal{S}(02)$  and  $\mathcal{S}(02_0^2)$  from the position and the magnitude of the effects, respectively. The cross section  $\mathcal{S}(02)$  is obtained from  $(H/p)_{1/2}$ , the value of  $H/p$  for which the effect reaches half its saturation value. For  $\text{CO}_2$ ,  $\text{OCS}$ ,  $\text{N}_2\text{O}$ ,  $\text{SF}_6$ ,  $\text{CHF}_3$ ,  $\text{PF}_3$  and  $\text{NF}_3$  one has from eqs. (21) and (31c)

$$\mathcal{S}(02) = 2 \left| g_L \left[ 1 + \frac{g_H - g_L}{g_L} \left\langle \frac{K^2}{J(J+1)} \right\rangle_0 \right] \right| \frac{\mu_N k T}{\hbar \langle v \rangle_0} \left( \frac{H}{p} \right)_{1/2} \quad (33)$$

Here we used the fact that the curve described by eq. (31c) reaches half its saturation value for  $\langle \xi_{02} \rangle_0 = 1/2$ . Values for the thermally averaged g-factor were calculated according to

$$\langle g \rangle_0 = g_L \left[ 1 + \frac{g_H - g_L}{g_L} \left\langle \frac{K^2}{J(J+1)} \right\rangle_0 \right] \quad (34)$$

and are given in table II.

For  $\text{CH}_3\text{F}$  the simple formula (31c) with an averaged g-factor cannot be used because of the spread in precession frequencies. Performing numerical calculation for  $\text{CH}_3\text{F}$  on the basis of eq. (31a), one finds

$$\mathcal{S}(02) = 1.595 \frac{|g_L| \mu_N k T}{\hbar \langle v \rangle_0} \left( \frac{H}{p} \right)_{1/2} \quad (35a)$$



and from eq. (31b)

$$\mathfrak{S}(02) = 1.479 \frac{|g_L| \mu_N kT}{h \langle v \rangle_0} \left( \frac{H}{p} \right)^{\frac{1}{2}} \quad (35b)$$

Values of  $\mathfrak{S}(02)$  thus found from the experiment are listed in table V.

The saturation value of the effect, as described by eqs. (31a) or (31b), equals  $\Psi_{02}$ . From eq. (14), the absolute value of the cross section  $\mathfrak{S}_{(20)}^{(02)}$  is therefore found to be

$$|\mathfrak{S}_{(20)}^{(02)}| = \sqrt{\Psi_{02} \mathfrak{S}(02) \mathfrak{S}(20)}. \quad (36)$$

For the calculation of  $\mathfrak{S}_{(20)}^{(02)}$  the values of  $\mathfrak{S}(02)$  from eqs. (33) and (35) have been used as well as the values of  $\mathfrak{S}(20)$  obtained from the field free viscosity data, using eq. (13). The sign of  $\mathfrak{S}_{(20)}^{(02)}$  can be determined from flow birefringence experiments<sup>54</sup>) and it was found to be positive for  $\text{CO}_2$ ,  $\text{OCS}$ ,  $\text{N}_2\text{O}$ ,  $\text{CH}_3\text{F}$ ,  $\text{PF}_3$  and  $\text{NF}_3$ . For  $\text{SF}_6$  the sign was not determined, but it is probably also positive. The experimental values for  $(H/p)^{\frac{1}{2}}$  and  $\Psi_{02}$  as well as the calculated values for the effective cross sections  $\mathfrak{S}(20)$ ,  $\mathfrak{S}(02)$  and  $\mathfrak{S}_{(20)}^{(02)}$  are given in table V, together with the literature values of  $\eta(0)$ . The magnitudes of these cross sections will be discussed in section 5.3. For  $\text{CH}_3\text{F}$  two sets of results are listed; one set is obtained by fitting the theoretical curve of eq. (31a) to the experimental results and the second set by using eq. (31b). Since, as discussed above, either curve gives a good fit to the experimental data, it is not possible from the present results to determine which choice has to be made. This point will be discussed further in section 6.1.

**5.2.  $\text{NH}_3$  and  $\text{ND}_3$ .** While for the gases discussed in the previous section the viscosity decreases in a magnetic field, for  $\text{NH}_3$  and  $\text{ND}_3$  an increase of viscosity is observed. Only an odd-in- $\underline{J}$  polarization can explain this increase. From the experimental results it is found that the ratio of the saturation values of the curves  $\frac{1}{2}\eta_2^+ + \frac{1}{2}\eta_0^+$  and  $\eta_2^+$  is  $2.6 \pm 0.2$  for  $\text{NH}_3$  and  $2.5 \pm 0.2$  for  $\text{ND}_3$  (see figs. 16, 17). From the theoretical expressions in table I one finds for this ratio  $\frac{5}{2} \cdot \frac{55}{52}$  and  $\frac{1}{2}$  for the odd-in- $\underline{J}$  polarizations  $\underline{W}\underline{W}\underline{J}$ ,  $\underline{W}\underline{W}\underline{J}\underline{J}\underline{J}$  and  $\underline{W}\underline{J}\underline{J}$ , respectively. Using eq. (6) it can be shown that with increasing rank of the tensors  $[\underline{W}]^{(p)}$   $[\underline{J}]^{(q)}$  the ratio tends to 1. Thus, one is tempted to conclude that the effect has to be attributed almost entirely to the  $\underline{W}\underline{W}\underline{J}$  term, which is the only term that gives a ratio near the experimental value. One cannot, however, exclude the possibility that a positive and a negative contribution of comparable magnitude cooperate to give the observed ratio. In figs. 16 and

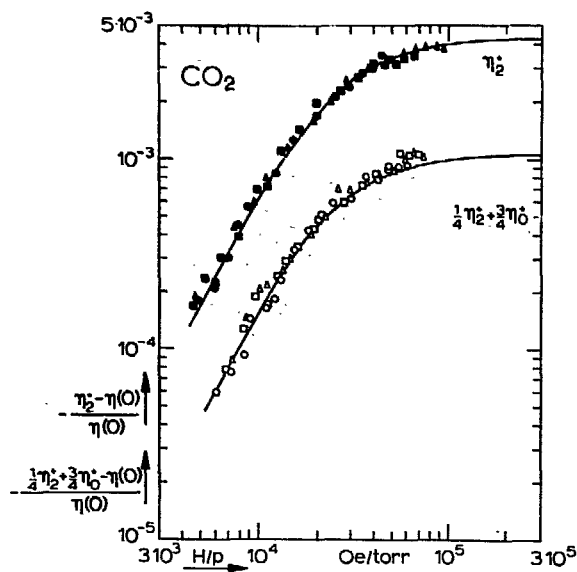


Fig. 8  $-\frac{[\eta_2^* - \eta(0)]}{\eta(0)}$  and  $-\frac{[\frac{1}{4}\eta_2^* + \frac{3}{4}\eta_0^* - \eta(0)]}{\eta(0)}$  versus  $H/p$  for  $\text{CO}_2$ .  
 ● 1.50 torr; ■ 1.12 torr; ▲ 0.76 torr;  
 ○ 1.13 torr; □ 0.97 torr; △ 0.86 torr.  
 — theoretical  $H/p$  dependence for  $\overline{II}$ -polarization according to eqs. (10).

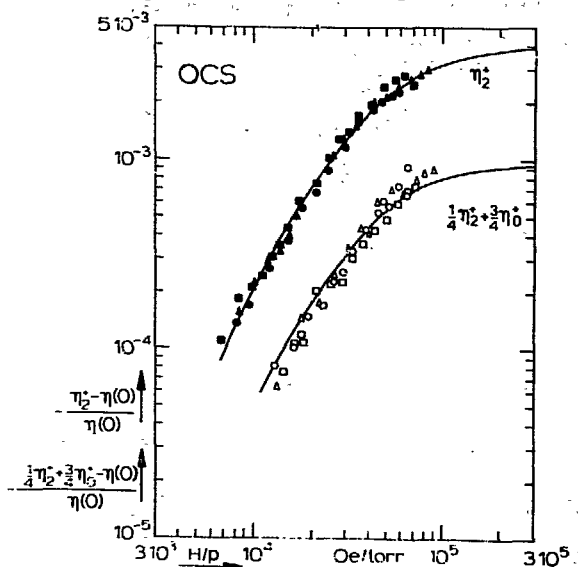


Fig. 9  $-\frac{[\eta_2^* - \eta(0)]}{\eta(0)}$  and  $-\frac{[\frac{1}{4}\eta_2^* + \frac{3}{4}\eta_0^* - \eta(0)]}{\eta(0)}$  versus  $H/p$  for  $\text{OCS}$ .  
 ● 1.24 torr; ■ 1.05 torr; ▲ 0.85 torr;  
 ○ 1.15 torr; □ 1.01 torr; △ 0.80 torr.  
 — theoretical  $H/p$  dependence for  $\overline{II}$ -polarization according to eqs. (10).

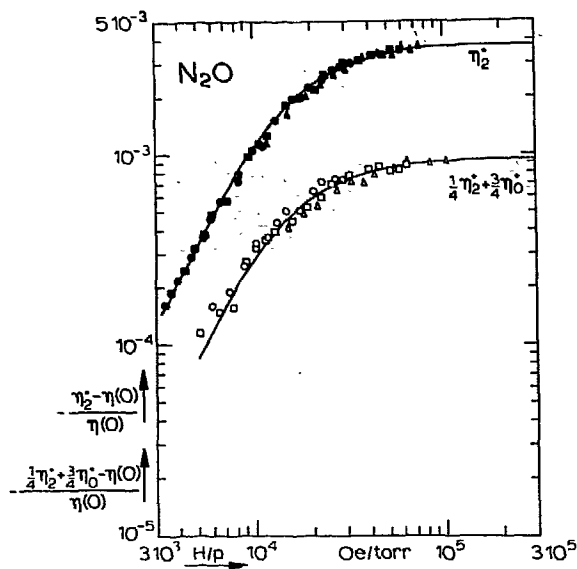


Fig. 10  $-\frac{[\eta_2^+ - \eta(O)]}{\eta(O)}$  and  $-\frac{[\frac{1}{4}\eta_2^+ + \frac{3}{4}\eta_0^+ - \eta(O)]}{\eta(O)}$  versus  $H/p$  for  $N_2O$ .  
 ● 2.21 torr; ■ 1.18 torr; ▲ 0.91 torr;  
 ○ 2.49 torr; □ 1.08 torr; △ 0.60 torr;  
 — theoretical  $H/p$  dependence for  $\overline{II}$ -polarization according to eqs. (10).

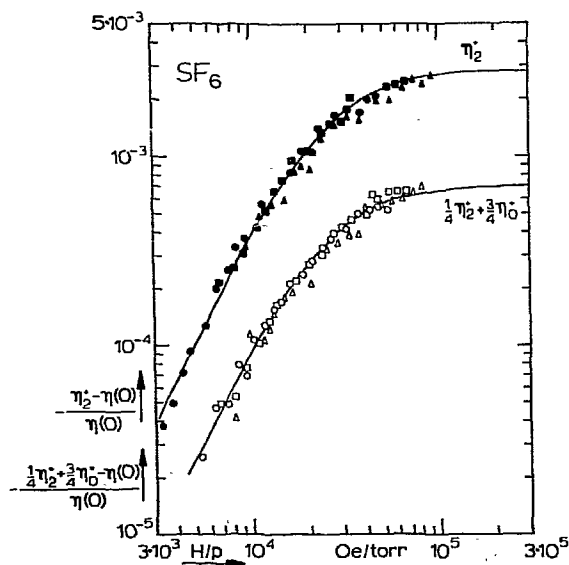


Fig. 11  $-\frac{[\eta_2^+ - \eta(O)]}{\eta(O)}$  and  $-\frac{[\frac{1}{4}\eta_2^+ + \frac{3}{4}\eta_0^+ - \eta(O)]}{\eta(O)}$  versus  $H/p$  for  $SF_6$ .  
 ● 1.55 torr; ■ 1.07 torr; ▲ 0.75 torr;  
 ○ 1.35 torr; □ 1.05 torr; △ 0.88 torr.  
 — theoretical  $H/p$  dependence for  $\overline{II}$ -polarization according to eqs. (10).

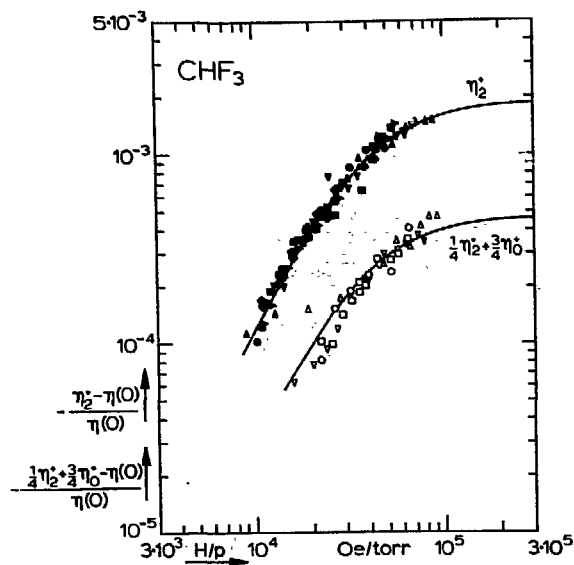


Fig. 12  $-\frac{[\eta_2^+ - \eta(0)]}{\eta(0)}$  and  $-\frac{[\frac{1}{4}\eta_2^+ + \frac{3}{4}\eta_0^+ - \eta(0)]}{\eta(0)}$  versus  $H/p$  for  $\text{CHF}_3$ .  
 • 1.58 torr; ■ 1.37 torr; ◆ 1.30 torr; ▶ 1.18 torr; ▼ 0.99 torr; ▲ 0.74 torr;  
 ○ 1.15 torr; □ 1.09 torr; △ 0.85 torr; △ 0.80 torr.  
 — theoretical  $H/p$  dependence for  $\overline{II}$ -polarization according to eqs. (31a, b and c)  
 For this gas the curves corresponding to eqs. (31a, b and c) are indistinguishable.

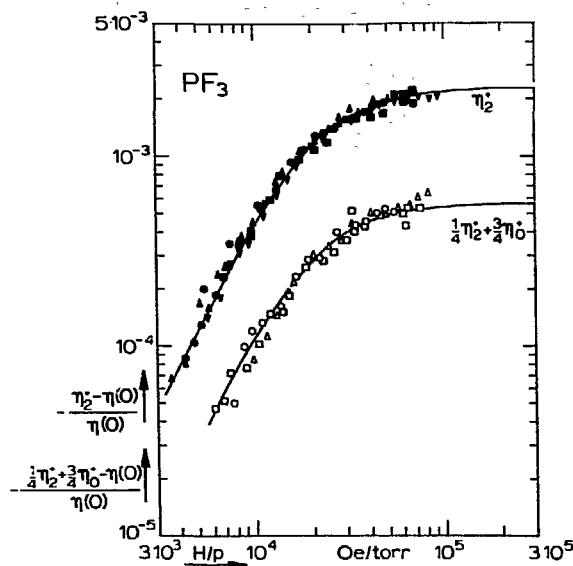


Fig. 13  $-\frac{[\eta_2^+ - \eta(0)]}{\eta(0)}$  and  $-\frac{[\frac{1}{4}\eta_2^+ + \frac{3}{4}\eta_0^+ - \eta(0)]}{\eta(0)}$  versus  $H/p$  for  $\text{PF}_3$ .  
 • 1.36 torr; ■ 1.04 torr; ▲ 1.00 torr; ▼ 0.76 torr;  
 ○ 1.32 torr; □ 0.95 torr; △ 0.86 torr.  
 — theoretical  $H/p$  dependence for  $\overline{II}$ -polarization according to eqs. (31a, b and c). For this gas the curves corresponding to eqs. (31a, b and c) are indistinguishable.

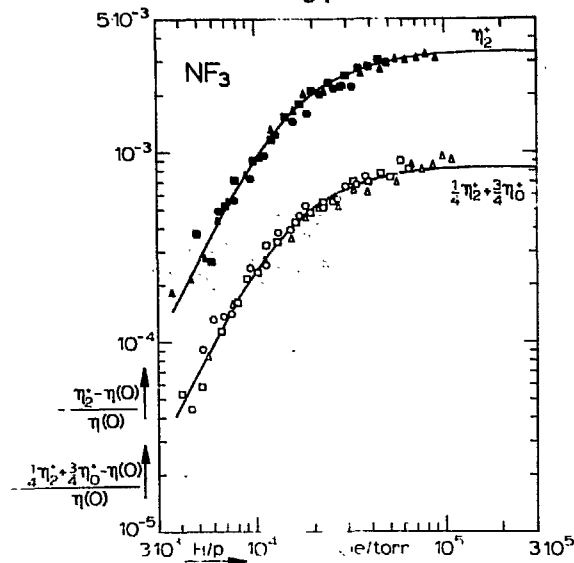


Fig. 14  $-\frac{[\eta_2^+ - \eta(0)]}{\eta(0)}$  and  $-\frac{[\frac{1}{4}\eta_2^+ + \frac{3}{4}\eta_0^+ - \eta(0)]}{\eta(0)}$  versus  $H/p$  for  $\text{NF}_3$ .  
 • 2.43 torr; ■ 1.57 torr; ▲ 0.86 torr;  
 ○ 2.05 torr; □ 1.19 torr; △ 0.70 torr.  
 — theoretical  $H/p$  dependence for  $\overline{J_1}$ -polarization according to eqs. (31a, b and c). For this gas the curves corresponding to eqs. (31a, b and c) are indistinguishable.

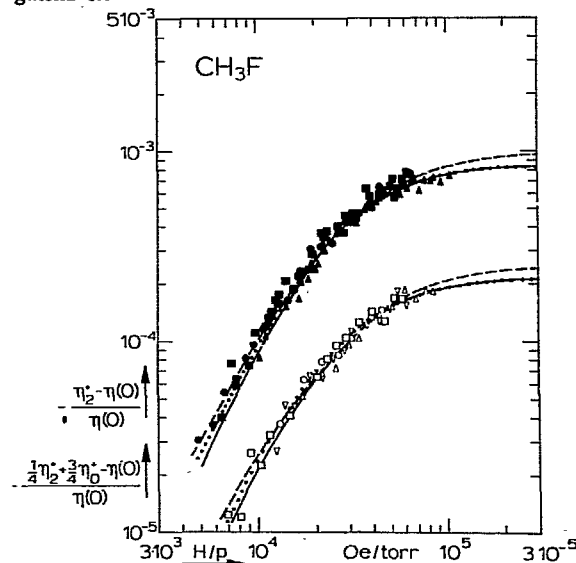


Fig. 15  $-\frac{[\eta_2^+ - \eta(0)]}{\eta(0)}$  and  $-\frac{[\frac{1}{4}\eta_2^+ + \frac{3}{4}\eta_0^+ - \eta(0)]}{\eta(0)}$  versus  $H/p$  for  $\text{CH}_3\text{F}$ .  
 • 1.44 torr; ■ 1.04 torr; ▲ 0.65 torr;  
 ○ 1.65 torr; □ 1.24 torr; ▽ 1.15 torr; △ 0.81 torr.  
 The curves represent the theoretical  $H/p$  dependence for  $\overline{J_1}$ -polarization according to eqs. (20).  
 ---- based on a normalized angular momentum polarization (eqs. (22) and (31a)).  
 ..... based on a unnormalized angular momentum polarization (eqs. (24) and (31b)).  
 — single parameter curve (eq. (31c)).

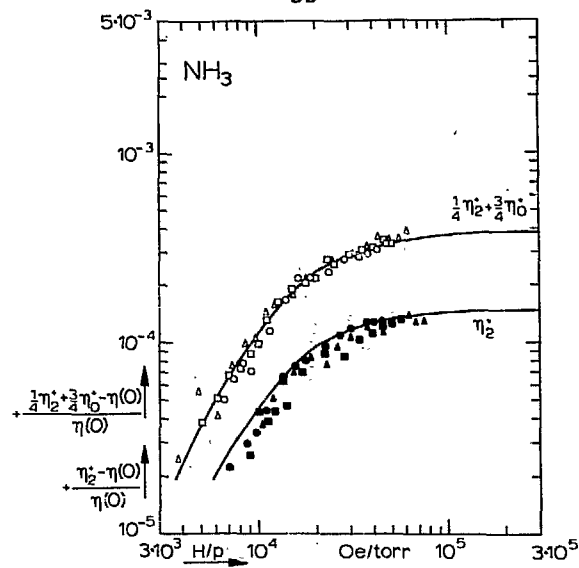


Fig. 16  $+\frac{1}{4}\eta_2^+ + \frac{3}{4}\eta_0^+ - \eta(0)]/\eta(0)$  and  $+\frac{1}{4}\eta_2^+ - \eta(0)]/\eta(0)$  versus  $H/p$  for  $\text{NH}_3$ .  
 ○ 1.55 torr; □ 1.43 torr; △ 1.17 torr;  
 ● 1.59 torr; ◆ 1.25 torr; ▲ 0.91 torr.

— theoretical  $H/p$  dependence for  $\overline{W\overline{W}}$   $I$ -polarization (see eqs. (37, 38)), scaled to the experimental points of  $\frac{1}{4}\eta_2^+ + \frac{3}{4}\eta_0^+$ .

Note that the sign of the viscomagnetic effects for  $\text{NH}_3$  and  $\text{ND}_3$  are opposite to the other effects measured in this thesis.

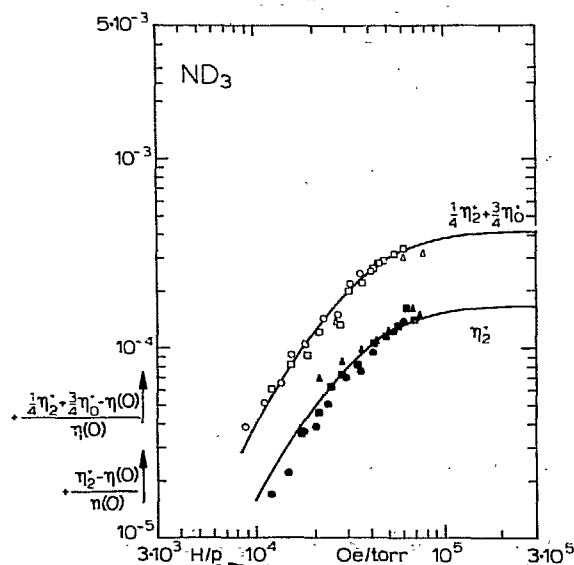


Fig. 17  $+\frac{1}{4}\eta_2^+ + \frac{3}{4}\eta_0^+ - \eta(0)]/\eta(0)$  and  $+\frac{1}{4}\eta_2^+ - \eta(0)]/\eta(0)$  versus  $H/p$  for  $\text{ND}_3$ .  
 ○ 1.57 torr; □ 1.14 torr; △ 0.75 torr;  
 ● 1.19 torr; ◆ 1.01 torr; ▲ 0.95 torr.

— theoretical  $H/p$  dependence for  $\overline{W\overline{W}}$   $I$ -polarization (see eqs. (37, 38)), scaled to the experimental points of  $\frac{1}{4}\eta_2^+ + \frac{3}{4}\eta_0^+$ .

Note that the sign of the viscomagnetic effects for  $\text{NH}_3$  and  $\text{ND}_3$  are opposite to the other effects measured in this thesis.

17 the experimental results are compared with theoretical curves based on the  $\overline{W W J}$  polarization only. Since  $g_J$  and  $g_I$  differ very little (cf. discussion in section 2.2) we can use the single parameter formulae

$$+ \frac{\eta_2^+ - \eta(0)}{\eta(0)} = \frac{2}{4} \Psi_{21} \frac{\langle \xi_{21} \rangle_0^2}{1 + \langle \xi_{21} \rangle_0^2} \quad (37)$$

and

$$+ \frac{\frac{1}{2}\eta_2^+ + \frac{3}{2}\eta_0^+ - \eta(0)}{\eta(0)} = \frac{5}{4} \Psi_{21} \frac{\langle \xi_{21} \rangle_0^2}{1 + \langle \xi_{21} \rangle_0^2} \quad (38)$$

where  $\Psi_{21} = \mathfrak{S}^2 \binom{21}{20} / \{ \mathfrak{S}(20) \mathfrak{S}(21) \}$  (see eq. (14)).

When trying to fit the curves for both  $\eta_2^+$  and for  $\frac{1}{2}\eta_2^+ + \frac{3}{2}\eta_0^+$  simultaneously to the experimental data, it is seen that the fit is reasonable but not quite perfect (see figs. 16 and 17). For  $\text{NH}_3$  this suggests a (small) contribution of even-in- $J$  polarizations. Since the influence of such polarizations on the field effects is smallest on the upper curve ( $\frac{1}{2}\eta_2^+ + \frac{3}{2}\eta_0^+$ ), effective cross sections  $\mathfrak{S}(21)$  and  $\mathfrak{S} \binom{21}{20}$  are derived from the upper curve. Using eqs. (21) and (38) one has

$$\mathfrak{S}(21) = \left| g_I \left[ 1 + \frac{g_J - g_I}{g_I} \left\langle \frac{K^2}{J(J+1)} \right\rangle_{cl} \right] \frac{\mu_N k T}{\hbar \langle v \rangle_0} \left( \frac{H}{p} \right)^{\frac{1}{2}} \right| \quad (39)$$

and

$$|\mathfrak{S} \binom{21}{20}| = \sqrt{\Psi_{21} \mathfrak{S}(20) \mathfrak{S}(21)}, \quad (40)$$

where  $\frac{5}{4} \Psi_{21}$  equals the saturation value of the effect. The results are listed in table V. A more refined analysis of the data using a superposition of a dominant  $\overline{W W J}$ -term and a  $\overline{J J}$  or a  $\overline{W W J J}$ -term has also been tried. This method yields for  $\text{NH}_3$  the value of  $\Psi_{21} \approx 0.31 \times 10^{-3}$  and values of  $\Psi_{02}$  and  $\Psi_{22}$  of at most  $0.05 \times 10^{-3}$ . A similar conclusion was drawn by Korving<sup>10</sup>) from his viscosity results for  $\text{NH}_3$ , who found  $\Psi_{21} = (0.32 \pm 0.03) \times 10^{-3}$  which agrees well with the present results (see table V). The conclusion must be drawn that the values of  $\Psi_{02}$  and  $\Psi_{22}$  for  $\text{NH}_3$  and  $\text{ND}_3$  are too small to make any further analysis meaningful.

Since a contribution to the field effect from a polarization of type  $\overline{J J}$  would be expected to show up in the  $\frac{H}{p}$  range studied in these measurements, the smallness of  $\Psi_{02}$  suggests a very small production of  $\overline{J J}$ -polarization from velocity polarization, i.e.,  $\mathfrak{S} \binom{02}{20}$  is very small. This is confirmed by flow birefringence measurements on  $\text{NH}_3$  and  $\text{ND}_3$ <sup>54</sup>). As the cross section  $\mathfrak{S} \binom{02}{20}$  is related to  $\mathfrak{S} \binom{1010}{1200}$  by

$\mathfrak{S}_{20}^{(02)} = -\sqrt{3} \mathfrak{S}_{1200}^{(1010)}$ , one should also expect  $\mathfrak{S}_{1200}^{(1010)}$  to be quite small. Since this cross section plays an important role in the thermomagnetic torque and the thermomagnetic pressure difference, it is not surprising that the thermomagnetic torque effect was found to be very small<sup>58</sup>) and that the thermomagnetic pressure difference could not be detected for  $\text{NH}_3$ .

In first order Distorted Wave Born Approximation calculations only energetically inelastic collisions contribute to  $\mathfrak{S}_{20}^{(02)}$ <sup>59</sup>). Since molecules as  $\text{NH}_3$ ,  $\text{ND}_3$ ,  $\text{PH}_3$  and  $\text{AsH}_3$  possess widely separated rotational energy levels and furthermore selection rules for K-changing collisions prohibit conversion of, e.g., ammonia of A symmetry into ammonia with E symmetry, energetically inelastic collisions are expected to be rare. This, in turn, gives rise to a small value for  $\mathfrak{S}_{20}^{(02)}$ . One could be tempted to relate the positive effects for  $\text{NH}_3$  and  $\text{ND}_3$  to the molecular inversion. As the inversion frequencies ( $24 \times 10^9$  Hz for  $\text{NH}_3$  and  $1.6 \times 10^9$  Hz for  $\text{ND}_3$ ) are much higher than the collision frequency at the pressures studied ( $10^7$  Hz), it is improbable that the effect is related to the inversion, as was already pointed out by Levi *et al.*<sup>60</sup>). For instance, the polarizations involving  $J_l$  can be expected to average out. As was discussed above, this conclusion agrees with the experimental results. Furthermore, polarizations off-diagonal in the K quantum numbers ( $\tau_1$  and  $\tau_2$  in ref. 21) which can occur in an electric field, do not contribute in the magnetic field case because of parity restrictions.

Very recently Snider<sup>61</sup>) pointed out that for symmetric top molecules dipole-dipole interaction in first order Distorted Wave Born approximation can produce a vector polarization in angular momentum  $\underline{J}$  through elastic collisions. Such a dipole-dipole interaction can in this way not produce a tensor polarization of the form  $\overline{\underline{J}\underline{J}} R(J^2)$ , which is generally due to  $P_2$ -terms in the molecular interaction. As such terms can be expected to be small for  $\text{NH}_3$  and  $\text{ND}_3$  (the anisotropic part of the polarizability,  $\alpha_l - \alpha_1$ , being small) it is not surprising that for the ammonia molecules, where large electric dipole moments make themselves felt during the collisions (for  $\text{NH}_3$   $\mu_{e1} = 1.47\text{D}$  and for  $\text{ND}_3$   $\mu_{e1} = 1.51\text{D}$ ), a polarization vectorial in  $\underline{J}$  is produced:  $\overline{\underline{W}\underline{W}} \underline{J}$ . This is corroborated by results for the heat conductivity of  $\text{NH}_3$  where also a vectorial  $\underline{J}$ -term gives an important contribution:  $\underline{W}\underline{J}$ . For  $\text{PH}_3$  and  $\text{AsH}_3$  no viscomagnetic effect could be observed. Such a behavior can be understood because the cross sections determined by inelastic collisions will be small (the rotational constants of  $\text{PH}_3$  and  $\text{AsH}_3$  are comparable to those of  $\text{ND}_3$ , see table II) and cross sections determined by elastic collisions will be small because of the small dipole moments of  $\text{PH}_3$  and  $\text{AsH}_3$  (0.55 D and 0.16 D, respectively).

Finally, it is not to be expected that the rapid exchange of hydrogenic atoms in  $\text{NH}_3$  between colliding molecules might be a factor in determining the importance of the  $\overline{\underline{W}\underline{W}} \underline{J}$  term.



Table V. Experimental results together with data of electric dipole moments and field free viscosities. The gases CH<sub>4</sub> and CF<sub>4</sub> are listed for comparison. Note that 1D = 3.33567 × 10<sup>-30</sup> C.m, and 1P = 10<sup>-1</sup> Pa.s.

	$\mu_{el}^{42}$ (D)	$\eta(0)$ (10 <sup>-6</sup> P)	$(H/p)_{1/2}$ (kOe/torr)	$\Psi_{02} \cdot 10^3$		$(g)_0$	$\mathcal{G}(20)$ (Å <sup>2</sup> )		$\mathcal{G}(02)$ (Å <sup>2</sup> )		$\mathcal{G}(20^2)$ (Å <sup>2</sup> )		$\mathcal{G}_{nonres}$ (Å <sup>2</sup> )
				this exp.	litt.		this exp.	litt.	this exp.	litt.			
CO <sub>2</sub>	0	146.6 ± 0.1 <sup>43)</sup>	22.5 ± 1	4.2 ± 0.1	4.75 <sup>55)</sup>	-0.0551	52 ± 1	68 ± 3	69 <sup>55)</sup>	3.85 ± 0.2	4.1 <sup>55)</sup>		
OCS	0.72	122.1 ± 0.6 <sup>44)</sup>	43 ± 1	3.9 ± 0.1		-0.0287	73 ± 1	79 ± 3		4.7 ± 0.2			
N <sub>2</sub> O	0.16	146 ± 1 <sup>45)</sup>	15.2 ± 0.5	3.7 ± 0.1		-0.0761	52 ± 1	64 ± 2		3.5 ± 0.2			
HCl	1.08	142 ± 1 <sup>46)</sup>	?	<0.02		+0.4594	49 ± 1	?		small			
DCI	1.08	?	?	<0.02		?	?	?		small			
SF <sub>6</sub>	0	152 ± 1 <sup>47)</sup>	25.5 ± 1	2.75 ± 0.05		?	92 ± 1	?		?			
CH <sub>4</sub>	0	110.0 ± 0.5 <sup>48)</sup>			0.79 <sup>56)</sup>	+0.3133	42 ± 1		32 <sup>56)</sup>		1.06 <sup>56)</sup>		
CF <sub>4</sub>	0	170.6 ± 0.8 <sup>49)</sup>			3.1 <sup>56)</sup>	-0.031	63 ± 1		60 <sup>56)</sup>		3.4 <sup>56)</sup>		
CH <sub>3</sub> F	1.86	117 ± 2 <sup>50)</sup>	40.0 ± 0.7*	1.05 ± 0.05*			57 ± 1	95 ± 4*	634*	2.4 ± 0.1*			
			30.5 ± 0.6**	0.84 ± 0.05**	0.86 <sup>9)</sup>			67 ± 4**	148** †	1.8 ± 0.1**	2.8 <sup>22)</sup>	145 <sup>57)</sup>	
CHF <sub>3</sub>	1.64	148 ± 1 <sup>50)</sup>	39 ± 1	1.90 ± 0.08	1.72 <sup>9)</sup>	-0.034	65 ± 1	91 ± 4	110 <sup>9)</sup>	3.35 ± 0.2	3.5 <sup>22)</sup>	94 <sup>57)</sup>	
PF <sub>3</sub>	1.03	169 ± 2 <sup>51)</sup>	19.6 ± 0.9	2.3 ± 0.1		-0.072	64 ± 1	110 ± 7		4.0 ± 0.2			
NF <sub>3</sub>	0.23	178 ± 2 <sup>51)</sup>	16.0 ± 0.4	3.5 ± 0.1	3.3 <sup>9)</sup>	-0.069	54 ± 1	77 ± 4	63 <sup>9)</sup>	3.8 ± 0.2	3.4 <sup>22)</sup>		
PH <sub>3</sub>	0.55	115 ± 1 <sup>52)</sup>	?	<0.05			58 ± 1	?		small			
AsH <sub>3</sub>	0.16	158 ± 2 <sup>52)</sup>	?	<0.02		?	64 ± 1	?		small			

	$\mu_{el}^{42}$ (D)	$\eta(0)$ (10 <sup>-6</sup> P)	$(H/p)_{1/2}$ (kOe/torr)	$\Psi_{21} \cdot 10^3$		$(g)_0$	$\mathcal{G}(20)$ (Å <sup>2</sup> )		$\mathcal{G}(21)$ (Å <sup>2</sup> )		$\mathcal{G}(20^2)$ (Å <sup>2</sup> )		$\mathcal{G}_{nonres}$ (Å <sup>2</sup> )
				this exp.	litt.		this exp.	litt.	this exp.	litt.			
NH <sub>3</sub>	1.47	98.4 ± 0.5 <sup>53)</sup>	16 ± 1	0.31 ± 0.03	0.33 <sup>10)</sup>	+0.538	48 ± 1	146 ± 9	133 <sup>10)</sup>	1.5 ± 0.2	1.45 <sup>10)</sup>		
ND <sub>3</sub>	1.51	-----	31 ± 2	0.34 ± 0.03	0.18 <sup>11)</sup>	?	?	?		?			

\* Results obtained assuming normalized angular momentum polarization. For the magnetic field effect, this corresponds to eqs. (31a) and (35a).

\*\* Results obtained assuming unnormalized angular momentum polarization. For the magnetic field effect, this corresponds to eqs. (31b) and (35b).

† This value is calculated on the basis of the half value of 935 V/cm torr which is obtained by fitting a curve of the form of eq. (24) (obtained by quantum mechanical calculation) to the experimental data. It should be noted that the value of 1100 V/cm torr as given in ref. 22 is obtained on the basis of the classical calculation.

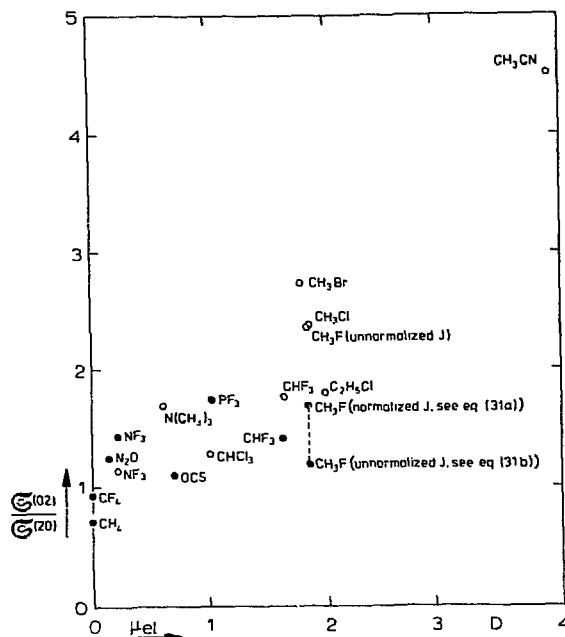


Fig. 18  $\mathcal{S}(02)/\mathcal{S}(20)$  for various molecules as a function of electric dipole moment.  
 ● from the present measurements.  
 ○ from the measurements in ref. 22.

**5.3 The magnitudes of the cross sections.** In table V the results for the cross sections  $\mathcal{S}(20)$  as obtained from field free viscosity data,  $\mathcal{S}(02)$  as obtained from the position of the viscomagnetic effect on the  $\frac{H}{p}$ -axis, and  $\mathcal{S}_{(20)}^{(02)}$  as obtained from the magnitude of the effect are given for the various gases investigated. Results from other field effect measurements for  $\text{CO}_2$ ,  $\text{NF}_3$ ,  $\text{CH}_3\text{F}$ ,  $\text{CHF}_3$ ,  $\text{NH}_3$  and  $\text{ND}_3$  are also listed. The agreement between our data for  $\text{CO}_2$  and  $\text{NH}_3$  with those obtained by Korving<sup>10,55</sup>) from viscomagnetic effect measurements is quite good (see also section 5.2). For  $\text{NF}_3$ ,  $\text{CHF}_3$  and  $\text{CH}_3\text{F}$  the magnitudes, *i.e.*,  $\Psi_{02}$ , do agree with the results from the visco-electric effect. One should realize in such a comparison that the molecules with  $K = 0$  (and  $J \neq 0$ ) do not contribute to the electric field effect, while in the magnetic case they do contribute. Only for  $\text{CH}_3\text{F}$  this difference is of some importance (about 10%). Our data for  $\mathcal{S}(02)$  for  $\text{NF}_3$  and  $\text{CHF}_3$  which have been obtained using estimated values for  $g_l$  compare quite well with the results for the visco-electric effect in these gases<sup>22,9</sup>). The same is true for  $\mathcal{S}_{(20)}^{(02)}$ .

For  $\text{CH}_3\text{F}$ , however, our value of  $\mathcal{S}(02)$  is approximately a factor 2 smaller than the corresponding value found in the visco-electric effect. As both experiments

give approximately the same value for the magnitude of the effect (*i.e.*,  $\Psi_{02}$ ), the values for  $\mathcal{S}_{20}^{(02)}$  have a discrepancy of about a factor of  $\sqrt{2}$ . The reason for this discrepancy is not clear. In a discussion the following points should be taken into account:

- the value of  $\mathcal{S}(02)$  for  $\text{CH}_3\text{F}$  as given in ref. 9 agrees with results from non-resonant absorption<sup>57</sup>) (see table V, and also table VIII in ref. 22);
- on the other hand the value of  $\mathcal{S}(02)$  given in ref. 9 seems surprisingly large when compared with the value of  $\mathcal{S}(12)$  for this gas ( $120 \text{ \AA}^2$ ) as obtained in measurements of the electric field effect on the thermal conductivity<sup>9</sup>); for all gases investigated it was found that  $\mathcal{S}(12) \geq \mathcal{S}(02)$  which is not surprising since in  $\mathcal{S}(12)$  elastic and reorientation collisions contribute while in  $\mathcal{S}(02)$  only reorientation collisions contribute;
- It is seen from table V that the choice of the averaging has a considerable influence on the value of  $\mathcal{S}(02)$  that is obtained for this gas. As the physical situation may require an even more sophisticated approach, the values of  $\mathcal{S}(02)$  as obtained from the present analysis should be treated with care for  $\text{CH}_3\text{F}$ .

When comparing the cross sections  $\mathcal{S}_{20}^{(02)}$  and  $\mathcal{S}(02)$  with the viscosity cross section  $\mathcal{S}(20)$ , the same trend is found as in earlier experiments on simpler molecules. That is, the energetically inelastic cross section  $\mathcal{S}_{20}^{(02)}$  is smaller than  $\mathcal{S}(20)$  by more than an order of magnitude, and  $\mathcal{S}(02)$  is roughly equal to  $\mathcal{S}(20)$ . The ratio  $\mathcal{S}(20)/\mathcal{S}(20)$  was, in earlier work<sup>22, 9</sup>), found to have a tendency to increase with increasing electric dipole moment, being close to 1 for  $\mu_{e1} = 0$  and approaching 4.5 for  $\mu_{e1} = 3.9 \text{ D}$  ( $\text{CH}_3\text{CN}$ ). The molecules investigated here fit well into this trend (see fig. 18). This is most clearly seen by comparing the ratio of  $\mathcal{S}(02)/\mathcal{S}(20)$  for  $\text{CH}_4$  and  $\text{CF}_4$  ( $\mu_{e1} = 0$ ) with the value for  $\text{CH}_3\text{F}$  and  $\text{CHF}_3$  ( $\mu_{e1} \approx 1.7$ ). This confirms the idea that the dipole-dipole interaction is crucial for the cross section  $\mathcal{S}(02)$ .

**6. Discussion. 6.1 The precise form of the angular momentum dependent polarizations.** As discussed in section 2.2, the question about the precise form of the polarization  $\overline{\mathbb{J}} \mathbb{R}(J^2)$  can, in principle, be settled by the present experiments. This is because the field dependence of the effect is sensitive to the precise form of the polarizations in those cases where state averaged field functions have to be used (cf. eqs. (22) and (24)). For such a procedure to be useful, a first requirement is that  $g_r$  and  $g_l$  of the molecule considered have widely different values. If the moments of inertia  $I_r$  and  $I_l$  are also widely different (as is the case for prolates like  $\text{CH}_3\text{Br}$ ) the distribution over  $K/J$  values is sharply peaked as discussed above (see fig. 5). The result will be a field dependence which is very nearly described by the approximate expression of eq. (27), irrespective of the averaging procedure. On the other hand, if the moments of inertia are almost equal, the distribution over  $K/J$  values will be rather

uniform. In this case, an appreciable broadening of the field dependence curve will be produced by the spread in precession frequencies. However, for  $I_2/I_1 = 1$ , the two averages of eqs (22) and (24) become exactly the same (see eq. (26)), since the distribution over  $K/J$  values becomes insensitive to the exponent  $3/2$  and  $7/2$  respectively.

In other words, neither  $\frac{I_2}{I_1} = 1$  nor  $\frac{I_2}{I_1} \ll 1$  will provide a good test case in these magnetic field measurements. Intermediate values for  $I_2/I_1$  will show some distinction between the two averages of eqs. (22) and (24) (e.g.,  $\text{CH}_3\text{F}$ , see fig. 15), but experimental results will have to be very accurate for such a test to be conclusive.

Electric field effects on the transport properties look more promising in this respect. As the precession frequency is given by

$$\omega = \frac{K}{J(J+1)} \frac{\mu_{e1} E}{\hbar}, \quad (41)$$

with  $\mu_{e1}$  being the electric dipole moment and  $E$  the electric field, for prolate molecules like  $\text{CH}_3\text{F}$  or  $\text{CH}_3\text{Br}$  the sharply peaked distribution around  $K = 0$  gives rise to precession frequencies which are widely different. Consequently, an appreciable broadening of the electric field dependence curve will result. This broadening is still sensitive to the precise form of averaging, since in this case  $I_2/I_1 \ll 1$ . In using electric field effect measurements as a means of deciding on the correct form of the average, the thermal conductivity is less suited because in the thermal conductivity of polar molecules, like  $\text{CH}_3\text{F}$ , more polarizations play a role. This leaves the electric field effect on the viscosity (the visco-electric effect) as test case. There it was found that the role played by odd-in- $J$  polarizations is negligible. We will reexamine the viscosity data of  $\text{CH}_3\text{Br}$  obtained by Tommasini *et al.*<sup>22</sup>). The authors found their experimental results to coincide with the theoretical description corresponding to the averaging of eq. (24), which was the only theoretical description available at that time. This is shown in fig. 19 where we have also given the theoretical curve corresponding to the averaging of eq. (22), *i.e.*, normalized  $\underline{J}$ . As is seen, the results seem to favor slightly the averaging of eq. (24), which would lead one to assume that the direction of  $\underline{J}$  as well as its magnitude are to be considered. One should however be somewhat cautious in drawing such a conclusion, since it contradicts results from different sources. Experiments on flow birefringence<sup>54</sup>) yield indications that the normalized angular momentum tensor polarization as used in eq. (22) is the correct type. Moreover, Moraal<sup>62</sup>) calculated the cross section for decay of tensor polarization for  $\text{CH}_3\text{F}$  in the case of a normalized polarization ( $127 \text{ \AA}^2$ ) and for a polarization of the (unnormalized) form  $\underline{J}\underline{J}$  ( $4 \text{ \AA}^2$ ). A comparison of these values with our results ( $95 \text{ \AA}^2$  and  $67 \text{ \AA}^2$ , respectively) seems to favour the use of the normalized angular momentum dependent polarization in the description of the field effects on the visco-

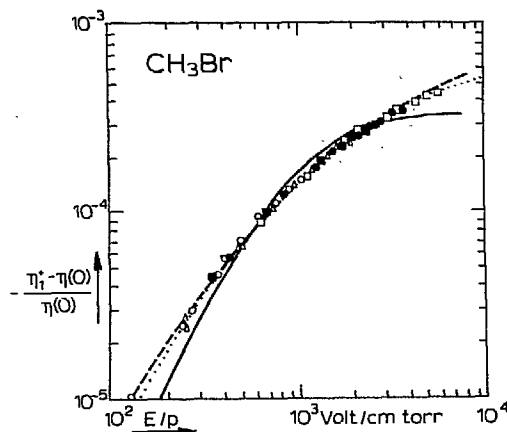


Fig. 19  $-\frac{[\eta_1^* - \eta(0)]}{\eta(0)}$  versus  $E/p$  for  $\text{CH}_3\text{Br}$  taken from ref. 22. The curves represent the theoretical field dependence according to eq. (20b) for  $\overline{\text{II}}$ -polarization.  
 ----- based on a normalized angular momentum polarization (eqs. (22) and (31a)).  
 ..... based on a unnormalized angular momentum polarization (eqs. (24) and (31b)).  
 — single parameter curve (eq. (31c)).

sity. An explanation of the apparent contradiction might be obtained from a consideration derived from the results of Depolarized Rayleigh scattering<sup>19</sup>). It was found that the data for heavier linear molecules ( $\text{N}_2$ ,  $\text{CO}_2$ ,  $\text{OCS}$ ) suggest transfer of polarization between different rotational J-states on collision. If a tensor polarization persists over a time corresponding to several inelastic collisions, each molecule would sample several K and J-states and thus several precession frequencies. For the field effect this would result in a behavior more near the single parameter curve. Consequently, the curves corresponding to eqs. (22) and (24) would have to be modified to become less broadened. Thus the curve corresponding to the assumption of normalized  $\overline{\text{I}}$  (eq. (22)) might give the better fit to the experimental results.

In the above equations we have furthermore assumed that the decay of angular momentum tensor polarization is governed by one relaxation time  $\tau$ . The broadening of the curves due to a dependence of the reorientation efficiency on the rotational quantum number can be expected to be small because of the occurrence of transfer of polarization.

In conclusion one can say that more information is needed before this question can be unambiguously settled.

**6.2 The importance of the various polarizations.** For the gases  $\text{SF}_6$ ,  $\text{N}_2\text{O}$ ,  $\text{CH}_3\text{F}$ ,  $\text{CHF}_3$ ,  $\text{PF}_3$  and  $\text{NF}_3$  the  $\overline{\text{II}}$ -type of polarization is found to be by far dominant.

The measurements on CO<sub>2</sub> and OCS at high H/p values indicate that small contributions from different polarizations (e.g.,  $\overline{W \overline{W}} \overline{J \overline{J}}$ ) might be present for these gases. In principle such contributions can be determined by combining the data for  $\eta_2^+$  and  $\frac{1}{4}\eta_2^+ + \frac{3}{4}\eta_0^+$ . However, these contributions are too small for such a treatment to be meaningful in this case, since both for CO<sub>2</sub> and for OCS the description on the basis of the  $\overline{J \overline{J}}$ -type of polarization is quite good. From the electric field effect measurements on the thermal conductivity<sup>22, 9)</sup> it was concluded that for molecules with strong electric dipole moments the odd-in-J polarization  $\overline{W \overline{J}}$  is important. In some cases (CH<sub>3</sub>F, CH<sub>3</sub>CN), the contribution of this odd-in-J term can even dominate the even-in-J term. In case of viscosity, both for magnetic and for the electric field effects no such correlation can be deduced. In fact, hardly any odd-in-J contribution has been found to date in the viscosity effects, except for NH<sub>3</sub> and ND<sub>3</sub>, where this contribution was found to be dominant (see also refs. 10, 11).

On the basis of the present measurements one may conclude that the presence of a strong electric dipole moment does not lead to the occurrence of an odd-in-J polarization in a viscous flow. This is, in contrast to the thermal conductivity, where the electric field measurements<sup>9)</sup> and magnetic field measurements<sup>12)</sup> suggest a connection between the dipole moment and the odd-in-J polarization. Further analysis on this point will be possible only after all quantitative data from the magnetic field measurements on the thermal conductivity have become available.

#### References

1. Beenakker, J.J.M. and McCourt, F.R., *Ann. Rev. Phys. Chem.* **21** (1970) 47.
2. Beenakker, J.J.M., Knaap, H.F.P. and Sanctuary, B.C., *AIP Conference Proc.* **11** (1973) 12.
3. Beenakker, J.J.M., *Lecture Notes in Physics*, Vol. **31**, Springer-Verlag, Berlin, 1974, p. 414; Snider, R.F., *ibid.*, p. 469.
4. Coope, J.A.R. and Snider, R.F., *J. Chem. Phys.* **56** (1972) 2056.
5. Coope, J.A.R. and Snider, R.F., *J. Chem. Phys.* **57** (1972) 4266.
6. Moraal, H., *Physics Reports* **17** (1975) 225.
7. Hulsman, H., Van Kuik, F.G., Walstra, K.W., Knaap, H.F.P. and Beenakker, J.J.M., *Physica* **57** (1972) 501.
8. Burgmans, A.L.J., Van Ditzhuyzen, P.G., Knaap, H.F.P. and Beenakker, J.J.M., *Z. Naturforsch.* **28a** (1973) 835.
9. De Groot, J.J., Van den Broeke, J.W., Martinius, H.J., Van den Meijdenberg, C.J.N. and Beenakker, J.J.M., *Physica* **56** (1971) 388.
10. Korving, J., *Physica* **46** (1970) 619.
11. Tommasini, F., Levi, A.C. and Scoles, G., *Z. Naturforsch.* **26a** (1971) 1098.

12. Thijsse, B.J., to be published.
13. De Groot, S.R. and Mazur, P., *Non-Equilibrium Thermodynamics*, North-Holland Publishing Comp., Amsterdam, 1962, p. 311.
14. Hooyma, G.J., Mazur, P. and De Groot, S.R., *Physica* 21 (1955) 355.
15. Mikhailova, Yu.V. and Maksimov, L.A., *Sov. Phys. JETP* 24 (1967) 1265.
16. Eggermont, G.E.J., Vestner, H. and Knaap, H.F.P., *Physica* 82A (1976) 23.
17. Edmonds, A.R., *Angular momentum in Quantum Mechanics*, Princeton University Press, Princeton, N.J., 1957.  
Rotenberg, M., Bivins, R., Metropolis, N. and Wooten, J.K., *The 3j- and 6j-symbols*, The Technology Press, M.I.T., Cambridge, Mass., 1969.
18. Snider, R.F., *Physica* 78 (1974) 387.
19. Keijser, R.A.J., Van den Hout, K.D., De Groot, M. and Knaap, H.F.P., *Physica* 75 (1974) 515.
20. Levi, A.C. and McCourt, F.R., *Physica* 38 (1968) 415.
21. Levi, A.C., McCourt, F.R. and Tip, A., *Physica* 39 (1968) 165.
22. Tommasini, F., Levi, A.C., Scoles, G., De Groot, J.J., Van den Broeke, J.W., Van den Meijdenberg, C.J.N. and Beenakker, J.J.M., *Physica* 49 (1970) 299.
23. Cederberg, J.W., Anderson, C.H. and Ramsey, N.F., *Phys. Rev.* 136 (1964) A960.
24. Flygare, W.H., Hüttner, W., Shoemaker, R.L. and Foster, P.D., *J. Chem. Phys.* 50 (1969) 1714.
25. Flygare, W.H., Schoemaker, R.L. and Hüttner, W., *J. Chem. Phys.* 50 (1969) 2414.
26. De Leeuw, F.H. and Dymanus, A., *Symp. Mol. Struct. Spectr.*, Columbus, Ohio, (1971), paper R 10.
27. Anderson, C.H. and Ramsey, N.F., *Phys. Rev.* 149 (1966) 14.
28. Cederberg, J.W., Anderson, C.H. and Ramsey, N.F., *Phys. Rev.* 136 (1964) A960.
29. Johnson, C.M., Trambarulo, R. and Gordy, W., *Phys. Rev.* 84 (1951) 1178.  
Jones, E.W., Popplewell, R.J.L. and Thompson, H.W., *Proc. Royal Soc. London* 290 (1966) 490.
30. Sullivan, T.E. and Frenkel, L., *J. Mol. Spectry.* 39 (1971) 185.
31. Hirota, E. and Morino, Y., *J. Mol. Spectry.* 33 (1970) 460.
32. Otake, M., Matsuniwa, C. and Morino, Y., *J. Mol. Spectry.* 28 (1968) 316.
33. Yin, P.K.L. and Narahari Rao, K., *J. Mol. Spectry.* 51 (1974) 199.
34. Sarka, K., Paporisek, D. and Narahari Rao, K., *J. Mol. Spectry.* 37 (1971) 1.
35. Benedict, W.S. and Plyler, E.K., *Can. J. Phys.* 35 (1957) 1235.
36. Norris, C.L., Pearson, E.F. and Flygare, W.H., *J. Chem. Phys.* 60 (1974) 1758.
37. Flygare, W.H. and Benson, R.C., *Mol. Phys.* 20 (1971) 225.
38. Stone, R.G., Pochan, J.M. and Flygare, W.H., *Inorg. Chem.* 8 (1969) 2647.

39. Kukolich, S.G. and Flygare, W.H., Chem. Phys. Lett. 6 (1970) 45.
40. Kukolich, S.G. and Flygare, W.H., Mol. Phys. 17 (1969) 2647.
41. Hulsman, H. and Knaap, H.F.P., Physica 50 (1970) 565.
42. Maryott, A.A. and Buckley, F., N.B.S. Circular 537 (1953).
43. Kestin, J. and Leidenfrost, W., Physica 25 (1959) 1033.
44. Smith, C.J., Phil. Mag. 44 (1922) 289.
45. Johnston, H.L. and McCloskey, K.E., J. Phys. Chem. 44 (1940) 1038.
46. Trautz, A. and Narath, A., Ann. Phys. 79 (1926) 637.
47. Douve, R.A., Maitland, G.C., Rigby, M. and Smith, E.B., Trans. Faraday Soc. 66 (1970) 1955.
48. Data Book, edited by Thermophysical Properties Research Center, Purdue University, Lafayette, Indiana, 1966, Vol. 2.
49. McCoubey, J.C. and Singh, N.M., Trans. Faraday Soc. 53 (1957) 877.
50. Casparian, A.S. and Cole, R.H., J. Chem. Phys. 60 (1974) 1106.
51. Svehla, R.A., NASA Technical Report R-132, 1962.
52. Rankine, A.O. and Smith, C.J., Phil. Mag. 42 (1921) 601.
53. Iwasaki, H., Kestin, J. and Nagashima, A., J. Chem. Phys. 40 (1964) 2988.
54. Baas, F., Phys. Letters 36A (1971) 107;  
Baas, F., Thesis Leiden (1976);  
Baas, F. *et al.*, Physica, to be published.
55. Korving, J., Physica 50 (1970) 27.
56. Hulsman, H., Van Waasdijk, E.J., Burgmans, A.L.J., Knaap, H.F.P. and Beenakker, J.J.M., Physica 50 (1970) 53.
57. Birnbaum, G., J. Chem. Phys. 27 (1957) 360.
58. Adair, III, T.W. and McClurg, G.R., Phys. Rev. A2 (1970) 1986.
59. Köhler, W.E., Hess, S. and Waldmann, L., Z. Naturforsch. 25a (1970) 336.
60. Levi, A.C. and Tommei, G.E., Z. Naturforsch. 26a (1971) 952.
61. Snider, R.F., private communication.
62. Moraal, H., Z. Naturforsch. 29a (1974) 299.



## CHAPTER II

THE TEMPERATURE DEPENDENCE OF THE VISCOMAGNETIC  
EFFECT IN THE HYDROGEN ISOTOPES

1. *Introduction.* The Senftleben-Beenakker effect, *i.e.*, the change in transport properties of polyatomic gases by external fields, has proven to be a useful tool in the study of collision processes between nonspherical molecules. For a survey see *e.g.*, refs. 1 through 5. Experiments on the influence of magnetic fields on the shear viscosity were performed earlier for gases like  $N_2$ , CO,  $CH_4$  and HD at various temperatures (see *e.g.*, refs. 6, 7, 8 and Chapter I). For these gases the relative change in viscosity was found to be of the order  $10^{-3}$ . For the homonuclear hydrogen isotopes which are almost spherical the effect was found to be of the order  $10^{-5}$  <sup>9)</sup>. This is the reason that no accurate experimental results have as yet been published on these systems notwithstanding the fact that the hydrogen isotopes are of special interest. Below 300 K  $H_2$  and  $D_2$  are in low rotational states due to their small moments of inertia (see fig. 1). Therefore, by performing measurements as a function of temperature the dependence of the viscomagnetic effect on the rotational quantum number can be studied. Further information can be obtained by investigating the ortho and para modifications of these gases. The various characteristics of these modifications are presented in Table I.

Table I

Some properties of $H_2$ , $D_2$ and HD				
rotational temperature $\theta = \frac{\hbar^2}{2I_0 K}$ (K)	modification	total nuclear spin I	statistical weight $g_I$	rotational states J
$H_2$ 85.3	ortho	1	3	1, 3, 5, ...
	para	0	1	0, 2, 4, ...
$D_2$ 43.0	ortho	2 0	5 1	0, 2, 4, ...
	para	1	3	
HD      64.3	no ortho and para modifications			0, 1, 2, ...

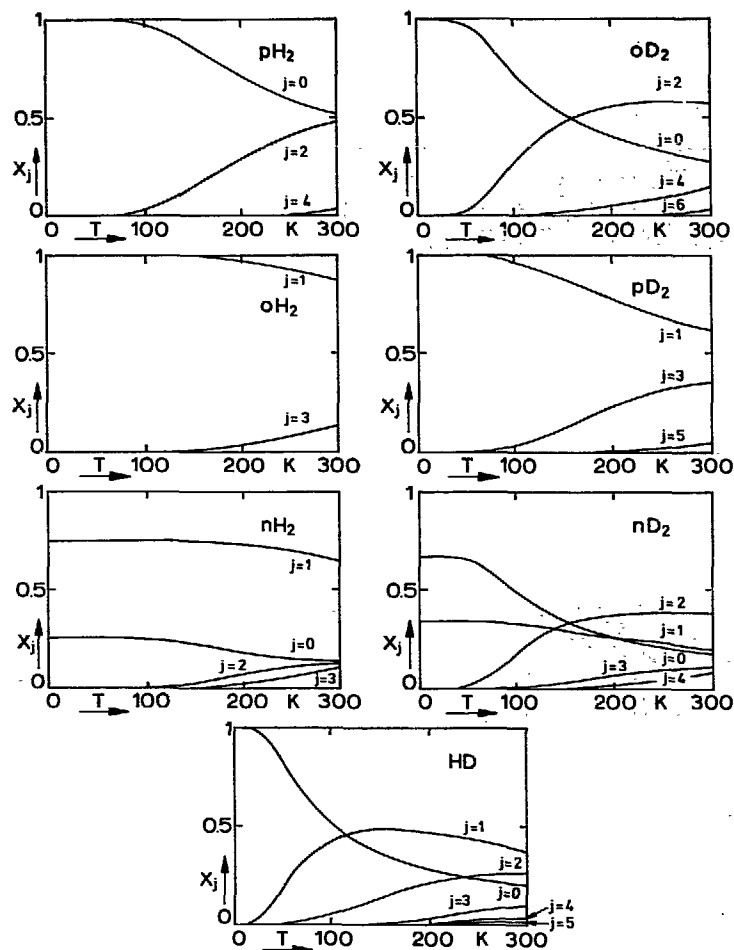


Fig. 1 The occupation of rotational energy levels as a function of temperature for the different modifications of  $H_2$  and  $D_2$  and for HD (see also table I).

In this paper measurements are reported on the viscomagnetic effect for normal hydrogen ( $nH_2$ ,  $\frac{3}{4}$  ortho and  $\frac{1}{4}$  para), para hydrogen ( $pH_2$ ), normal deuterium ( $nD_2$ ,  $\frac{2}{3}$  ortho and  $\frac{1}{3}$  para) and ortho deuterium ( $oD_2$ ) in the temperature range from 100 to 300 K. The experimental results are given in terms of effective cross sections. The results are discussed together with those of HD as obtained by Burgmans *et al.*<sup>8</sup>). Qualitative conclusions on various collision processes will be drawn.

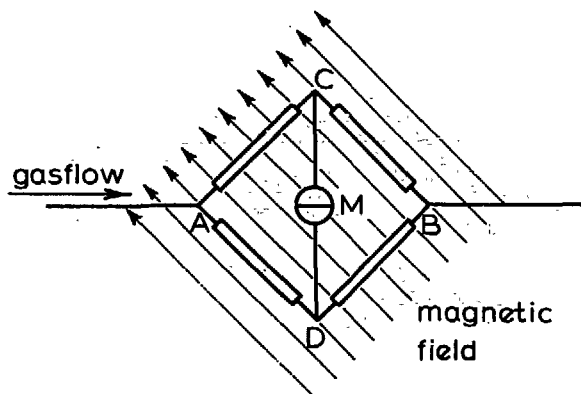


Fig. 2 Schematic diagram of the experimental set up.

**2. Measuring procedure and calculation of the results.** The apparatus is essentially the one described as apparatus II in ref. 8 with changes to improve the temperature stability. It consists of a Wheatstone bridge arrangement of four circular glass capillaries (length 65 mm, inner diameter 0.5 mm) placed in a magnetic field. Two capillaries are parallel and two perpendicular to the field (fig. 2). The viscosity change in a capillary parallel to the field is different from the change in a capillary perpendicular to the field. This difference shows up as a pressure difference between the points C and D which is measured by means of a capacitance manometer M. The observed pressure difference is related to the field effect on the viscosity by

$$-\frac{\eta_2^+ - \eta_1^+}{2\eta(0)} = 2 \frac{p_C - p_D}{p_A - p_B} f, \quad (1)$$

where  $\eta_1^+$  and  $\eta_2^+$  are (field dependent) elements of the shear viscosity tensor (see section 4) and  $\eta(0)$  is the field free viscosity coefficient. The correction factor  $f$  is given by (see also ref. 8):

$$f = \frac{2(p_C + K_\alpha)}{(p_A + K_\alpha) + (p_B + K_\alpha)} \left[ 1 + \frac{1}{16} (m + \frac{1}{2} \ln \frac{p_A}{p_B}) \frac{R}{\rho} \right] \left( 1 + \frac{K_\beta}{p} \right), \quad (2)$$

where the symbols have the same meaning as in eq. (30) of chapter I. The formula contains correction factors for (a), the expansion of the gas in the capillary (at most 1.04), for (b), the pressure losses caused by acceleration of the gas at the entrance of the capillary and in the capillary (at most 0.01) and for (c), Knudsen effect (at most 1.25).

The Knudsen correction is caused by the fact that in the experimental situation the mean free path of the molecules is not negligible as compared to the diameter of the capillaries. A Knudsen correction has also to be applied to the position along the  $H/p$  axis. This correction on the experimental  $H/p$  values is of the form

$$H/p = (H/p)_{\text{exp}} / (1 + K_{\gamma}/p). \quad (3)$$

The quantities  $K_{\beta}$  and  $K_{\gamma}$  (see table II) are experimentally determined by extrapolation to  $p = \infty$  following a procedure described earlier<sup>6</sup>). The correction for the magnitude of the effect is at most 25% and for the  $H/p$  values at most 33% in this experiment. Analogous to the procedure used in chapter I Knudsen numbers  $n_{\beta}$  and  $n_{\gamma}$  are introduced, defined by  $K_{\beta,\gamma} = n_{\beta,\gamma} p \xi / R$  where  $p = (p_A + p_B)/2$  is the mean pressure,  $R$  is the radius of the capillary and  $\xi$  is the mean free path, defined by  $\xi = \frac{4}{5} \frac{\eta}{p} \sqrt{\frac{8kT}{\pi m}}$ , where  $m$  is the molecular mass. This definition is in agreement with the definition used in refs. 7, 8. The numbers  $n_{\beta}$  and  $n_{\gamma}$  were found to be independent of temperature within the measuring accuracy, which is in agreement with ref. 8. Note that the

Table II

Knudsen correction parameters									
nH <sub>2</sub>					pH <sub>2</sub>				
T (K)	K <sub>β</sub> (torr)	K <sub>γ</sub> (torr)	n <sub>β</sub>	n <sub>γ</sub>	T (K)	K <sub>β</sub> (torr)	K <sub>γ</sub> (torr)	n <sub>β</sub>	n <sub>γ</sub>
293	4.0	7.5	12	24	293	5.0	8.0	12	25
247	4.4	7.7			243	4.5	8.5		
198	2.5	5.7			198	3.0	5.7		
140	2.2	4.2			151	1.6	4.1		
nD <sub>2</sub>					oD <sub>2</sub>				
T (K)	K <sub>β</sub> (torr)	K <sub>γ</sub> (torr)	n <sub>β</sub>	n <sub>γ</sub>	T (K)	K <sub>β</sub> (torr)	K <sub>γ</sub> (torr)	n <sub>β</sub>	n <sub>γ</sub>
293	1.7	6.4	5	18	293	1.8	6.1	5	21
248	1.4	5.8			249	1.3	7.1		
186	1.4	5.2			200	1.3	5.9		
140	0.7	2.6			155	0.9	3.9		
					102	0.5	2.2		

corresponding Knudsen number for the field free flow is given by  $n_{\alpha} = 4^{6,8}$ ). Within the experimental accuracy the values of  $n_{\beta}$  for  $nH_2$  and  $pH_2$  (see Table II) are the same as those for gases like  $N_2$ ,  $CO$ ,  $CH_4$  and  $HD^{7,8}$ ) whereas for  $nD_2$  and  $oD_2$  the values of  $n_{\beta}$  are about a factor two smaller. The Knudsen numbers  $n_{\gamma}$  for  $H_2$  and  $D_2$  are found to be much larger than those obtained for heavier molecules like  $N_2$ ,  $CO$  and  $CH_4$ . This is also found for  $HD^{7,8}$ ). This means that for the hydrogen isotopes the wall makes itself felt over a larger distance in the gas corresponding to the fact that the reorientation time for the angular momentum is long compared to the time scale of elastic collisions. For a detailed discussion on this subject see ref. 10.

**3. Purity of the gases.** Since the effects of  $H_2$  and  $D_2$  are two or three orders of magnitude smaller than those of gases like  $N_2$ ,  $O_2$  or even  $HD$ , great care must be taken with respect to the purity of the gases. Nonisotopic impurities were removed by the standard method of condensing the gases at 20.4 K which reduces the fraction of nonisotopic impurities to less than  $1 \times 10^{-4}$  as shown in previous experiments<sup>11</sup>). Air in such minute amounts will not seriously affect the results; this is the more true because the effects for  $H_2$  and  $D_2$  occur at  $H/p$  values which are far different from those for  $O_2$  and  $N_2$ . With the above mentioned method isotopic impurities like  $HD$  are not removed. These could seriously affect the measurements: one percent of  $HD$  causes an effect which is of the same order of magnitude as the effect of  $H_2$  or  $D_2$ . In  $H_2$ , the (natural) abundance of  $HD$  is 0.03% and can be neglected. In commercial  $D_2$  in general more  $HD$  is present. This was removed by rectification at 20 K as described in ref. 12. Thus the fraction of  $HD$  in  $oD_2$  was reduced to less than 0.2% in  $oD_2$  and to less than 0.1% in  $nD_2$  as measured by a mass spectrometer. Above 180 K this purity is sufficient. As the effect of  $D_2$  decreases with temperature as opposed to the behavior of  $HD$ , at still lower temperatures the small amount of  $HD$  might affect the  $D_2$  results as far as magnitude is concerned. Since the position of the curves of  $D_2$  and  $HD$  differ by a factor 2 only, the influence of the small amount of  $HD$  on the position of the effects for  $D_2$  can be neglected.

**4. Experimental results. 4.1 General.** The gases  $nH_2$ ,  $pH_2$ ,  $nD_2$  and  $oD_2$  have been investigated. In figs. 3, 4, 5 and 6 the relative viscosity changes  $-(\eta_2^+ - \eta_1^+)/2\eta(0)$  (see eq. (1)) are presented as a function of  $H/p$  at various temperatures. The notation as introduced by Coope and Snider is used<sup>13</sup>), where  $\eta_0^+$ ,  $\eta_1^+$  and  $\eta_2^+$  are even-in-field coefficients and  $\eta_1^-$  and  $\eta_2^-$  are odd-in-field coefficients. The viscosity change measured here can also be given in the notation of De Groot and Mazur<sup>14,15</sup>)

$$-\frac{\eta_2^+ - \eta_1^+}{2\eta(0)} = -\frac{2\eta_2 - \eta_1 - \eta_3}{2\eta(0)} \quad (4)$$

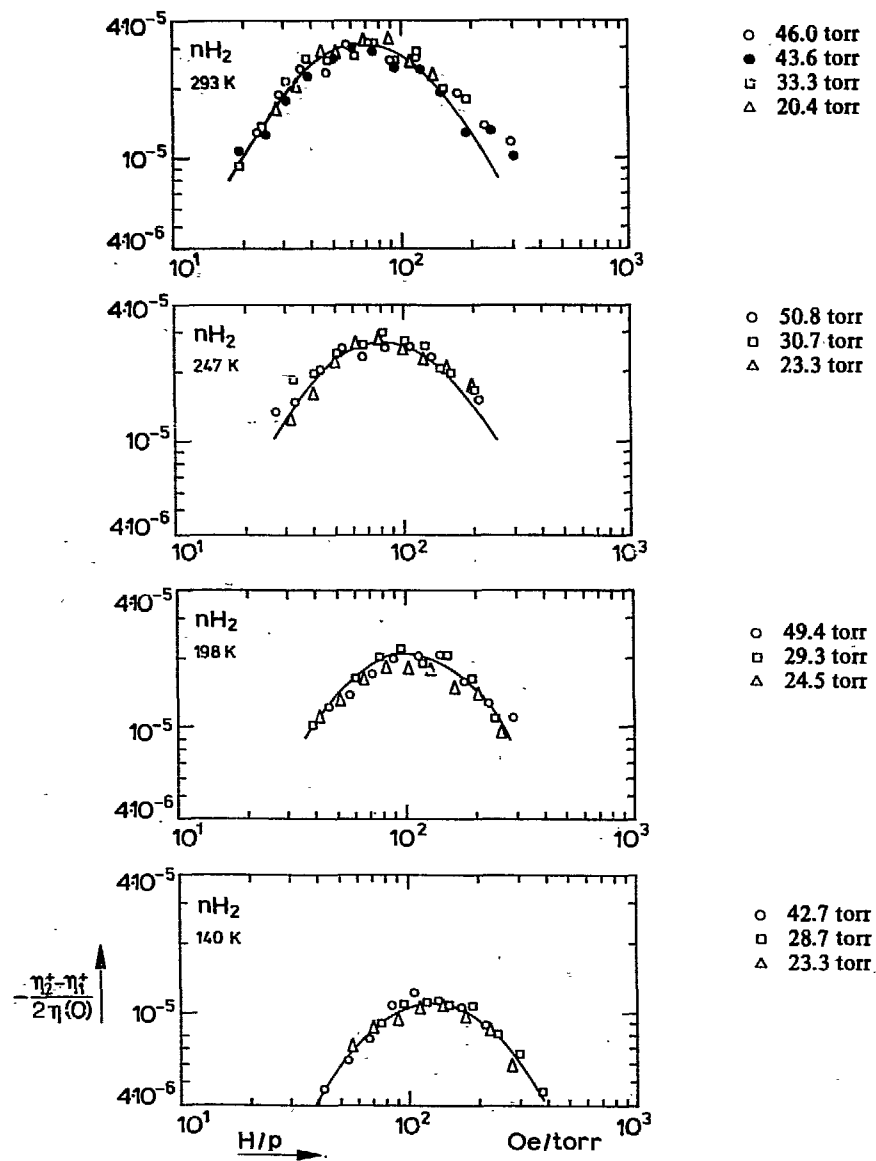


Fig. 3  $-(\eta_2^+ - \eta_1^+)/2\eta(0)$  versus  $H/p$  for  $nH_2$  at various temperatures.  
 — theoretical  $H/p$  dependence for the angular momentum tensor polarization of type  $\overline{II}$  scaled to the experimental points.

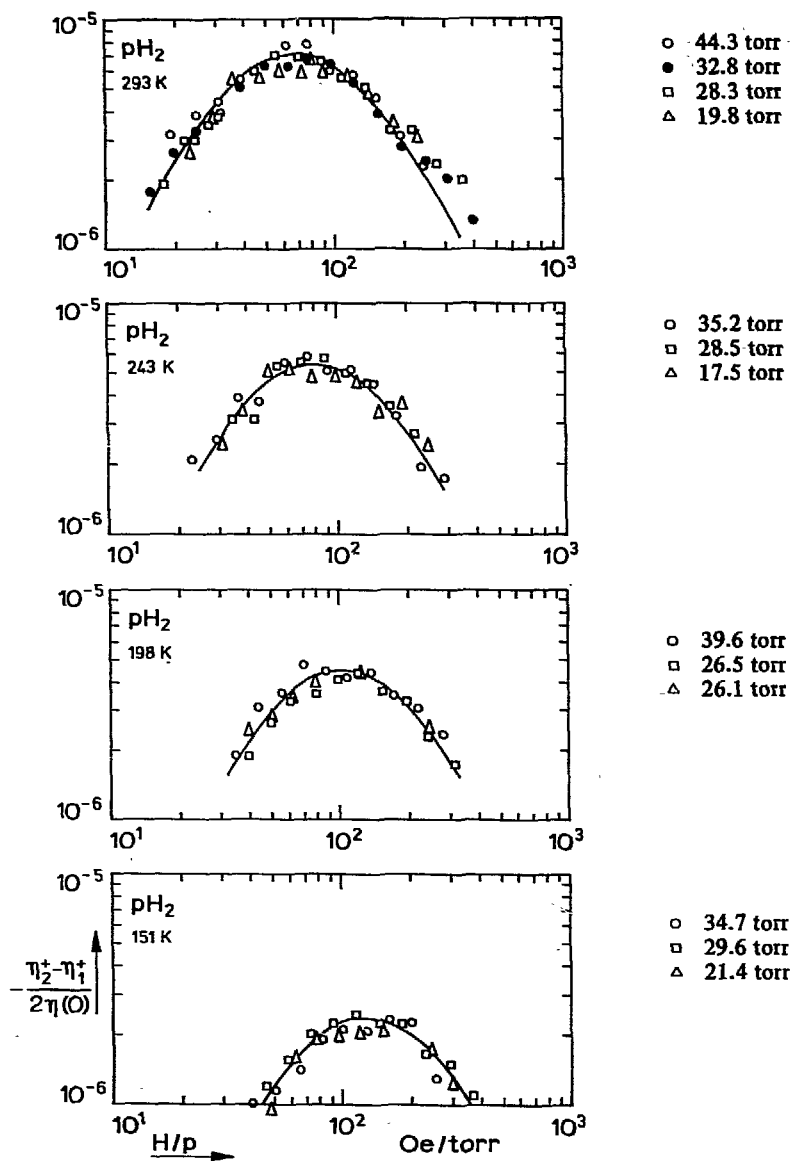


Fig. 4  $-(\eta_2^+ - \eta_1^+)/2\eta(0)$  versus  $H/p$  for  $pH_2$  at various temperatures.  
 — theoretical  $H/p$  dependence for the angular momentum tensor polarization of type  $\overline{II}$  scaled to the experimental points.

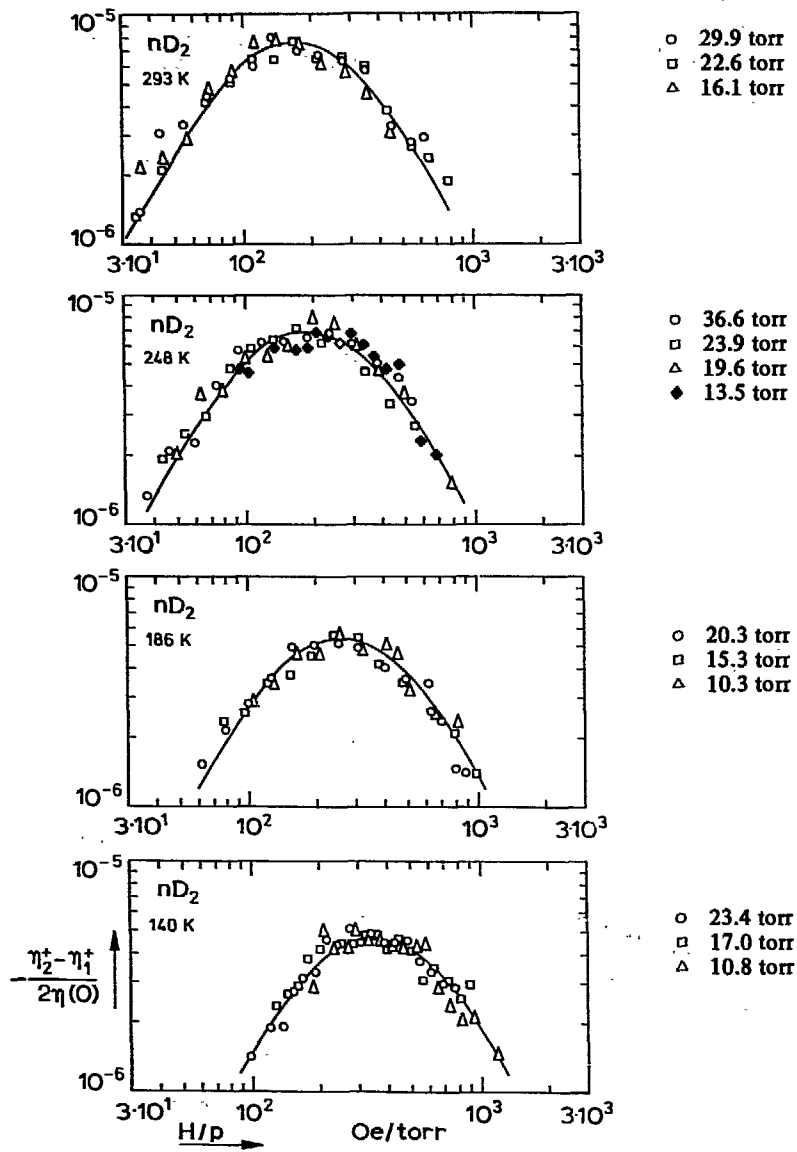


Fig. 5  $-(\eta_2^+ - \eta_1^+)/2\eta(0)$  versus  $H/p$  for  $nD_2$  at various temperatures.  
 — theoretical  $H/p$  dependence for the angular momentum tensor polarization of type  $\underline{II}$  scaled to the experimental points.



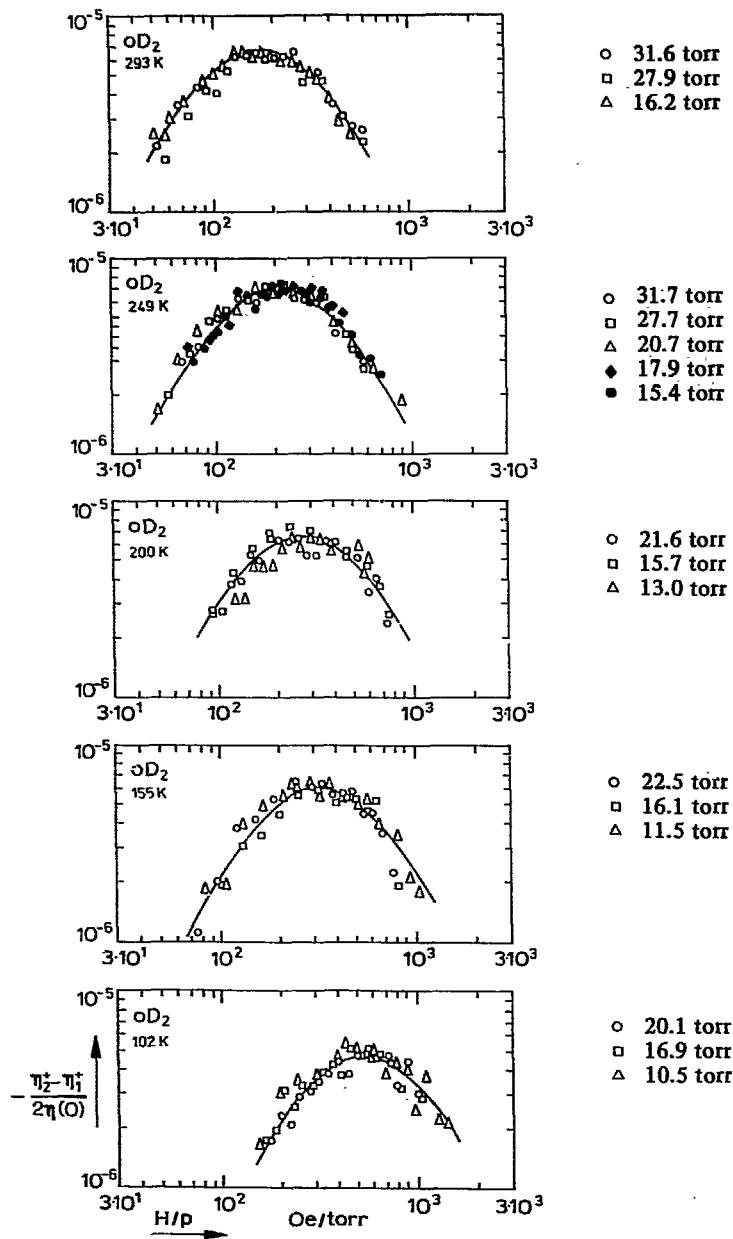


Fig. 6  $-(\eta_2^* - \eta_1^*)/2\eta(0)$  versus  $H/p$  for  $oD_2$  at various temperatures.  
 — theoretical  $H/p$  dependence for the angular momentum tensor polarization of type  $\underline{J}$  scaled to the experimental points.

The data shown in the figures have been corrected according to eqs. (1) through (3). For each curve, the coordinates of the maximum are given in table III. Below 100 K no effect could be detected. The solid lines drawn in figs. 3, 4, 5 and 6 are theoretical curves. These are derived under the assumption that only one angular momentum dependent tensor polarization of the form  $\overline{J_i J_j} R(J^2)$ , plays a role ( $R(J^2)$  is a function of  $J^2$ , with  $\underline{J}$  the angular momentum, and  $\overline{\quad}$  indicates the symmetric traceless part of a tensor e.g.,  $\overline{J_i J_j} = \frac{1}{2} J_i J_j + \frac{1}{2} J_j J_i - \frac{1}{3} \delta_{ij} J^2$ ). The field dependence arising from such a polarization is given by<sup>2)</sup> (see e.g., chapter I)

$$-\frac{\eta_2^+ - \eta_1^+}{2\eta(0)} = \frac{1}{2} \Psi_{02} \left[ \frac{4\xi_{02}^2}{1 + 4\xi_{02}^2} - \frac{\xi_{02}^2}{1 + \xi_{02}^2} \right]. \quad (5)$$

The maximum of the curve occurs at  $\xi_{02} = 2^{-1/2}$  and has the value  $\frac{1}{6} \Psi_{02}$ . The quantities  $\Psi_{02}$  and  $\xi_{02}$  are given by

$$\Psi_{02} = \frac{\mathfrak{S}_{(20)}^2 \mathfrak{S}_{(20)}^{(02)}}{\mathfrak{S}(20) \mathfrak{S}(02)}, \quad (6)$$

$$\xi_{02} = \frac{1}{\langle v \rangle_0} \frac{g \mu_N k T}{\hbar} \frac{H}{p}. \quad (7)$$

The field free viscosity coefficient  $\eta(0)$  is given by

$$\eta(0) = \frac{kT}{\langle v \rangle_0 \mathfrak{S}(20)} \quad (8)$$

with  $\langle v \rangle_0 = \sqrt{16kT/\pi m}$  is the mean relative velocity. The quantities,  $k$ ,  $\hbar$ ,  $T$  and  $p$  have their usual meanings.  $g$  is the molecular  $g$ -factor,  $\mu_N$  the nuclear magneton and  $m$  the molecular mass. The  $\mathfrak{S}$ 's are effective cross sections, already defined in ref. 8.  $\mathfrak{S}(20)$  is the viscosity cross section describing the decay of the velocity polarization of the form  $\overline{W W}$  ( $W$  is the reduced velocity). The effective cross section  $\mathfrak{S}(02)$  describes the decay of the (tensorial) polarization of the angular momentum. The coupling cross section  $\mathfrak{S}_{(20)}^{(02)}$  describes the production of angular momentum polarization from velocity polarization. Figs. 3, 4, 5 and 6 show that the experimental data can be well described by the  $H/p$  dependence as given by eq. (5), with the possible exception of  $nH_2$  and  $pH_2$  at room temperature (see section 5). The fit of the theoretical curve to the experimental data has been performed with two adjustable parameters:  $\mathfrak{S}(02)$  for the position of the curve along the  $H/p$  axis and  $\Psi_{02}$  for the magnitude of the effect.

Table III

Experimental results at various temperatures						
T	$\eta(0)$	$16) \left(\frac{H}{p}\right)_{\max}$	$\left(-\frac{\eta_2^+ - \eta_1^+}{2\eta(0)}\right) 10^6$	$\mathcal{C}(20)$	$\mathcal{C}(02)$	$\mathcal{C}(\frac{02}{10}) 10^3$
(K)	$(10^{-6} \text{ P})^*$	(Oe/torr)		(A <sup>2</sup> )	(A <sup>2</sup> )	(A <sup>2</sup> )
nH <sub>2</sub>						
293	87.2 ± 0.9	70 ± 4	3.1 ± 0.6	18.7 ± 0.2	0.51 ± 0.05	13.3 ± 0.8
247	78.8 ± 0.8	84 ± 5	2.7 ± 0.2	19.0 ± 0.2	0.56 ± 0.05	13.4 ± 0.8
198	67.8 ± 0.7	104 ± 5	2.1 ± 0.1	19.8 ± 0.2	0.62 ± 0.04	12.4 ± 0.5
140	53.7 ± 0.5	130 ± 5	1.1 ± 0.1	21.0 ± 0.2	0.66 ± 0.04	9.7 ± 0.4
pH <sub>2</sub>						
293	87.2 ± 0.9	67 ± 4	7 ± 1	18.7 ± 0.2	0.49 ± 0.05	19 ± 1
243	78.0 ± 0.8	80 ± 2	5.4 ± 0.4	19.0 ± 0.2	0.53 ± 0.04	18 ± 1
198	67.8 ± 0.7	104 ± 4	4.5 ± 0.4	19.8 ± 0.2	0.62 ± 0.04	18.3 ± 0.8
151	56.5 ± 0.6	130 ± 5	2.4 ± 0.2	20.7 ± 0.2	0.66 ± 0.04	14.0 ± 0.8
nD <sub>2</sub>						
293	124 ± 1	170 ± 15	7.4 ± 0.6	18.7 ± 0.2	0.88 ± 0.08	27 ± 2
248	110 ± 1	190 ± 20	7.0 ± 0.8	19.0 ± 0.2	0.91 ± 0.09	27 ± 2
186	90.8 ± 0.9	260 ± 20	5.4 ± 0.4	19.9 ± 0.2	1.07 ± 0.08	26 ± 2
140	75.2 ± 0.8	350 ± 25	4.7 ± 0.3	21.1 ± 0.2	1.26 ± 0.09	27 ± 2
oD <sub>2</sub>						
293	124 ± 1	175 ± 15	6.6 ± 0.3	18.7 ± 0.2	0.91 ± 0.08	26 ± 2
249	110 ± 1	210 ± 20	7.0 ± 0.4	19.0 ± 0.2	1.0 ± 0.1	28 ± 2
200	95.5 ± 0.9	270 ± 30	6.6 ± 0.5	19.7 ± 0.2	1.2 ± 0.1	30 ± 2
155	80.6 ± 0.8	320 ± 30	6.0 ± 0.6	20.6 ± 0.2	1.2 ± 0.1	30 ± 2
102	60.0 ± 0.6	530 ± 50	4.6 ± 0.5	22.7 ± 0.2	1.6 ± 0.2	30 ± 2

\*  $10^{-6} \text{ P} = 10^{-7} \text{ Pa.s}$

4.2. *The position of the curve.* Values of  $H/p$  for which the effect reaches a maximum,  $(H/p)_{\max}$ , are given in table III. Using eqs. (5) and (7) an expression can be obtained for the effective cross section  $\mathcal{C}(02)$  in terms of  $(H/p)_{\max}$ :

$$\mathcal{C}(02) = 2^{1/2} \frac{g \mu_N k T}{\hbar \langle v \rangle_0} \left(\frac{H}{p}\right)_{\max} \quad (9)$$

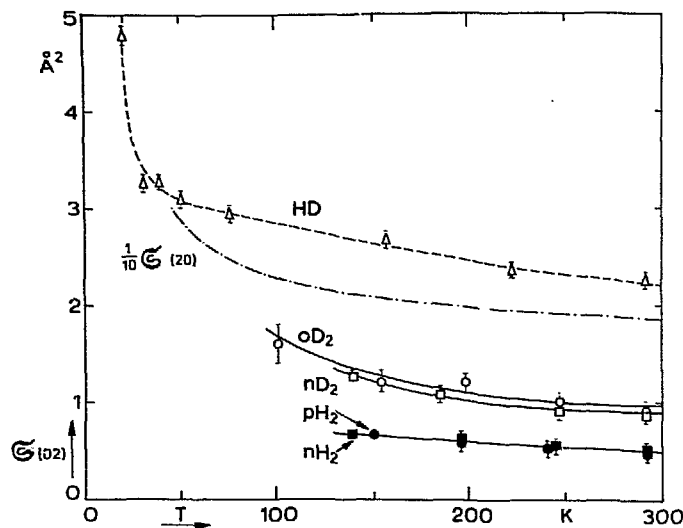


Fig. 7 Effective (reorientation) cross section  $\mathcal{S}(02)$  versus temperature for  $nH_2$ ,  $pH_2$ ,  $nD_2$ ,  $oD_2$ , and HD. The values for HD have been taken from ref. 8. For comparison the viscosity cross section  $\mathcal{S}(20)$  for these hydrogen isotopes is given as well.

Using for hydrogen  $g = +0.883$  and for deuterium  $g = +0.443$  values for this cross section at various temperatures are listed in table III, together with the values of the viscosity cross section  $\mathcal{S}(20)$ , which have been calculated from data on the field free viscosity coefficient using eq. (8)<sup>16</sup>. In fig. 7  $\mathcal{S}(02)$  is plotted versus temperature for  $nH_2$ ,  $pH_2$ ,  $nD_2$  and  $oD_2$ . For comparison the cross section  $\mathcal{S}(02)$  for HD is also given. For a discussion of the results see section 5.

4.3. *The magnitude of the viscosity change.* In fig. 8 the maximum of the viscomagnetic effect is plotted versus temperature for  $nH_2$ ,  $pH_2$ ,  $nD_2$  and  $oD_2$  (see also table III). Note that the magnitude of the effect for  $oD_2$  may be somewhat too large at the lowest temperatures due to small amounts of HD as described in section 3. With eq. (6) the value of  $|\mathcal{S}_{20}^{(02)}|$  can be obtained from

$$|\mathcal{S}_{20}^{(02)}| = [6 \{-(\eta_2^* - \eta_1^*)/2\eta(0)\}_{\max} \mathcal{S}(20) \mathcal{S}(02)]^{1/2}, \quad (10)$$

using the values of  $\mathcal{S}(20)$  and  $\mathcal{S}(02)$  as determined in the preceding section. The sign of this coupling cross section can not be determined by this experiment and has been obtained from flow birefringence experiments<sup>17,18</sup> where  $\mathcal{S}_{20}^{(02)}$  was found to be positive for all four gases. Values for  $\mathcal{S}_{20}^{(02)}$  are listed in table III and are plotted versus temperature in fig. 9. The coupling cross section of HD as determined by Burgmans *et al.*<sup>8</sup> is given as well.

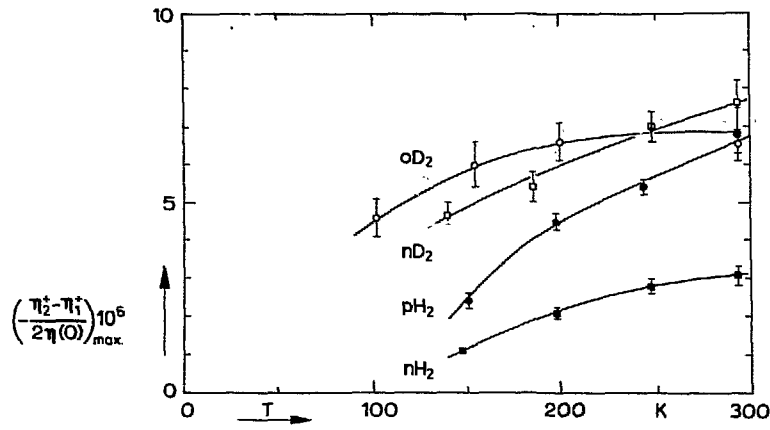


Fig. 8 The maximum of the measured viscosity change  $\{-(\eta_2^+ - \eta_1^+)/2\eta(0)\}_{\max}$  for  $\text{nH}_2$ ,  $\text{pH}_2$ ,  $\text{nD}_2$  and  $\text{oD}_2$  versus temperature.

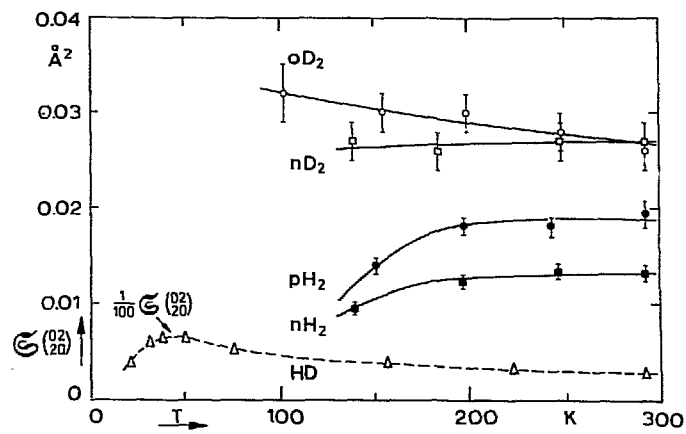


Fig. 9 The coupling cross section  $\mathcal{S}_{(02)/(20)}^2$  for  $\text{nH}_2$ ,  $\text{pH}_2$ ,  $\text{nD}_2$ ,  $\text{oD}_2$  and  $\text{HD}$  versus temperature. The values for  $\text{HD}$  have been taken from ref. 8.

5. *Discussion.* The equation for the field dependence of the viscosity (eq. (5)) is valid under the assumption that only one relaxation time describes the decay of the angular momentum polarization. It has been shown in measurements of the Depolarized Rayleigh line<sup>19</sup>, that in general more relaxation times are needed to describe the decay of the angular momentum polarization. These have been shown to correspond to the decay of the angular momentum polarization in different rotational states. However, the distribution of relaxation times has such a narrow shape (see table V of ref. 19) that the effective relaxation times do not differ more than about 2% for H<sub>2</sub> while for HD and D<sub>2</sub> the spread is not more than 10%. One should not expect that this (narrow) distribution of relaxation times will show up in our experiment as a curve that is considerably broader than the one relaxation time curve of eq. (5). Therefore, the one relaxation time description has been used throughout and effective cross sections have been calculated on this basis. This may to some extent introduce a systematic error in the values of  $\mathcal{S}(02)$  and  $\mathcal{S}_{20}^{(02)}$ . Especially for D<sub>2</sub> and HD the values of these cross sections found from this experiment and from ref. 8 may deviate about 10% from the values found in the Depolarized Rayleigh experiments.

It is seen from the room temperature measurements of H<sub>2</sub> (see figs. 3 and 4) that slight deviations from the curve of eq. (5) occur. These cannot be attributed to the occurrence of a  $\overline{W\overline{W}} \overline{J\overline{J}}$  polarization as this would narrow the experimental curves, as can be seen from eq. (10) in chapter I. Instead, they may be caused by e.g., a  $\overline{W\overline{W}} \underline{J}$  polarization. However, the deviations are too small to draw any more definite conclusions.

Finally, it should be remarked that on the basis of the experimental single parameter curve only it is not possible to decide on the precise form of the angular momentum tensor polarization. In this paper therefore the symbol 02 in  $\mathcal{S}(02)$  stands for a polarization of the form  $\overline{J\overline{J}} R(J^2)$  where  $R(J^2)$  is some function of  $J^2$ .

6. *The behavior of the cross sections.* In the following a qualitative discussion will be given of the results of  $\mathcal{S}(02)$ , the reorientation cross section, and of  $\mathcal{S}_{20}^{(02)}$ , the cross section which describes the production of angular momentum polarization from velocity polarization. As energetically inelastic collision processes play an important role both in  $\mathcal{S}(02)$  and  $\mathcal{S}_{20}^{(02)}$ , the purely inelastic cross section  $\mathcal{S}(0001)$ , which is determined from sound absorption measurements, will also be considered. The values of  $\mathcal{S}(0001)$  for H<sub>2</sub> and D<sub>2</sub> are given in tables IV and V. These tables give also the cross sections obtained from the Senftleben-Beenakker effect for heat conductivity and viscosity and from Depolarized Rayleigh light scattering experiments for H<sub>2</sub>, D<sub>2</sub> and HD.

Concerning the temperature dependence of the effective cross sections it can, in general, be stated that the effective cross sections that are governed by elastic collisional processes (e.g.,  $\mathcal{S}(20)$ ) will increase at lower temperatures approximately

Table IV

Effective cross sections for  $H_2$  from various experimental sources represented in  $\text{Å}^2$ . For method of calculation see appendix. Numbers between parentheses are interpolated values.

source	$\mathcal{E}(0001)$	$\mathcal{E}(0010)$	$\mathcal{E}(2000)$	$\mathcal{E}(0200)$	$\mathcal{E}(1010)$	$\mathcal{E}(1001)$	$\mathcal{E}(1200)$	$\mathcal{E}(\frac{1100}{1000})$	$\mathcal{E}(\frac{1101}{1001})$	$\mathcal{E}(\frac{1110}{1010})$	$\mathcal{E}(\frac{1111}{1011})$	$\mathcal{E}_{DPR}$	$\tilde{\mathcal{E}}_{DPR}$
	$\eta_v$	$\eta_v$	$\eta(0)$	$(\frac{H}{P})$	$\eta_v, \eta(0)$	$\lambda(0)$	$(\frac{H}{P})$	$\frac{\Delta\eta}{\eta}$	$\eta_v$	$\frac{\Delta\eta}{\eta}$	$\frac{\Delta\lambda}{\lambda}$	D.P.R.	D.P.R.
	20,21,22,23,24,		16,	this exp.		25,	11,26,	this exp.			11,26,	19,	19,
$oH_2$ T= 293 K	0.073	0.045	18.7		12.5								
269	0.073	0.042	18.8		12.6							0.037	
233	0.076	0.038	19.3		12.9							0.036	
170	0.049	0.013	20.2		13.5							0.035	
												0.016	
$pH_2$ T= 293 K	0.106	0.077	18.7	0.49	12.6	13	15	0.019	0.059	-0.009	0.20	0.53	0.53
243			19.0	0.53				0.018		-0.008			
198			19.8	0.62				0.018		-0.008			
170	0.065	0.064	20.2		13.5	22			0.042				
151			20.7	0.66				0.014		-0.006			
111	(0.043)	(0.029)	22.0		14.7	27	15		0.023		0.56		
100	(0.043)	(0.022)	22.7		(15.2)	(27)	15		(0.020)		0.45		
90	0.042	0.015	23.1		15.5	28			0.016				
86	(0.041)	(0.012)	23.8		(16.0)	(28)	15		(0.014)		0.44		
77.3	0.038	0.008	24.2		16.2	29			0.011				
$nH_2$ T= 293 K	0.087	0.056	18.7	0.51	12.6	14	17	0.013	0.045	-0.006	0.20	0.508	0.500
247			19.0	0.56				0.013		-0.006			
198			19.8	0.62				0.012		-0.005 <sup>s</sup>			
140			21.0	0.66				0.010		-0.004			
110			22.0										
100			22.7										
85			23.8										
77.3	0.050	0.003	24.3		16.3	29			0.007				
26.4			39.6										

$(-\frac{\lambda_{tr}}{\lambda})_{max} = 2 \times 10^{-4}$   
 $< 3 \times 10^{-4}$   
 $< 3 \times 10^{-4}$   
 $(-\frac{\lambda_{tr}}{\lambda})_{max} < 2 \times 10^{-4}$

Table V

source	$\tau_v$ 20,27,28,29	$\tau_v$ (0.010)	$\tau(0)$ (2000)	$\frac{H}{p}$ (0200)	$\tau_v, \tau(0)$ (1010)	$\lambda(0)$ (1001)	$\frac{H}{p}$ (1200)	$\frac{\Delta\tau}{\tau}$ (this exp., 8)	$\tau_v$ (1111)	$\frac{\Delta\tau}{\tau}$ (1111)	$\frac{\Delta\lambda}{\lambda}$ (11,26,31)	$\frac{\Delta\lambda}{\lambda}$ (11,26,31)	D.P.R. 19)	D.P.R. 19)
$\text{eD}_1$ T = 293	K 0.126	0.084	18.7	0.91	12.6	11	18	0.026	0.067	-0.012	0.21			
249			19.0	1.0	13.3	15		0.28		-0.013				
200	0.139	0.095	19.7	1.2	13.3	15		0.030	0.074	-0.014				
155			20.6	1.2	14.3	20		0.030		-0.014				
135	0.136	0.105	21.2	1.6	14.3	20		0.032	0.077	-0.014				
102			22.7											
90	0.100	0.096	23.4		15.8	27			0.064		1.13			
85	(0.094)	(0.092)	23.8		(16.1)	(27)	20		(0.060)					
77.3	0.087	0.083	24.5		16.5	29			0.055					
52.5	0.068	0.038	18.8		20.4	19			0.024					
44.5	0.065	0.021	30.5		21.4	18			0.022					
40.6	0.071	0.017	32.0		23.4	16			0.012					
31.2	0.073	0.005	34.9											
$\text{mD}_1$ T = 293	K 0.145	0.096	18.7	0.88	12.6	11	14	0.027	0.077	-0.012	0.17			0.93
248			19.0	0.91				0.027		-0.012				
186			19.9	1.07				0.026		-0.012				
141			21.1	1.26				0.027		-0.012				
85	(0.118)	(0.087)	23.7		(15.9)	(30)	18		(0.065)		0.21			
77.3	0.116	0.080	24.2		16.3	31			0.063					
26.4			39.6											
$\text{HD T} = 293$	K 1.1	0.76	18.7	2.26	13.2	13.5	14	0.28	0.58	-0.13	0.67			2.95
224	(1.2)	(0.81)	19.5	2.3	(13.9)	(14)	(15)	0.32	(0.64)	-0.14	(0.69)			
190	(1.3)	(0.89)	20.0	(2.4)	(14.2)	(14.5)	(15)	(0.34)	(0.69)	(-0.15)	(0.70)			
157	(1.5)	(1.0)	20.7	2.67	(14.9)	(15)	(16)	0.38	(0.79)	(-0.17)	(0.75)			
150	(1.6)	(1.1)	20.9	(2.70)	(15.1)	(15)	(16)	(0.39)	(0.85)	(-0.17)	(0.75)			
77.3	2.0	1.4	24.5	2.95	17.6	(19)	(19)	0.52	1.10	(-0.23)	(0.87)			
60	(2.3)	(1.7)	26.7	(3.05)	(19.3)	22	20	(0.61)	(1.26)	(-0.27)	(0.90)			
51	(2.4)	(1.8)	28.5	3.09	(20.8)	(24.5)	(21)	(0.64)	(1.33)	(-0.29)	(0.78)			
43	2.5	1.8	30.3	(3.20)	21.8	(25)	(22)	(0.65)	1.36	(-0.29)	(0.54)			
39.5	2.6	1.9	31.5	3.27	22.7	(26)	(23)	(0.64)	1.44	(-0.29)	(0.45)			
31.2	2.6	1.3	35.6	3.26	25.0	(20)	(25)	0.57	1.22	(-0.25)	(0.14)			
26.2	(2.6)	1.0	39.6	(3.85)	27.3	(17)	(26.5)	(0.48)	1.04	(-0.21)	(0.05)			
21.0	2.5	0.16	41.3	4.79	27.8	(18)	(28)	0.39	0.57	-0.17	(0.02)			

 $(-\frac{\lambda^{\text{tr}}}{\lambda})_{\text{max}} = 7 \times 10^{-3}$



as  $1/T$ . This is caused by the fact that the corresponding microscopic cross sections (squares of matrix elements) are proportional to the square of the duration of a collision, *i.e.*, proportional to  $1/v^2$  where  $v$  is the relative velocity. This corresponds to a  $1/T$  dependence which agrees well with the experimental observations (see fig. 7). For the effective cross section for energy exchange,  $\mathcal{S}(0001)$ , the same reasoning holds, as long as the rotational energy jumps are small compared with  $kT$ . However, if the jumps are no longer small compared with  $kT$ , it must be expected that  $\mathcal{S}(0001)$  decreases with decreasing temperature. This can be understood by realizing that  $\mathcal{S}(0001)$  is the sum of the excitation and deexcitation cross sections. The former becomes unimportant at low temperatures as it decreases exponentially while the deexcitation cross section which becomes dominant decreases weakly with temperature<sup>32,34</sup>). This explains the behavior of  $\mathcal{S}(0001)$  for the hydrogen isotopes (see *e.g.*, fig. 9); the data for HD suggest a maximum value for  $\mathcal{S}(0001)$  around 40 K; for  $H_2$  and  $D_2$  where the energy jumps are large due to the selection rule  $\Delta J = \pm 2$ , a decrease for  $\mathcal{S}(0001)$  is found with decreasing temperature in the whole temperature range studied. The temperature dependence of  $\mathcal{S}_{20}^{(02)}$  will be treated in section 6.1.2 where use is made of a relation between this cross section and  $\mathcal{S}(0001)$ .

When comparing the effective cross sections it should be realized that diagonal cross sections *e.g.*,  $\mathcal{S}(02)$  and  $\mathcal{S}(0001)$  are positive definite, each collisional event giving a positive contribution to the cross section. To off-diagonal effective cross sections *e.g.*,  $\mathcal{S}_{20}^{(02)}$  different collisional events may contribute with different signs, which tends to decrease the value of off-diagonal cross sections. We will first discuss the results for the homonuclear molecules  $H_2$  and  $D_2$  and subsequently the heteronuclear HD (see section 6.2).

6.1  $H_2$  and  $D_2$ . The homonuclear hydrogen isotopes differ in two respects from heavier homonuclears as  $N_2$  and  $O_2$ :

a) For  $H_2$  and  $D_2$  the angle dependent part in the intermolecular potential

$$V = V_0(r) + \epsilon V_2(r) \{P_2(\cos \chi_1) + P_2(\cos \chi_2)\} + V_{QQ} \quad (11)$$

is very weak:  $\epsilon \approx 0.05$ <sup>32,33</sup>). Here the spherical potentials  $V_0(r)$  and  $V_2(r)$  are of roughly the same magnitude and  $V_{QQ}$  is the (small) contribution arising from quadrupole-quadrupole interaction. The angles  $\chi_1$  and  $\chi_2$  determine the orientations of the molecular axes of both molecules relative to  $\underline{r}$ , the vector connecting the centers of mass.

b) Because of the large level spacing and the fact that transitions with  $\Delta J = \pm 1$  are spin forbidden, one has for inelastic collisions:  $\Delta E_{rot} \gtrsim kT$ .

As a consequence of these properties a) and b) the time scales for different collisional processes are widely separated. From argument a) it follows that the time

scale for gas kinetic processes (i) is shorter than the time scale for – energetically elastic – angular momentum reorientation processes (ii). From arguments a) and b) it is clear that the time scale for processes involving energy exchange with translation (iii) is still larger.

Keeping in mind the above considerations we will now discuss in some detail the relative magnitude and behavior of the various cross sections. As yet no complete close coupling calculations are available. However, Köhler, Hess and Waldmann<sup>35</sup>) performed calculations on the basis of a first order distorted wave Born approximation (DWBA). Assuming an anisotropic potential of the form of eq. (11) without the QQ-term they calculated for homonuclear molecules with small nonsphericity ( $\epsilon \ll 1$ ) the order of  $\epsilon$  in which the different collision processes contribute to the effective cross sections (see table VI). Especially for  $H_2$  and  $D_2$  ( $\epsilon \approx 0.05$ ) the results of these calculations are expected to be reliable. On this basis a qualitative discussion of the various cross sections will be done below. Finally, for a simple repulsive potential a few cross sections have been calculated<sup>36,37</sup>):  $\mathcal{S}_{1200}^{(1001)}$  for  $pH_2$  and  $\mathcal{S}(02)$  and  $\mathcal{S}_{20}^{(02)}$  for HD at room temperature. The results are in reasonable agreement with the experimental data (see table VII).

6.1.1  $\mathcal{S}(0001) \approx 0.1 \text{ \AA}^2$  for  $H_2$  and  $D_2$ . As seen from fig. 10, this cross section is found to be quite small for  $H_2$  and  $D_2$  (cf. the elastic cross section  $\mathcal{S}(20) \approx 20 \text{ \AA}^2$ ). In first order DWBA  $\mathcal{S}(0001)$  is proportional to  $\epsilon^2$ . Because  $\epsilon \approx 0.05$  and only inelastic collisions contribute to  $\mathcal{S}(0001)$ , it is not surprising that for  $\mathcal{S}(0001)$  small values of about  $0.1 \text{ \AA}^2$  are found. The difference between  $H_2$  and  $D_2$  can to a large extent be explained from the temperature dependence as discussed above. For  $D_2$ , which has the smaller rotational level spacing, the temperature at which the drop-off of  $\mathcal{S}(0001)$

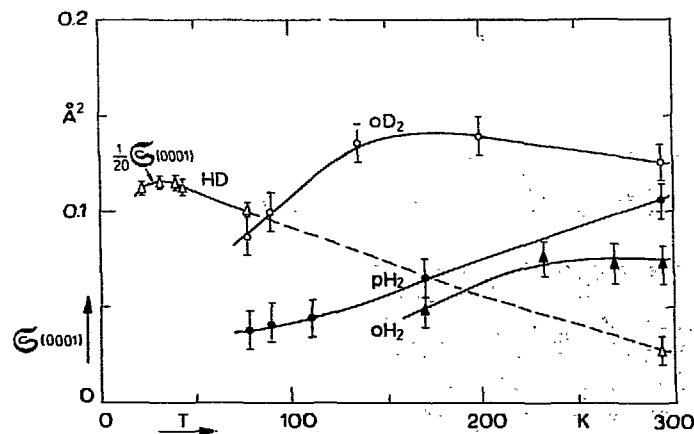


Fig. 10 The cross section  $\mathcal{S}(0001)$  versus temperature for  $pH_2$ ,  $oH_2$ ,  $oD_2$  and HD.

starts is much lower than for  $H_2$ . For the difference between  $oH_2$  and  $pH_2$  the same argument holds; at temperatures where  $kT$  is large compared to the level spacing,  $\mathcal{S}(0001)$  can be assumed to be equal for both systems. With decreasing temperature, however,  $\mathcal{S}(0001)$  for  $oH_2$  with its large energy jump  $J = 1 \leftrightarrow J = 3$  will start to fall off earlier than for  $pH_2$ .

Table VI

The various collision processes and the order of the non-sphericity parameter  $\epsilon$  in which they contribute to the various cross sections in first order DWBA<sup>35)</sup>

	energetically elastic collisions $\Delta J = 0$ $\Delta M_J = 0$	reorientation collisions $\Delta J = 0$ $\Delta M_J \neq 0$	energetically inelastic collisions $\Delta J \neq 0$ (and $\Delta M_J \neq 0$ )
$\mathcal{S}(0001)$	—	—	$\epsilon^2$
$\mathcal{S}(02)$	—	$\epsilon^2$	$\epsilon^2$
$\mathcal{S}_{20}^{(02)}$	—	$\epsilon^3$	$\epsilon^2$

Table VII

Comparison of some experimental results with (first order) DWBA calculations<sup>36,37)</sup> at room temperature

	$\mathcal{S}_{1200}^{(1001)}$ ( $\text{\AA}^2$ )		$\mathcal{S}(02)$ ( $\text{\AA}^2$ )		$\mathcal{S}_{20}^{(02)}$ ( $\text{\AA}^2$ )	
	exp.	calc.	exp.	calc.	exp.	calc.
HD	0.67 <sup>31)</sup>	—	2.3 <sup>6)</sup>	2.58 <sup>36)</sup>	0.28 <sup>6)</sup>	0.55 <sup>36)</sup>
$pH_2$	0.31 <sup>38)</sup>	0.286 <sup>37)</sup>	0.49	—	0.019	—

6.1.2.  $\mathcal{S}_{(20)}^{(02)} \approx 0.02 \text{ \AA}^2$  for  $H_2$  and  $D_2$ . In first order DWBA the contribution to  $\mathcal{S}_{(20)}^{(02)}$  from elastic collisions is proportional to  $\epsilon^3$  and is moreover connected with the non-self-adjoint part of the Waldmann-Snyder collision operator. It can therefore be neglected as compared to the contribution from inelastic collisions which is of the order  $\epsilon^2$ . As such inelastic collisions will be rare in  $H_2$  and  $D_2$ ,  $\mathcal{S}_{(20)}^{(02)}$  can be expected to be small (see section 6.1.1). In fig. 9 the results for  $\mathcal{S}_{(20)}^{(02)}$  are given for  $pH_2$ ,  $nH_2$ ,  $oD_2$  and  $nD_2$ . No measurements were performed on  $oH_2$  and  $pD_2$ , because these gases were not available in large enough quantities. The cross section values of  $\mathcal{S}_{(20)}^{(02)}$  obtained for  $nH_2$  and  $nD_2$  are as such of limited value, because these gases have to be considered as non-reacting gas mixtures of even  $J$  and odd  $J$  molecules. However, by combining the data for pure  $pH_2$  with those for  $nH_2$  ( $\frac{1}{4}$  para and  $\frac{3}{4}$  ortho) one can obtain qualitative information about the difference in behavior between  $oH_2$  and  $pH_2$ . For  $D_2$  this is also true but to a lesser extent because extrapolation to  $pD_2$  is more speculative using the data for  $oD_2$  and  $nD_2$  ( $\frac{2}{3}$  ortho and  $\frac{1}{3}$  para).

Keeping in mind the above considerations the relatively large difference in magnitude of  $\mathcal{S}_{(20)}^{(02)}$  between  $pH_2$  and  $nH_2$  can be well understood, since inelastic transitions between  $J=0$  and  $J=2$  take place more easily than between  $J=1$  and  $J=3$ . The difference between the values of  $\mathcal{S}_{(20)}^{(02)}$  for  $oD_2$  and  $nD_2$  is much less pronounced mainly because  $nD_2$  consists for  $\frac{2}{3}$  of  $oD_2$ . The cross sections for  $H_2$  are considerably smaller than those for  $D_2$ . Again, the main reason for this has to be sought in the fact that inelastic collisions can occur less easily in  $H_2$  than in  $D_2$  because of the larger level spacing in  $H_2$ . We will now consider the temperature dependence of  $\mathcal{S}_{(20)}^{(02)}$ . In  $pH_2$  only  $J=0 \rightarrow 2$  transitions are efficient in producing from a velocity polarization a  $\underline{J}\underline{J}$ -polarization since the reverse process leaves the molecule in the  $J=0$  state and thus unable to contribute to the  $\underline{J}$  polarization. Consequently, the fraction of  $J=0$  molecules in combination with the excitation cross section determines  $\mathcal{S}_{(20)}^{(02)}$  in this case. At decreasing temperature, the exponential decrease of the excitation cross section is partly compensated for by the increasing fraction of  $J=0$  molecules. Therefore, the temperature dependence is much less steep than could be expected. In  $oH_2$ , both  $J=1 \rightarrow 3$  and  $J=3 \rightarrow 1$  transitions contribute to  $\mathcal{S}_{(20)}^{(02)}$  so that both excitation and deexcitation cross section have to be considered. Since the deexcitation cross section is only weakly dependent on temperature, a weak temperature dependence of  $\mathcal{S}_{(20)}^{(02)}$  must also be expected (see fig. 9). For  $D_2$ , no drop-off at lower temperatures is observed in the temperature range studied because the level spacing is a factor 2 smaller than for  $H_2$ .

Moraal<sup>39</sup>) and Snider<sup>40</sup>), using a modified Born approximation, derived an approximate relation between  $\mathcal{S}_{(20)}^{(02)}$  and  $\mathcal{S}(0001)$  for diatomics assuming that only one type of nonspherical potential dominates; for a single  $P_1$ -potential with  $l=1$  or 2, this relation is given by

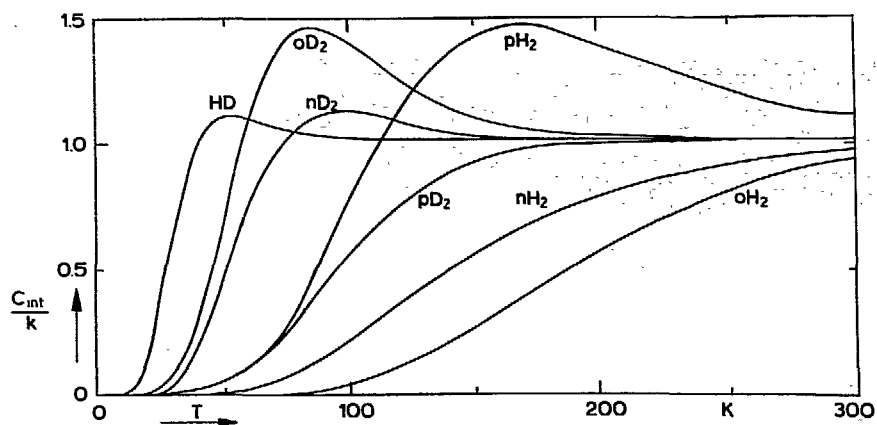


Fig. 11 Internal (rotational) specific heat per molecule versus temperature for different hydrogen isotopes and their modifications.

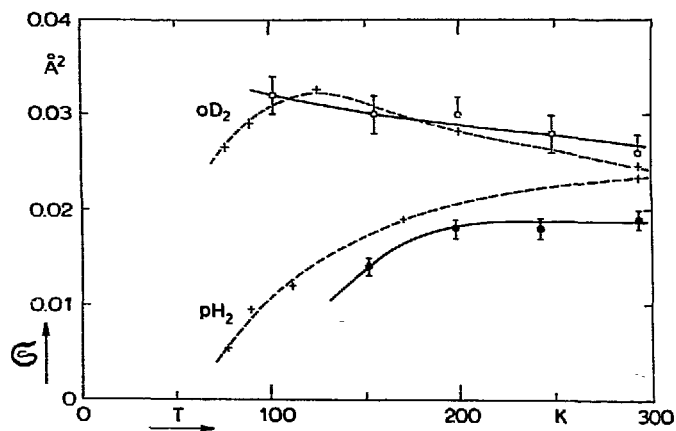


Fig. 12 Comparison of  $S(0,0)$  and  $S(0001)$  for  $pH_2$  and  $oD_2$  as a function of temperature;

•  $S(0,0)$  for  $pH_2$

○  $S(0,0)$  for  $oD_2$

+  $\frac{1}{\sqrt{15}} \frac{C_{int} T}{k \theta} (J^2 (J^2 - 3/4))_0^{-1/2} S(0001)$ ,  $P_2$ -potential dominant.

$$\mathcal{S}_{(20)}^{(02)} \approx \frac{1}{\sqrt{15}} \frac{C_{\text{int}}}{k} \frac{T}{\theta} (J^2 - 3/4)_0^{-1/2} \mathcal{S}(0001) \quad (12)$$

where  $C_{\text{int}}$  is the internal specific heat per molecule (fig. 11) and  $\theta$  the rotational temperature (see table I). Eq. (12) reduces in the high temperature limit to the already known relation<sup>41,42)</sup>

$$\mathcal{S}_{(20)}^{(02)} = \frac{1}{\sqrt{30}} \mathcal{S}(0001). \quad (13)$$

In fig. 12  $\mathcal{S}_{(20)}^{(02)}$  for  $\text{pH}_2$  and  $\text{oD}_2$  has been plotted versus temperature together with the quantity appearing on the right hand side of eq. (12) as calculated from the experimentally obtained cross section  $\mathcal{S}(0001)$ . As can be seen the relation of eq. (12) is quite well obeyed over the whole temperature range.

6.1.3.  $\mathcal{S}(02) \approx 0.5 - 1 \text{ \AA}^2$  for  $\text{H}_2$  and  $\text{D}_2$ . In first order DWBA (elastic) reorientation collisions as well as inelastic collisions contribute to  $\mathcal{S}(02)$ , both in order  $\epsilon^2$ . As  $\mathcal{S}(02)$  is considerably larger than  $\mathcal{S}(0001)$  it must be concluded that elastic reorientation collisions give an important contribution to  $\mathcal{S}(02)$ . This is consistent with the slight increase of  $\mathcal{S}(02)$  at lower temperatures, as seen in fig. 7. The value of  $\mathcal{S}(02)$  for  $\text{D}_2$  is found to be a factor of 2 larger than for  $\text{H}_2$ . Since  $\mathcal{S}(02)$  is mainly determined by elastic collisions, which are governed by the interaction time during the collisions, the smaller velocity of  $\text{D}_2$  fully explains this difference.

For  $\mathcal{S}(02)$  differences between ortho and para modifications are found to be negligible, both in  $\text{H}_2$  and in  $\text{D}_2$ . The same was found from measurements on the Depolarized Rayleigh line<sup>19)</sup>. The reorientation process is apparently rather insensitive to the rotational quantum number. This is not surprising, since on one hand high rotational quantum numbers tend to make reorientation more difficult by the larger gyroscopic stability. On the other hand they tend to make reorientation easier since there are more  $M_J$  states to be occupied.

Using this conclusion, another interesting statement can be made. From a comparison of fig. 1 and fig. 7 it is seen that in para  $\text{H}_2$  between 150 K and 300 K, the occupation of the  $J = 0$  level changes drastically while the value of  $\mathcal{S}(02)$  behaves like that of ortho  $\text{H}_2$  where only a slight shift from  $J = 1$  to  $J = 3$  molecules takes place over that temperature region. Consequently, the efficiencies of  $J = 0$  molecules and  $J = 2$  molecules in reorienting  $J = 2$  molecules must be roughly equal.

The fact that  $\mathcal{S}(02)$  was found to be equal for  $\text{pH}_2$  and  $\text{oH}_2$  is in accordance with DWBA calculation<sup>43)</sup>. Taking into account only elastic collisions of  $J = 1$  with  $J = 1$  molecules in  $\text{oH}_2$  and  $J = 0$  with  $J = 2$  molecules in  $\text{pH}_2$ , these calculations

yield a ratio of 1.04 between the reorientation cross section for  $\text{oH}_2$  and  $\text{pH}_2$  for a pure  $P_2$ -potential. This value changes only slightly if also quadrupole-quadrupole (QQ) interaction is included. However, the QQ interaction (which gives rise to resonance collisions  $0 + 2 \leftrightarrow 2 + 0$  in  $\text{pH}_2$ , and to elastic reorientation collisions  $1 + 1 \leftrightarrow 1 + 1$  in  $\text{oH}_2$ ) can be expected to give only a small contribution to  $\mathcal{S}(02)$  in  $\text{H}_2$ . This is suggested by Raman scattering experiments<sup>44)</sup> where the cross section for resonance collisions was found to be comparable with the purely inelastic cross section which is an order of magnitude smaller than the reorientation cross section.

Also from NMR, molecular cross sections can be obtained which are related to the reorientation of the molecules. Hence it is useful to compare  $\mathcal{S}(02)$  obtained from our experiments with the NMR cross sections. Since for  $\text{H}_2$  both spin-spin and spin-rotation interactions contribute to the relaxation, these contributions cannot be disentangled from the experimental results only. On the other hand, in the case of  $\text{D}_2$  which has a nuclear quadrupole, the nuclear spin relaxation is dominated by one process: the quadrupole interaction. In this case the reorientation cross section is related to the NMR relaxation time  $T_1$  or  $T_2$  by<sup>8)</sup>

$$\mathcal{S}'(02) = \frac{3}{8} \left( \frac{eqQ}{\hbar} \right)^2 \left\langle \frac{J(J+1)}{(2J-1)(2J+3)} \right\rangle_0 \frac{T_2}{n \langle v \rangle_0} \quad (14)$$

The average has to be taken for  $\text{pD}_2$  over odd  $J$  and for  $\text{oD}_2$  over even  $J$ . The prime refers to the collision superoperator used in NMR which differs from that used in the viscosity cross sections in that the collision partner does not explicitly appear in NMR. This is a consequence of assuming that collisions cannot change nuclear spin states. The results for  $\text{oD}_2$  obtained by Hardy<sup>45)</sup> in the temperature range from 32 K to 330 K agree very well with our results (see fig. 13).

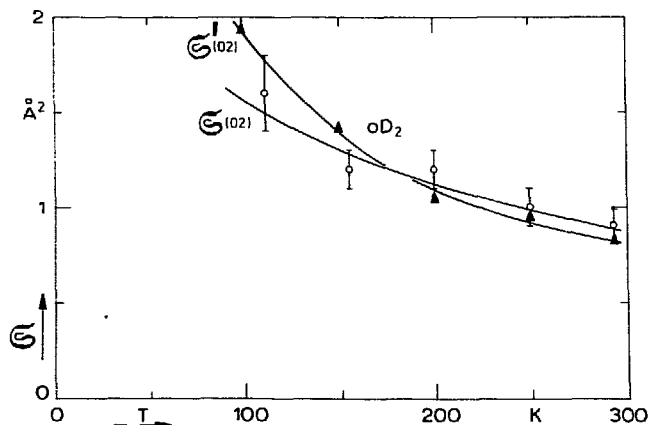


Fig. 13 Comparison for  $\text{oD}_2$  between the reorientation cross section  $\mathcal{S}(02)$  and the NMR cross section  $\mathcal{S}'(02)$ .  
 $\circ$   $\mathcal{S}(02)$ ,  $\blacktriangle$   $\mathcal{S}'(02)$ .

6.2 HD. Although the interaction potential between two HD molecules in terms of the vector connecting the geometrical centers of the molecules is also given by eq. (11), the interaction potential contains a strong  $P_1$  term when the potential is written in terms of the vector connecting the centers of mass of the molecules<sup>32,35</sup>). Therefore collisional transitions  $\Delta J = \pm 1$ , which are allowed here, can be supposed to occur far more frequent than transitions  $\Delta J = \pm 2$ .

6.2.1  $\mathcal{S}(0001) \approx 1.2 \text{ \AA}^2$  for HD. The value of  $\mathcal{S}(0001)$  is 10 times larger than for  $H_2$  and  $D_2$ . This is caused by the presence of the strong  $P_1$  term.

6.2.2  $\mathcal{S}_{20}^{(02)} \approx 0.3 \text{ \AA}^2$  for HD. As  $\mathcal{S}_{20}^{(02)}$  is predominantly an inelastic cross section (see section 6.1.2) the inclusion of a  $P_1$  term gives rise to a relatively large value of  $\mathcal{S}_{20}^{(02)}$ .

6.2.3  $\mathcal{S}(02) \approx 3 \text{ \AA}^2$  for HD. For  $\mathcal{S}(02)$  the contribution arising from the  $P_1$  term occurs in first order DWBA only through inelastic collisions. Even so, this contribution is rather large due to the rather large non-sphericity parameter associated with this  $P_1$  term. For the contribution arising from this  $P_1$  term, Köhler<sup>36</sup>), using the quantum mechanical version of the loaded sphere model, calculated the value  $\mathcal{S}(02) = 2.6 \text{ \AA}^2$  for HD at 300 K. As seen in table VII the experimental value is  $2.3 \text{ \AA}^2$ . Since it is expected that the contribution arising from the  $P_2$  term will be roughly equal to that for  $H_2$  and  $D_2$ , some  $0.7 \text{ \AA}^2$  of this last value will be due to the  $P_2$  term. One might thus conclude that the above mentioned model<sup>36</sup>) which is based on purely repulsive interaction, overestimates the inelastic cross sections. This is supported by the fact that this model also gives too high values for  $\mathcal{S}_{20}^{(02)}$ :  $0.55 \text{ \AA}^2$  compared with the experimental value of  $0.28 \text{ \AA}^2$  for HD at 300 K (see table VII).

*Appendix.* The method of calculation for the various cross sections appearing in tables IV and V is given below:

$\mathcal{S}(0001)$  is obtained from the volume viscosity  $\eta_v$ ,

$$\mathcal{S}(0001) = \frac{kT}{\langle v \rangle_0} \frac{C_{int}/k}{(C_{int}/k + 3/2)^2} \frac{1}{\eta_v} \quad (A1)$$

$\mathcal{S}(0010)$  from the exact relation

$$\mathcal{S}(0010) = \frac{2}{3} \frac{C_{int}}{k} \mathcal{S}(0001) \quad (A2)$$



$\mathfrak{S}(2000)$  from the field free viscosity coefficient  $\eta(0)$

$$\mathfrak{S}(2000) = \frac{kT}{\langle v \rangle_0} \frac{1}{\eta(0)} \quad (\text{A3})$$

$\mathfrak{S}(1010)$  from the exact relation

$$\mathfrak{S}(1010) = \frac{2}{3} \mathfrak{S}(2000) + \frac{5}{9} \frac{C_{\text{int}}}{k} \mathfrak{S}(0001) \quad (\text{A4})$$

$\mathfrak{S}_{(1001)}^{(1010)}$  from the exact relation

$$\mathfrak{S}_{(1001)}^{(1010)} = \frac{1}{3} \sqrt{\frac{5C_{\text{int}}}{2k}} \mathfrak{S}(0001) \quad (\text{A5})$$

$\mathfrak{S}(1001)$  using the field free thermal conductivity coefficient  $\lambda(0)$

$$\mathfrak{S}(1001) = \frac{\lambda(0) \mathfrak{S}_{(1001)}^{(1010)2} + a \sqrt{\frac{10C_{\text{int}}}{k}} \mathfrak{S}_{(1001)}^{(1010)} + a \frac{C_{\text{int}}}{k} \mathfrak{S}(1010)}{\lambda(0) \mathfrak{S}(1010) - \frac{5}{2} a} \quad (\text{A6})$$

$$\text{with } a = \frac{k^2 T}{m \langle v \rangle_0}$$

$\mathfrak{S}(0200)$  from the position of the viscomagnetic effect

$$\mathfrak{S}(0200) = \frac{|g| \mu_N kT}{\hbar \langle v \rangle_0} \left( \frac{H}{p} \right)_{\xi_{02}=1} \quad (\text{cf. eq. (7)}) \quad (\text{A7})$$

$\mathfrak{S}(1200)$  from the position of the Senftleben-Beenakker effect for the thermal conductivity

$$\mathfrak{S}(1200) = \frac{|g| \mu_N kT}{\hbar \langle v \rangle_0} \left( \frac{H}{p} \right)_{\xi_{12}=1} \quad (\text{A8})$$

$|\mathfrak{S}_{(2000)}^{(0200)}|$  from the magnitude  $\Psi_{02}$  of the viscomagnetic effect

$$|\mathfrak{S}_{(2000)}^{(0200)}| = \sqrt{\Psi_{02} \mathfrak{S}(0200) \mathfrak{S}(2000)} \quad (\text{cf. eq. (5)}) \quad (\text{A9})$$

$\mathcal{S}_{1200}^{(1010)}$  from the exact relation

$$\mathcal{S}_{1200}^{(1010)} = -\frac{1}{\sqrt{5}} \mathcal{S}_{2000}^{(0200)} \quad (\text{A10})$$

$\mathcal{S}_{1200}^{(1001)}$  from the magnitude  $\Psi_{12}$  (see ref. 31) of the Sentfleben-Beenakker effect for the heat conductivity

$$\mathcal{S}_{1200}^{(1001)} = \frac{1}{C_3} (C_2 \pm \sqrt{\frac{\Psi_{12}}{C_1}}) \quad (\text{A11})$$

where

$$C_1 = \frac{5k^2 T}{4m\lambda(0) \langle v \rangle_0} \frac{1}{\mathcal{S}_{1200} \{ \mathcal{S}_{1010} \mathcal{S}_{1001} - \mathcal{S}_{1001}^{(1010)^2} \}^2}$$

$$C_2 = \mathcal{S}_{1200}^{(1010)} \{ \mathcal{S}_{1001} + \sqrt{\frac{2C_{\text{int}}}{5k}} \mathcal{S}_{1001}^{(1010)} \}$$

$$C_3 = \mathcal{S}_{1001}^{(1010)} + \sqrt{\frac{2C_{\text{int}}}{5k}} \mathcal{S}_{1010}.$$

Following the argument used in ref. 31 only the plus sign of eq. (A11) is considered.

The cross sections  $\mathcal{S}_{\text{DPR}}$  and  $\tilde{\mathcal{S}}_{\text{DPR}}$  are obtained from the Fourier transform  $F_R(t)$  of the Depolarized Rayleigh line profile (see ref. 19)

$$\mathcal{S}_{\text{DPR}} = -\frac{1}{n \langle v \rangle_0} \left( \frac{d F_R}{dt} \right)_{t=0} \quad (\text{A12})$$

$$\tilde{\mathcal{S}}_{\text{DPR}} = \frac{1}{n \langle v \rangle_0} \left[ \int_0^\infty F_R(t) dt \right]^{-1} \quad (\text{A13})$$

where  $n$  is the number density.

In the above equations the mean relative velocity is defined by  $\langle v \rangle_0 = \sqrt{16kT/\pi m}$  where  $m$  is the molecular mass. The exact relations (A2), (A4), (A5) and (A10) have been derived in refs. 41, 42 and 46.

## References

1. Beenakker, J.J.M. and McCourt, F.R., *Ann. Rev. Phys. Chem.* 21 (1970) 47.
2. Beenakker, J.J.M., Knaap, H.F.P. and Sanctuary, B.C., *AIP Conference Proc.* 11 (1973) 21.
3. Beenakker, J.J.M., *Lecture Notes in Physics*, Vol. 31, Springer-Verlag, Berlin, 1974, p. 414; Snider, R.F., *ibid.*, p. 469.
4. Coope, J.A.R. and Snider, R.F., *J. Chem. Phys.* 57 (1972) 4266.
5. Moraal, H., *Physics Reports* 17 (1975) 225.
6. Hulsman, H., Van Waasdijk, E.J. Burgmans, A.L.J., Knaap, H.F.P. and Beenakker, J.J.M., *Physica* 50 (1970) 53.
7. Hulsman, H., Van Kuik, F.G., Walstra, K.W., Knaap, H.F.P. and Beenakker, J.J.M., *Physica* 57 (1972) 501.
8. Burgmans, A.L.J., Van Ditzhuyzen, P.G., Knaap, H.F.P. and Beenakker, J.J.M., *Z. Naturforsch.* 28a (1973) 385.
9. Korving, J., Hulsman, H., Scoles, G., Knaap, H.F.P. and Beenakker, J.J.M., *Physica* 36 (1967) 177.
10. Vestner, H., *Z. Naturforsch.* 29a (1974) 663.
11. Hermans, L.J.F., Schutte, A., Knaap, H.F.P. and Beenakker, J.J.M., *Physica* 51 (1971) 319.
12. Van Ee, H., Thesis Leiden, 1966, p. 21.
13. Coope, J.A.R. and Snider, R.F., *J. Chem. Phys.* 56 (1972) 2056.
14. Hooyman, G.J., Mazur, P. and De Groot, S.R., *Physica* 21 (1955) 355.
15. De Groot, S.R. and Mazur, P., *Non-Equilibrium Thermodynamics*, North-Holland Publishing, Amsterdam, 1962, p. 311.
16. Rietveld, A.O., Van Itterbeek, A. and Velds, C.A., *Physica* 25 (1959) 205.
17. Baas, F., *Phys. Letters* 36A (1971) 107; Baas, F., Thesis Leiden (1976).
18. Baas, F. et al., *Physica*, to be published.
19. Keijser, R.A.J., Van den Hout, K.D. and Knaap, H.F.P., *Physica* 75 (1974) 515.
20. Sluyter, C.G., Knaap, H.F.P. and Beenakker, J.J.M., *Physica* 30 (1964) 745.
21. Sluyter, C.G. and Jonkman, R.M., *Physica* 30 (1964) 1670.
22. Jonkman, R.M., Prangma, G.J., Ertas, I., Knaap, H.F.P. and Beenakker, J.J.M., *Physica* 38 (1968) 441.
23. Narayana, H. and Woods, S.B., *Can. J. Phys.* 48 (1970) 303.
24. Prangma, G.J., Borsboom, L.J.M., Knaap, H.F.P., Van den Meijdenberg, C.J.N. and Beenakker, J.J.M., *Physica* 61 (1972) 527.
25. *Data Book*, edited by Thermophysical Properties Research Center, Purdue University (Lafayette, Indiana) 1966, Vol. 2.

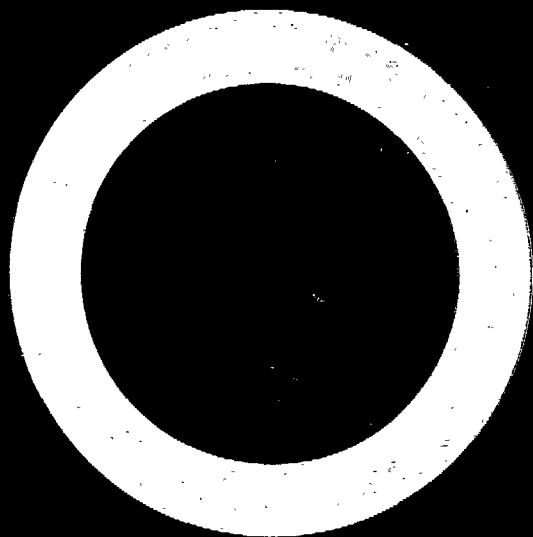
Since only for  $n\text{H}_2$  and  $n\text{D}_2$  heat conductivity data are available, for  $p\text{H}_2$  the heat conductivity data are calculated by

$$\lambda^{p\text{H}_2} = \lambda^{n\text{H}_2} \frac{C_{\text{int}}^{p\text{H}_2} / k + 3.75}{C_{\text{int}}^{n\text{H}_2} / k + 3.75}$$

where the data for the specific heat (fig. 11) are taken from A. Farkas, Ortho-hydrogen, Parahydrogen and Heavy hydrogen (University Press, Cambridge, 1935). The heat conductivity of  $o\text{D}_2$  has been analogously calculated from that of  $n\text{D}_2$ .

26. Hermans, L.J.F., Koks, J.M., Hengeveld, A.F. and Knaap, H.F.P., *Physica* **50** (1970) 410.
27. Jonkman, R.M., Prangma, G.J., Keijser, R.A.J., Aziz, R.A. and Beenakker, J.J.M., *Physica* **38** (1968) 451.
28. Van der Meulen, J.P. and Harpe, J.P., unpublished results.
29. Prangma, G.J., Heemskerk, J.P.J., Knaap, H.F.P. and Beenakker, J.J.M., *Physica* **50** (1970) 433.
30. The thermal conductivity of HD at room temperature was taken from Van Dael, W. and Cauwenbergh, H., *Physica* **54** (1971) 347 :  $\lambda = 1.538 \text{ mW cm}^{-1} \text{ K}^{-1}$  at 296.8 K. At lower temperatures the unpublished data measured by Heemskerk are used:  $\lambda$  ( $\text{mW cm}^{-1} \text{ K}^{-1}$ ): 0.31 at 38.2 K, 0.41 at 49.6 K, 0.525 at 60.0 K, 0.555 at 69.5 K, 0.60 at 86.2 K, 0.88 at 150 K, 1.1 at 199 K and 1.55 at 300 K. This last value is in good agreement with the value of Van Dael and Cauwenbergh at 296.8 K.
31. Heemskerk, F.G., Van Kuik, F.G., Knaap, H.F.P. and Beenakker, J.J.M., *Physica* **71** (1974) 484.
32. Takayanagi, K., Sc. Repts. Saitama Univ. **A III** (1959) 2.
33. Hess, S. and Köhler, W.E., *Z. Naturforsch.* **23a** (1968) 1903.
34. Davison, W.D., *Disc. Faraday Soc.* **33** (1962) 71.
35. Köhler, W.E., Hess, S. and Waldmann, L., *Z. Naturforsch.* **25a** (1970) 336.
36. Köhler, W.E., *Z. Naturforsch.* **26a** (1971) 1926; *ibid* **30a** (1975) 117.
37. Köhler, W.E., *Z. Naturforsch.* **28a** (1973) 815.
38. Hermans, L.F.J., Schutte, A., Knaap, H.F.P. and Beenakker, J.J.M., *Physica* **46** (1970) 491.
39. Moraal, H., *Z. Naturforsch.* **28a** (1973) 824.
40. Snider, R.F., *Physica* **78** (1974) 387.
41. Moraal, H. and Snider, R.F., *Chem. Phys. Letters* **9** (1971) 401.
42. Chen, F.M., Moraal, H. and Snider, R.F., *J. Chem. Phys.* **57** (1972) 542.
43. Köhler, W.E., private communication.

44. Keijser, R.A.J., Lombardi, J.R., Van den Hout, K.D., De Groot, M., Sanctuary, B.C. and Knaap, H.F.P., Phys. Letters 45A (1973) 3.  
Keijser, R.A.J., Thesis Leiden, 1973, Chapter III.
45. Hardy, W.N., Thesis University of British Columbia, Vancouver (1964).
46. Köhler, W.E., Z. Naturforsch. 29a (1974) 1705.



## SAMENVATTING

De invloed van elektrische en magnetische velden op de transporteigenschappen van meeratomige gassen staat bekend onder de naam Senftleben-Beenakker effect. In dit proefschrift wordt de invloed van magneetvelden op de viscositeit onderzocht. Als in een meeratomig gas een snelheidsgradiënt aanwezig is, ontstaat ten gevolge van botsingen een impulsmoment-polarisatie, d.w.z. een ophijning van de moleculen. Hierbij speelt het hoekafhankelijke deel van de interactie-potentiaal een essentiële rol. Onder invloed van een magneetveld wordt deze polarisatie verstoord en zal de viscositeit van het gas veranderen. De polarisaties kunnen even of oneven in het impulsmoment zijn. Dit correspondeert met respectievelijk een afname en een toename van de viscositeit.

Experimenteel is tot nu toe gebleken, dat voor alle gemeten gassen met uitzondering van  $\text{NH}_3$  de viscositeit afneemt onder invloed van een magneetveld en dat de gemeten effecten goed kunnen worden beschreven met één type polarisatie, dat even in het impulsmoment is. Metingen van transporteigenschappen van enkele symmetrische tot moleculen in een elektrisch veld hebben echter aangetoond dat eveneens polarisaties die oneven in het impulsmoment zijn kunnen optreden. Om na te gaan of de sterkte van het elektrische dipoolmoment en/of de meer gecompliceerde moleculaire structuur verantwoordelijk is voor de aanwezigheid van deze polarisaties is een meer systematisch onderzoek noodzakelijk. Omdat dit experimenteel eenvoudiger te verwezenlijken is met behulp van magneetvelden dan met elektrische velden, is een onderzoek opgezet naar de invloed van magneetvelden op de warmtegeleiding en de viscositeit van polaire moleculen met verschillende structuren. Het onderzoek aan de warmtegeleiding, dat wordt verricht door drs. B.J. Thijsse, is nog in volle gang. De resultaten van het onderzoek naar de viscositeit van dergelijke gassen in een magneetveld (het z.g. viscomagnetisch effect) zijn beschreven in hoofdstuk I van dit proefschrift. Allereerst is de apparatuur beschreven, die nodig is om de veranderingen van de viscositeit te kunnen meten in twee verschillende oriëntaties van het magneetveld. Onderzocht zijn de lineaire moleculen  $\text{CO}_2$ ,  $\text{OCS}$ ,  $\text{N}_2\text{O}$ ,  $\text{HCl}$ ,  $\text{DCl}$  en de symmetrische tot moleculen  $\text{CH}_3\text{F}$ ,  $\text{CHF}_3$ ,  $\text{PF}_3$ ,  $\text{NF}_3$ ,  $\text{PH}_3$ ,  $\text{AsH}_3$ ,  $\text{NH}_3$ ,  $\text{ND}_3$  en  $\text{SF}_6$ . Vanwege de kleine magnetische momenten van deze moleculen was het noodzakelijk gebruik te maken van een supergeleidende magneet die zeer hoge velden levert (75 kOe). De metingen van beide viscositeitsveranderingen maakte het mogelijk een kwantitatieve uitspraak te doen over het optreden van verschillende polarisaties. Met uitzondering van  $\text{NH}_3$  en  $\text{ND}_3$  bleek in alle gevallen, onafhankelijk van de moleculaire structuur en de grootte van het elektrisch dipoolmoment, het viscomagnetisch effect beschreven te kunnen worden door slechts één polarisatie, die even in het impulsmoment is.

De experimentele resultaten zijn vergeleken met de theorie, en de daaruit verkregen effectieve botsingsdoorsneden worden vergeleken met die welke afkomstig zijn van metingen aan het visco-elektrische effect.

Het viscomagnetische effect geeft informatie over verschillende botsingsprocessen, die daarbij een rol spelen: elastische botsingen, d.w.z. botsingen waarbij alleen de snelheid verandert en botsingen waarbij ook de oriëntatie van de moleculen verandert, en (energetisch) inelastische botsingen, waarbij uitwisseling van translatie- en rotatie-energie plaats vindt. In het algemeen zal bij kamertemperatuur het onderscheid tussen energetisch elastische en inelastische botsingen niet erg pregnant zijn omdat  $kT$  veel groter is dan de afstand tussen de rotatie-energieniveaux. Een gedetailleerde studie van deze botsingsprocessen is dus voor de meeste moleculen moeilijk. Uitzondering hierop vormen de waterstofisotopen, waar de afstand tussen de rotatie-energieniveaux groot is ten opzichte van  $kT$  bij kamertemperatuur. Dientengevolge zijn slechts weinig rotatieniveaux bezet ( $J = 0, 1, 2, 3, 4$ ). Bovendien komen bij de mononucleaire moleculen  $H_2$  en  $D_2$  twee modificaties voor, waarbij de ene slechts even en de andere slechts oneven rotatieniveaux heeft. De invloed van de specifieke rotatieniveaux op de verscheidene botsingsprocessen kan derhalve worden bestudeerd door metingen te doen aan de ortho- en para-modificaties van  $H_2$  en  $D_2$  bij verschillende temperaturen. Daarom is een systematisch onderzoek gedaan naar het viscomagnetisch effect van  $H_2$  en  $D_2$  in het temperatuurgebied van 140 K tot 300 K. De relatieve viscositeitsverandering van  $H_2$  en  $D_2$  is van de orde  $10^{-5}$  hetgeen ongeveer een factor 100 kleiner is dan het effect van andere moleculen zoals  $O_2$ ,  $N_2$ ,  $CO$  en  $HD$ . Daarom moesten hoge eisen worden gesteld aan de experimentele opstelling. De metingen zijn vergeleken met de reeds eerder verrichte metingen aan  $HD$ . Tevens zijn de resultaten afkomstig van rotatie-relaxatiemetingen aan deze waterstofisotopen in de discussie betrokken.



## CURRICULUM VITAE

Op verzoek van de faculteit der Wiskunde en Natuurwetenschappen volgt hier een overzicht van mijn studie. In 1964 behaalde ik het diploma Gymnasium  $\beta$  aan het Gereformeerd Gymnasium te Leeuwarden. Hierna vervulde ik gedurende twee jaar mijn militaire dienstplicht. In 1966 begon ik mijn studie aan de Rijksuniversiteit te Leiden. In 1969 legde ik het kandidaatsexamen Natuurkunde en Wiskunde met bijvak Sterrenkunde af. Het experimentele werk voor het doctoraalexamen heb ik verricht in het Kamerlingh Onnes Laboratorium. Het eerste half jaar heb ik dr. J.A. Roest geassisteerd bij zijn onderzoek aan paramagnetische relaxatie. Vanaf augustus 1969 ben ik werkzaam geweest in de werkgroep voor Molecuulfysica, die onder leiding staat van prof. dr. J.J.M. Beenakker en prof. dr. H.F.P. Knaap. Ik heb gewerkt aan een onderzoek naar de invloed van magneetvelden op de viscositeit van meeratomige gassen bij dr. A.L.J. Burgmans. In 1970 was ik gedurende twee maanden werkzaam in het Departement voor Natuurkunde van de Katholieke Universiteit van Leuven. Na in 1971 het doctoraalexamen experimentele natuurkunde te hebben afgelegd trad ik als wetenschappelijk medewerker in dienst van de Stichting voor Fundamenteel Onderzoek der Materie (F.O.M.) en begon ik het in dit proefschrift beschreven onderzoek. In 1971 ben ik assistent geweest op het natuurkunde practicum voor pre-kandidaten natuurkunde. Vervolgens had ik tot 1974 als hoofdassistent de leiding van het natuurkunde practicum voor studenten in de chemie en de farmacie. Sinds augustus 1974 ben ik als docent natuurkunde in dienst bij de Stichting Lerarenopleiding Zuidwest-Nederland in Delft, tot 1976 in een deelbetrekking, daarna in een volledige betrekking.

Van de velen, die een bijdrage hebben geleverd aan het tot stand komen van dit proefschrift, wil ik dr. L.J.F. Hermans noemen, die steeds weer bereid was de interpretatie van de resultaten te bediscussiëren. Zeer dankbaar ben ik prof. dr. J.J.M. Beenakker voor de stimulerende gesprekken, die hebben bijgedragen tot een beter inzicht in de resultaten van het in dit proefschrift beschreven onderzoek. De discussies met dr. C.J.N. van den Meijdenberg, dr. W.E. Köhler van de Universiteit van Erlangen, dr. D.A. Coombe van de Universiteit van Vancouver, drs. G.E.J. Eggermont en drs. G.W. 't Hooft mogen niet onvermeld blijven. Drs. B.J. Thijsse ben ik zeer erkentelijk voor de prettige samenwerking tijdens het verrichten van de eerste experimenten. In een later stadium van het onderzoek werd ik geassisteerd door drs. L.K. van der Meij, drs. W.C.M. Henkens en A.P.M. van Slingerland. Veel dank ben ik verschuldigd aan de technische staven van het Kamerlingh Onnes Laboratorium en het Huygens Laboratorium, in het bijzonder aan de heren P. Zwanenburg, J.M. Verbeek, J. Turenhout en J.F. Benning. Nooit deed ik vergeefs een beroep op de cryogene afdeling. In het bijzonder de heer J.D. Sprong voorzag mij telkens van de noodzakelijke hoeveelheid helium. Zeer dankbaar ben ik Anneke Aschoff, die met veel geduld en grote nauwgezetheid het manuscript en alle correcties heeft getypt. De Engelse tekst werd gecorrigeerd door dr. D.A. Coombe. De tekeningen en de foto zijn op vakkundige wijze verzorgd door de heren W. Rijnsburger en W.J. Brokaar.

